CHAPTER ONE

1. INTRODUCTION

1.1 Area of Research:

The research project was executed at the Khartoum Refinery. The influence of aqueous solvent on increased the rate of absorption was investigated for wide range of operation parameters. These parameters include flow rate of aqueous solvent and refinery flue gas, and concentration. The Simulation result was used as pattern and develop to design and analyses performance columns refinery for chemical absorption of H_2S from refinery flue gas, and also for other similar systems.

1.2 Statement of the Problem:

Refinery flue gas contains hydrogen sulfide gas besides ammonia. The existence of hydrogen sulfide in refinery flue gas is very disturbing, besides it smells bad, on combustion it will produce (SO_2) gas which pollutes the environment, in global, it will cause green house effect which causes global warming. So that, also needs to be eliminated from refinery flue gas

Therefore, it is necessary to purify the refinery flue gas first before combustion. Hydrogen sulfide in the Refinery flue gas is controlled by a combustion process where hydrogen sulfide (1036.6 kg/h) is converted to sulfur dioxide, which is also an air pollutant, hence the combustion process not the best way to remove hydrogen sulfide. To operate a successful refinery you need to have a clean production, clean technology and be environmentally friendly.

The effect of ammonia and sulphur dioxide in areas west and south-west of the Khartoum Refinery at stable weather even a distance of 4 km (including

residential complex for employees of the refinery Sudanese and Chinese), and in the event of a thunderstorm and windy (June - July - August - September) the effect extend to the village of Gilin (18 - 20 kilometers southwest of the refinery), causing harassment and complaint about odors for most of the residents of the village.

Health, safety and environment of great importance in human life, therefore, the pollutants that result from petroleum products and their effect on air, water and land should be explained.

1.3 Background:

H_2S is a colorless, toxic and flammable gas, with ρ=1.39 g/l (at 25 °C and 1 bar) and boiling point - 60 °C. Currently, H_2S removal is one of the most important aspects for the development of a new oil-gas field due to the reduction of the conventional oil resources (J.S.Gudmundsson, 2011). H_2S must be removed both to protect workers and environment (a H_2S concentration equal to 600 ppm causes breathing problems and even death among the exposed people), and because it reduces the economic value of the oil-gas field. In fact, oil companies must use special materials for equipments, like metal and corrosion resistant alloys, whose costs are about 10 times greater than the common carbon steel piping. In addition, the sulphur that is produced from the H_2S of the refinery flue gas can be extracted and marketed on its own (J.S.Gudmundsson, 2011).

Since H_2S is extremely toxic, it must be removed with efficiency close to 100%, and it must be transformed to a less dangerous chemical compound, elemental sulfur. Sulfur it is a bright yellow powder-like material, which can be sold and used in other chemical plants. Hydrogen sulfide is being produced by many industrial activities such as petroleum refining, natural gas and petrochemical plants, viscose rayon manufacturing craft, pulp manufacturing, food processing, aerobic and

anaerobic wastewater treatments and many other industries (Wang et al, 2012). The presence of H_2S usually prohibits the direct use of these gases because of its toxic properties, the formation of SO_2 upon combustion (acid rain), and the problems it (usually) gives in downstream processing. This means that it is often necessary to remove H_2S from gas stream prior to use. Many processes have been developed to remove H_2S from gas streams, (Ter Maat, 2005). Most of the process use gas-liquid contactors in which the H_2S is absorbed into a complexing reagent to give either another dissolved sulfide containing component and problems are the degradation of the solvent, (S. Ebrahimi, 2003).

Nowadays, researchers and scientists are focusing on developing effective, stable, and practicable methods for hydrogen sulfide removal from gaseous streams. Various solid materials have been developed to capture H_2S from a number of industrial gas effluent streams (Wang et al., 2008; Katoh et al., 1995; Jianwen et al., 2011; Liang et al., 2011; Li et al., 2007; Feng et al., 2009; Nguyen-Thanh et al., 2005). Several commercial techniques are available for the removal of H_2S, including aqueous NaCl (Duan et al, 2007), iron-based sorbents (Xie et al, 2010; Wang et al, 2012), activated carbon (Nguyen-Thanh et al, 2005), Fe_2O_3, metal oxides (Ko et al, 2005; Van Dijk et al, 2011), and removal of H_2S using aqueous red mud (Pandey et al, 2003) which is a caustic waste product of aluminum industry (Sahu et al, 2011). Iron (Fe) is an excellent oxidizing agent to convert H_2S to elemental sulfur (S). During the1960s, intensive researches focused on increasing the solubility of elemental Fe^{3+} in aqueous solutions and they realized that Iron is an excellent oxidizing agent to convert H_2S to elemental sulfur (S^0) (Heguy and et al, 2003). However, there is always research for the development of effective and low-cost method.

The importance of health, safety and environment at refinery area needs efforts that based on scientific information to avoid air, land and water pollution. Toxic and hazardous byproducts of petroleum and the waste water are to be in investigated to minimize environmental problems. Hence, waste water tests must be of high accuracy and feedback evaluation and recommendations should be considered.

Of the impurities which usually are found in oil fractions are sulfur compounds. In light hydrocarbon fractions, sulfur is usually in the form of hydrogen sulfide (H_2S), carbonyl sulfide (COS), carbon disulfide (CS_2) and mercaptan (RSH). These sulfur contaminates not only make odor in oil fraction but also during the combustion they will be oxidized and make the air polluted. Furthermore, corrosion problems of these compounds are important and have undesirable effects on downstream catalysts.

Sulfur compounds of oil fraction are:

- LPG, contains H_2S (usually at high concentration) and methyl and ethyl mercaptans.
- NGL, contain H_2S and methyl and ethyl mercaptans and sometimes may have CS_2 and COS.
- Gasoline, contains H_2S plus light and heavy mercaptans, and even Butyl mercaptan. For example hydrogenated and debutanized light gasoline have trace H_2S and / or produced gasoline from hydrocracking has also trace H_2S and a considerable amount of mercaptans.

Refinery flue gas is generally a mixture of gases coming from several different units within the refinery. The quantity and quality of gases in the refinery flue gas depends on refining capacity, severity of cracking unit and the quality of

refinery crude. refinery flue gas has been recognized as one of the major sources of sulfur emissions from refineries.

In KRC normal processing capacity of refinery flue gas incinerator is 2.401t/h. Refinery flue gas is split into two streams to enter the burner of refinery flue gas incinerator. One stream comes from sour water stripping (SWS) (1670 t/h) , the other path comes from Resid Fluid Catalytic Cracking RFCC (594t/h) and Delayed Coking Unit DCU (137t/h) units passes through refinery flue gas knockout drum for liquid separation, then each stream enters the burner separately. The flow rate and composition of sour refinery flue gas is shown in the Table 1.1

Table 1.1 Khartoum Refinery Flue Gas

Unit	H_2S kg/h	NH_3 kg/h	CO_2 kg/h	H_2O kg/h	Total kg/h
SWS	625	620.6	8.4	416	1670
RFCC	356.4	237.6	-	-	594
DCU	82.2	54.8	-	-	137
Total	**1036.6**	**913**	**8.4**	**416**	**2401**

The refinery flue gas streams contains varying amounts of hydrogen sulfide, ammonia and, in certain instances, carbon dioxide. The presence of each of the before-mentioned contaminants, as well as the amounts of same in a refinery flue gas stream will vary depending on the nature of the feed stock to the refinery and the specific refinery processing operations from which the refinery flue gas streams are recovered for use as a suitable feed in practicing the process of the present treatment.

The refinery flue gas incinerator incinerates refinery flue gas to convert H_2S into S_2O and ammonia into nitrogen, the vent gas is emitted directly to atmosphere.

The incinerator works 1350～1400℃, and the tail gas discharged to the atmosphere by stack.

$$H_2S + 3/2O_2 \rightarrow SO_2 + H_2O \quad (1.1)$$

$$2NH_3 + 3/2O_2 \rightarrow 3H_2O + N_2 \quad (1.2)$$

The acid gas from hydrotreating and hydrocracking essentially contains H_2S and ammonia. The gas treating pressures and H_2S specifications vary for individual applications.

The refinery flue gas emissions can cause damage to the environment due to the presence of the pollutant hydrogen sulfide, which is harmful to human beings and animals. At lower concentrations, this gas has an unpleasant odor, at higher concentrations; it can be life-threatening. The recommended industrial exposure limits are from 8 to 10 ppm (Horikawa, 2001).

Hydrogen sulfide is a colorless, flammable, and highly toxic gas which characteristic rotten-egg odor. The threshold value of odor is only several ppb. Therefore, H_2S is one of the malodorous air pollutants in the community. Hydrogen sulfide is a naturally occurring component of crude oil and natural gas. Petroleum oil and natural gas are the products of thermal conversion of decayed organic matter (called kerogen) that is trapped in sedimentary rocks. High-sulfur kerogens release hydrogen sulfide during decomposition, and this H_2S stays trapped in the oil and gas deposits. Hydrogen sulfide is produced in nature by anaerobic decomposition of sulfur-containing organic and inorganic matter. In recent years, industrial activities have contributed substantially to H_2S emissions through hydrogenation and hydro desulfurization processes. Hydrogen sulfide enters the refinery in the crude oil and is removed during the refining process to ensure no H_2S is present in the finished

product or emitted to air. Any hydrogen sulfide present in fuel gas is burnt in the furnaces.

The combustion of H_2S resulting from the oil refining operations directly in the gas incinerator before cleaning the refinery flue gas leads to the production of sulphur dioxide (SO_2), which is another toxic pollutant and a major contributor to acid rain.

Hydrogen sulfide emissions from oil and gas development may pose a significant human health risk, as the studies discussed below reveal. Workers in the oil and gas industry are trained to recognize and respond to high-concentration accidental releases of H_2S. The American Petroleum Institute (API), an oil and gas industry technical organization publishes recommendations for practices that help prevent hazardous H_2S concentrations from occurring in the workplace. People living near oil and gas development sites may be chronically exposed to much lower, but nonetheless dangerous ambient H_2S levels, as well as to accidental high concentration releases. Considerable amounts of hydrogen sulfide are emitted from industrial activities such as petroleum refining (Henshaw, 1999), pulp and paper manufacturing (Wani, 1999), food processing, livestock farming (Chung, 2001), biogas production (Schieder, 2003), and natural gas processing (Kim, 1992). No matter how it is produced, H_2S poses a serious health risk, not to mention an obnoxious odor. The human nose can detect the "rotten egg" odor of H_2S at a concentration of 0.4 parts per billion (ppb). The maximum allowable exposure for prolonged periods is 10 parts per million (ppm). Hydrogen sulfide is a highly toxic and flammable gas. A 5-minute exposure to 1,000 ppm concentration in air can be fatal to humans (Patnaik, 1999). The symptoms are headache, nausea, nervousness, cough, eye irritation, and insomnia. High doses can produce unconsciousness and

respiratory paralysis. Hydrogen sulfide forms explosive mixtures with air; the LEL and UEL are 4.3 and 45.0% by volume in air, respectively. Its autoignition temperature is 260°C. Its reaction with soda-lime in oxygen can be explosive. Reactions with strong oxidizing agents can progress to incandescence.

As the Sudan concerns about climate changes, our vulnerable ecosystems, on which the vast majority of the population depends, already suffer from current droughts, over-use of marginal lands, and dominance of bio-mass use for energy. Even small changes in climate will have adverse effects on crops, grassland, and forest production because of the fragility representing emissions from oil industry. Thus, despite the fact that Sudan contributes an extremely small amount of hazardous air pollutants to the atmosphere compared to the rest of the world. This thesis tries to identify opportunities for mitigating emissions or enhancing sinks of (Khartoum Refinery) air pollutants.

The removal of hydrogen sulfide from the refinery flue gas stream depends on various factors e.g., raw feed composition, treated gas quality, economic analysis of the process of desulphurization, and the corrosion problems in existing operational units. The gaseous streams, therefore, require desulphurization through a techno-economically- viable process in order to meet the product purity requirement, to generate clean fuels (in case of gaseous fuels) and also to conform to the stringent sulfur emission standards (Pandey, 2003).

The two main purposes for removing H_2S from refinery flue gas streams are to purify refinery flue gas and to achieve air pollutants control. For these goals, numerous methodologies have been developed, and more than half a dozen have been demonstrated commercially.

When a choice is possible, preference is given to solvents with high solubility's for the target solute and high selectivity for the target solute over the other species in the gas mixture. A high solubility reduces the amount of liquid to be circulated. The solvent should have the advantages of low volatility, low cost, low corrosive tendencies, high stability, low viscosity, low tendency to foam, and low flammability. Since the exit gas normally leaves saturated with solvent, solvent loss can be costly and can cause environmental problems. The choice of the solvent is a key part of the process economic analysis and compliance with environmental regulations.

The choice of a liquid absorbent depends on the concentrations in the feed gas mixture and on the percent removal desired. I f the impurity concentration in the feed gas is high, perhaps ten to fifty percent, we can often dissolve most of the impurity in a nonvolatile, nonreactive liquid. Such a nonreactive liquid is called a physical solvent. If the impurity concentration is lower, around one to ten percent, a liquid capable of fast, reversible chemical reaction with the impurity is used. Such a reversibly reactive liquid is referred to as a "chemical solvent." If the impurity concentration in the feed is still lower, it is a liquid that reacts irreversibly is employed, and this is an expensive alternative that may produce solid waste.

There are many kinds of process that stated in literature for removing H_2S gas (Davidson, 1995; Kohl, 1985; Horikawa, 2001) which can be divided into two methods; those are chemical absorption and adsorption. Chemical absorption is an absorption which is followed by chemical reaction where the absorbed gas is reacted with the reactant in liquid phase, while adsorption is adsorption on the surface of solid particle which is called adsorbent. Chemical processes are available for the removal of H_2S from gaseous streams. Most of the processes use gas-liquid

contactors in which H_2S is absorbed into a complexing reagent to give either another dissolved sulfide containing component (e.g. alkanol-amine or hydroxide based processes) or elemental sulfur as a precipitate (Wubs et al, 1993). However, these have high capital costs, demand large energy inputs and result in the generation of secondary hazardous wastes (Pandey et al, 1999).

In case of H_2S gas, the adsorbent which commonly used is ZnO that reacts H_2S to give ZnS. Mostly, this process is only removing H_2S from the refinery flue gas, however it does not change the gas becomes a more stable and useful product. Many commercial processes are available for the removal of hydrogen sulfide from gaseous streams. Most of these processes use gas-liquid contactors in which the hydrogen sulfide is contacted with a reagent to give either another dissolved sulfide-containing component (for example, hydroxide based processes (sodium hydroxide),or alkanol-amine) or elemental sulfur as a precipitate (for example ferric sulfate).

The reaction rate seems to be independent of the ionic strength, and the pH dependency found can possibly be ascribed to the reactive species being hydroxy ferric chelate (DeBerry, 1991). Other systems in which hydrogen sulfide is converted to sodium sulfide by (D.Mamrosh, 2008), Scrubbing of hydrogen sulfide using sodium hydroxide solution is a well-established technology. Also, (Bontozoglou, 1993), Simultaneous absorption of H_2S and CO_2 in NaOH solutions: Experimental and numerical study of the performance of a short-time contactor.

The former authors absorbed hydrogen sulfide into an aqueous solution of ferric chloride $FeCl_3$ and found the reaction to be first-order in both ferric iron and hydrogen sulfide. Also, a dependency on the concentration of chloride ions was observed.

For the acidophilic process the kinetics of the reactive absorption of H_2S by aqueous $Fe_2(SO_4)_3$ solution has been studied and found to be secound order with respect to both H_2S and total Fe^{3+}concentration (Ebrahimi et al, 2003). This implies that the absorption rate of H_2S linearly increases with total $Fe_2(SO_4)_3$ concentration with a maximum at about 0.5 mol Fe^{3+}/l. However the studies of the biological regeneration stage indicated that maximum iron concentration applied in the integrated process is limited by biological regeneration stage to about 0.2M (Ebrahimi et al, 2005).

The desulfurization of gas streams using aqueous ferric sulfate solution $Fe_2(SO_4)_3$ as washing liquor is studied (Z. Gholami, 2009). Apart from sulfur, only H_2O is generated in the process, and consequently, no waste treatment facilities are required. A distinct advantage of the process is that the reaction of H_2S with is so rapid and complete that there remains no danger of discharging toxic waste gas. Ferric sulfate is used in many different municipal and industrial applications. In gaseous streams treatment and wastewater treatment operations, it is used as coagulants or flocculants for water clarification, odor control to minimize hydrogen sulfide release, for phosphorus removal, and as a sludge thickening, conditioning and dewatering agent. Ferric Sulfate is a low cost iron salt. If the dose efficiency is similar, ferric sulfate will usually be more cost effective than other coagulant salts. Ferric Sulfate can work better over a wider pH range than alum, so pH correction is not critical to good performance. Ferric Sulfate contains free acid which can make it better for wastewater treatment where low pHs are required (i.e. to remove fats and oils or high colour) Ferric Sulfate is also less corrosive to most metals and fittings than ferric chloride. For an aqueous solution containing ferric sulfate $Fe_2(SO_4)_3$ have been applied for H_2S treatment (Bedell,1988), H_2S is absorbed in an $Fe_2(SO_4)_3$ and

converted into elemental sulfur while $Fe_2(SO_4)_3$ is reduced to Fe_2SO_4 . The pH dependency found by these authors was ascribed to the reactive species, reportedly by the monohydroxy form of ferric iron. In accordance with (DeBerry, 1990), the observed reaction rate was independent of the ionic strength of the solution. (Broekhuis, 1992), stated that the H_2S conversion process becomes sulfur is by reaction with zinc natrium ferric. While Hix and Lynn steadied the absorption process of H_2S gas into SO_2 solution in polyglycol ether. (Horikawa,2004) proposes removing process of H_2S gas from biogas with changing it to become sulfur (S) applies absorption process into soluble chelate iron from Fe-EDTA. The advantage of these processes is the conversion of a pollutant into a chemical product or at least a solid residue that can be disposed of easily and safely.

(DeCoursey, 1982), have studied the effect of reversibility of the chemical reactions and unequal diffusivities on the enhancement of mass transfer due to a second-order gas-liquid chemical reaction. (Glasscock, 1993) used a modified form of the expression developed by DeCoursey for the enhancement factor to model the enhancement of the mass transfer of CO_2 when it is chemically absorbed in aqueous alkanolamine solutions.

The earlier researchers had done many theoretical and experimental studies about other chemical absorption system, such as, (Astarita, 1963; Glasscock,1993; Linek,1990; Qian,1995; Sanyal,1988; and Xu,1992).This theoretical study first estimated level of improvement the rate of absorption with existence of reaction in liquid phase (called as enhancement factor) based on assumption of interface mass transfer model applied . Some mass transfer models stated in literatures, such as, Film model (Whitman, 1923), Penetration model (Higbie, 1935), Dancwerts model (1951), Film Penetration model (Toor, 1958), Eddy diffusivity model (King, 1966;

Menez, 1974). (Brian, 1961), used penetration model to estimate enhancement factor for gas absorption followed by second order irreversible reaction numerically. (Hikita, 1964), studied absorption process followed by general irreversible reaction analyticall. (Altway, 1995), studied penetration model for absorption followed by general irreversible reaction numerically. (Hix, 1991) studied influence of dissolved volatility reactant on mass transfer rate by taking an example H_2S gas absorption into SO_2 solution in polyglycol ether. (Ubaidi, 1990) and (Bhattacharya, 1997), studied enhancement factor of gas absorption followed by second order irreversible reaction under non isothermal condition using film model. While (Bhat, 1997), used Penetration model analyzing gas absorption process followed by reversible reaction under non isothermal condition.

One of the most important information which needed to estimate mass transfer enhancement of gas-liquid on gas absorption followed by chemical reaction is kinetic data. Many researchers have been done to understand the kinetic reaction of gas-liquid. (Neumann, 1986), studied kinetic reaction of H_2S and SO_2 in organic solution. (Xu, 1992), studied kinetic reaction of CO_2 gas absorption into active MDEA solution. (Xu, 1993), studied kinetic reaction of CO_2 gas with 2-Piperedine ethanol solution. (Wubs, 1993), had studied kinetic reaction of gas absorption into chelat Fe-EDTA solution. (Asai, 1990) studied kinetic reaction of H_2S gas absorption into Ferric Sulfate solution. (Hikita, 1975), studied kinetic reaction of chlorine gas absorption into acidic Ferrous Chloride solution.

Hydrogen sulfide in the exhaust could be controlled by absorption, absorption, or by combustion processes. Because H_2S could be converted to SO_2, which is also an air pollutant, in combustion process, it is not the best way to remove H_2S by combustion.

Hydrogen sulfide could be effectively removed from gas mixture by adsorption because it is soluble in some solutions. Since H_2S is an acidic gas, it dissolves easily in basic solution. Absorption process of acidic gas is even more quickly and completely in strong basic solution.

The equipments used to absorption followed by chemical reaction are mainly tray (sieve tray column) and packed columns are most widely used for gas liquid contacting- namely for gas absorption. The process which occurred on gas absorption followed by chemical reaction in sieve tray column and packed column is quite complex, so that, to design and to analyze the performance of equipments needs to use numerical methods. The removal of the acid gas component H_2S from acid gas streams is often achieved by means of absorption into an aqueous hydroxide based processes (sodium hydroxide) and aqueous alkanolamine solution. These processes are usually carried out in sieve tray columns (Riesenfeld, 1979), operated in a countercurrent mode. In many cases, however, only the H_2S has to be removed and particularly for these situations selective gas treatment processes are required. (Danckwerts, 1966), presented design procedure for absorption followed by chemical reaction in packed column. (Kasiri, 2008), developed the model and simulation of sieve tray column for H_2S and CO_2 absorption using alkanolamine solutions. (Savitri, 2001), developed packed column model for absorption followed by second order irreversible reaction on non isothermal condition.

1.5 Objectives

1. To manage the air pollution resulting from flaring combustion of H_2S in Khartoum Refinery and to demonstrate that H_2S can be efficiently removed from a refinery flue gas stream by using $Fe_2(SO_4)_3$ solution.

2. To investigate the absorption process of H_2S in a sieve tray column under different operating conditions and its impact on the removal of H_2S as well as determination of operational conditions that would maximize the amount of hydrogen sulfide removed from the refinery flue gas.

3. To design a sieve tray column, and to establish the stability of the column by hydrodynamic phenomena of entrainment, weeping and flooding.

CHAPTER TWO

2. LITERATURE REVIEW

2.1 Introduction:

This chapter gives an overview of the process of absorption and the development of the theoretical models of a gas-liquid interface mass transfer. In this chapter, a steady state model was developed for contactor to analyze the simultaneous absorption of H_2S into the aqueous ferric sulfate solution $Fe_2(SO_4)_3$.

Processes have been known for producing sweet gas streams from refinery flue gas stream and for producing elemental sulfur from refinery flue gas stream. In this process contacting the refinery flue gas stream with a fresh aqueous ferric sulfate solution in continuous concurrent interfacial two-phase flow, such as a thin film contact apparatus, separating the gas phase into a sweet gas substantially free of hydrogen sulfide, and recovering the aqueous phase as a ferric sulfate free solution of ferrous sulfate. A mathematical model is developed here to describe the simultaneous absorption of H_2S from refinery flue gas using $Fe_2(SO4)_3$ solution. The bed is divided into small volume element (dv) and the two-film theory of mass transfer is applied on each element. In this chapter, is develop numerical solution for a set of ordinary differential , the most widely used methods of integration for ordinary differential equations are Runge-Kutta methods and Collocation Method.

2.1 Gas absorption:

Gas absorption, is a unit operation in chemical engineering whereby a soluble component of a gas mixture is dissolved in a liquid. There is mass transfer of the component of gas from the gas phase to the liquid phase and the solute transferred is absorbed by the liquid, gas absorption is not limited only to the process industries

alone but also in the biological process whereby oxygen from air is absorbed in the blood when we breathe. However, gas absorption will only be restricted to industrial applications in this work. Absorption is widely used in the removal of CO_2 and H_2S from natural gas or gas synthesis in amine solution or alkaline salt. Absorption comes either in physical or chemical process and the rate of absorption of gas is enhanced in the later than the former. Desorption or stripping is the reverse process of absorption when the dissolved gas is recovered from a solution for reuse and regenerates the solvent.

Absorption is a major chemical engineering unit operation that involves bringing contaminated effluent gas into contact with a liquid absorbent, a key aspect in an absorption system is the contact between gas and liquid phase. Gas absorption is a unit operation where one or more components in a effluent gas are selectively dissolved in a liquid (solvent). Key terms used when discussing the absorption process include:

• ***Absorbent:*** the liquid, usually water mixed with neutralizing agents, into which the contaminant is absorbed.

• ***Solute:*** the gaseous contaminant being absorbed, such as H_2S, and so forth.

• ***Carrier gas:*** the inert portion of the gas stream, usually flue gas, from which the contaminant is to be removed.

• ***Interface:*** the area where the gas phase and the absorbent contact each other.

• ***Solubility:*** the capability of a gas to be dissolved in a liquid.

Selection of solvent when choice is possible, preference is given to liquids with high solubility for the solute; a high solubility reduces the amount of solvent to be circulated. The solvent should be relatively nonvolatile, inexpensive, noncorrosive, stable, nonviscous, nonfoaming, and preferably nonflammable. Since

the exit gas normally leaves saturated with solvent, solvent loss can be costly and may present environmental contamination problems. Thus, low-cost solvents may be chosen over more expensive ones of higher solubility or lower volatility.

The absorption may either be a purely physical phenomenon or involve a chemical reaction, such as the reaction between H_2S and aqueous ferric sulfate solution $Fe_2(SO_4)_3$. The separation of components in a gaseous mixture by absorption is based on the difference in solubility of the components in a solvent (absorbent). Gas absorption is separation processes used in the chemical industry and for environmental control. Absorption involves no change in the chemical species present in the system. Absorption is used to separate gas mixtures, remove impurities, or recover valuable chemicals. Absorbers are normally used with strippers to permit regeneration (or recovery) and recycling of the absorbent.

Two methods of operation in gas absorption exist, which are counter-current and co-current operations. In co-current absorption, there is no minimum liquid-to-gas ratio and it is less efficient than counter-current operation. The advantage of concurrent operation is the lack of flooding limitation, and high gas flow rate can be used which reduces the required column diameter.

Most absorption operations are carried out in counter current flow processes, in which the gas flow is introduced in the bottom of the column and the liquid solvent is introduced in the top of the column.

Several processes have been proposed and studied for the removal of hydrogen sulfide from refinery flue gas. One of the most important gas purification techniques is absorption. It involves the transfer of hydrogen sulfide from the gaseous to the liquid phase through the phase boundary. At the process of absorption of gas into liquid, gas principally is absorbed through mechanism of diffusion

(molecular & turbulent) and convection into liquid through interface. Hydrogen sulfide absorption may be physical when merely dissolved in the absorbing solvent such as water, or it may be chemical when hydrogen sulfide reacts with the absorbing solution such ferric sulfate solutions.

Physical absorption: In this type of process, the component being absorbed is more soluble in the liquid absorbent than other components of the gas stream. Physical absorption occurs in situation where there is no chemical reaction between the solute and the solvent (absorbent) such as the use of water and hydrocarbon oils as solvent. It involves the transfer of mass that takes place at the interface between the liquid and the gas and the rate at which the gas diffuses into a liquid. This type of absorption depends on the solubility of gasses in a solvent, the pressure and the temperature. The equilibrium concentration of the absorbate in the liquid phase is strongly dependent on the partial pressure in the gas phase. (Smith, 2005).

Chemical absorption: chemical absorption or reactive absorption is a chemical reaction between the absorbed and the absorbing substances. However, in situation where aqueous solutions are used as absorbent, absorption are accompanied by chemical reaction in the liquid phase. Absorption with chemical reaction involves the reaction in the liquid phase to vehemently remove a solute from a mixture of gas. It has the capacity to increase the absorption coefficient of the liquid-film compared to an ordinary physical absorption. Reaction in the liquid phase greatly increases the driving force for mass transfer since there is reduction in the equilibrium partial pressure of the solute over the solution. Hence, the equilibrium partial pressure will be zero if the absorption reaction is irreversible. This type of absorption depends upon the stoichiometry of the reaction and the concentration of its reactants. The nature of chemical reaction influences the actual rate of absorption and the process

occurred by chemical reaction between the dissolved gas and the liquid, (Kohl, 1997; Smith, 2005).

2.2 Mass Transfer Models at Gas Liquid Interface:

Theoretical models of a gas-liquid interface mass transfer have been presented in the literature. All of these are based on the hypothesis that the velocity gradient in the liquid is zero. In fact, it can be shown that, in a majority of cases, the ratio of the rates of mass transfer in the liquid phase with and without chemical reaction does not depend on the particular hydrodynamic condition of the liquid.

The basic equation for diffusion accompanied by chemical reaction will be given here for the one-dimensional case only. Besides, the concentration of solute is uniform over any plane perpendicular to the x-axis, and transport of the solute only takes place in the x-direction .The flux F of transfer of diffusion across unit area of a plane perpendicular to the x-axis at a given moment is

$$N = -D \frac{\partial C}{\partial x} \tag{2.1}$$

Where $\frac{\partial C}{\partial x}$ is the concentration gradient at x at the given moment.

Chemical engineering processes always proceed under extremely complex hydrodynamic conditions. As a result of this situation and depending on weighing the hydrodynamic conditions of each process many theories (models) of mass transfer appeared.

2.2.1 Film Model:

This is first model proposed to describe the region around the gas-liquid interface. This is the simplest and oldest model which has been proposed for the description of mass transport processes is the so-called film theory. It was suggested by (Whitman, 1923) and first applied by (Hatta, 1928) for absorption with chemical reaction.

The film theory is based on the assumption that when two fluid phases are brought in contact with each other. The assumes that on either side of the interface exists a stationary fluid film thickness δ.

These films are free from convection currents and flow in them is laminar and parallel to the surface and they offer the only resistance to mass transfer. Transport of matter takes place through these stagnant films by simple molecular steady state diffusion. Beyond the thin layers the turbulence is sufficient to eliminate concentration gradients. Figure 2.1 shows the film model of mass transfer for the case of absorption of a gas in a liquid. The interfacial region is idealized as a hypothetical "unstirred layer". The constant partial pressure P_A implies no resistance to mass transfer in the gas phase

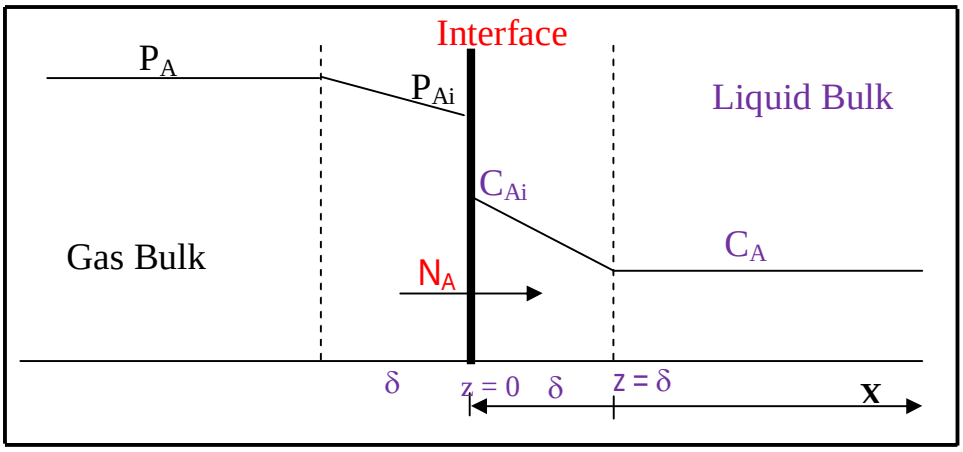

Figure 2.1 The Two film model of mass transfer

Conditions in the bulk of the phases a part from the film regions remain extremely constant. When applied to a process of liquid side controlled absorption, the film theory model allows the evaluation of the rate of absorption per unit area of surface R:

$$R = -D_A\left(\frac{\partial C_A}{\partial x}\right)_{X=0} \qquad (2.2)$$

The concentration gradient of A between x = 0 and x = δ is constant within the stagnant film; if no generation takes place (generation does take place when a chemical reaction is present):

$$\left(\frac{\partial C_A}{\partial x}\right)_{X=0} = \frac{C_{Ai} - C_{AL}}{\delta} \tag{2.3}$$

The absorption coefficient for physical absorption k_L ,defined as:

$$k_L = \frac{R}{(C_{Ai} - C_{AL})\ \delta} \tag{2.4}$$

substitution Eq (2.4) into Eq (2.3)

$$-\left(\frac{\partial C}{\partial x}\right)_{x=0} = \frac{R}{k_L\ \delta} \tag{2.5}$$

substitution Eq(2.5) into Eq (2.2)

$$R' = D_A \frac{R'}{k_L\ \delta}$$

$$\boxed{k_L = \frac{D_A}{\delta}} \tag{2.6}$$

Thus the mass transfer coefficient can be calculated from the film theory if the diffusivity and the film thickness are known. Whereas the former can possible be obtained from the literature or may be estimated by using a suitable correlation.

2.2.2 Mathematical Interpretations of Surface-Renewal Model:

It is becoming apparent that for the real understanding of the mass transfer processes the hydrodynamic behavior of fluids near the interface and the behavior of eddies as they approach the interface should be considered in depth. The surface renewal model suggests that every surface element will have been exposed for a different time period, and will therefore be absorbing from the gas phase at a different specific rate. There have been several attempts to describe this model mathematically. The most commonly used mathematical models are Higbie and Higbie-Danckwerts

➢ Higbie Model (1935):

In 1935 Higbie proposed that the gas-liquid interface is made up of small liquid elements which are continuously brought to the surface from the bulk of the liquid interior having the liquid local mean composition. These surface elements stay for the same period θ at the interface - exposed to the gas- before being replaced by

other fresh elements from the liquid bulk. During the expourse time θ , the elements absorb the same amount of gas if they were stagnant and infinitely deep. The mechanism of this model is described in Figure 2.2.

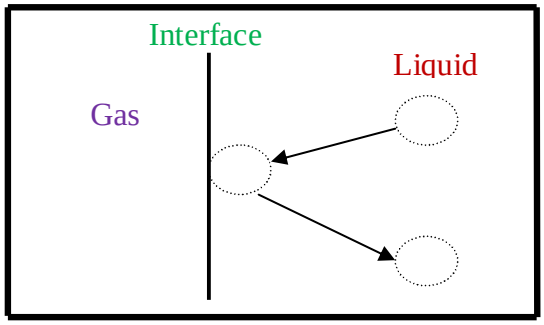

Figure 2.2 The Surface Renewal model of mass transfer

Mass transfer is accomplished by unsteady state molecular diffusion process in the various liquid elements at the surface. Conditions of steady state absorption are achieved only if the phase contact time is such longer than the penetration period. Solving the unsteady state differential equation:

$$D_A\left(\frac{\partial^2 C_A}{\partial x^2}\right)=\frac{\partial C_A}{\partial t} \tag{2.7}$$

Where t is the time elapsed from the moment the surface element considered has been brought to the surface. The appropriate initial and boundary conditions are:

Initial condition $C_A = C_{AL} \quad x>0 \quad t=0$ (2.8.a)

Boundary condition 1 $C_A = C_{Ai} \quad x=0 \quad t>0$ (2.8.b)

Boundary condition 2 $C_A = C_{AL} \quad x\to\infty \quad t>0$ (2.8.c)

The initial implies that in a fresh liquid element coming from the bulk, the concentration is uniform and is equal to the bulk concentration. The boundary condition 1 assumes that "interfacial equilibrium" exists at all time. The last condition means that if the contact time of an element with the gas is small, the 'depth of penetration' of the solute in the element should also be small and effectively the element can be considered to be of 'infinite thickness' in a relative sense. Equation (2.7) subject to the initial and boundary condition (2.8), can be solvent. The

integration of equation (2.7) satisfying initial conditions (2.8) is using Laplace transform method.

$$\frac{C_A - C_{AL}}{C_{Ai} - C_{AL}} = erfc\left[\frac{x}{2\sqrt{D_A t}}\right] \tag{2.9}$$

$$R = -D\left(\frac{\partial C_A}{\partial x}\right)_{X=0} \tag{2.2}$$

from Eq(2.9)

$$-\left(\frac{\partial C_A}{\partial x}\right)_{x=0} = (C_{Ai} - C_{AL})\left(\frac{-2}{\sqrt{\pi}} e^{\frac{x}{2\sqrt{D_A t}}}\right)\left(\frac{1}{2\sqrt{D_A t}}\right)_{x=0} \tag{2.10}$$

substitution x = 0 into Eq(2.10)

$$-\left(\frac{\partial C_A}{\partial x}\right)_{x=0} = (C_{Ai} - C_{AL})\left(\frac{-2}{\sqrt{\pi}}\right)\left(\frac{1}{2\sqrt{D_A t}}\right)_{x=0} = (C_{Ai} - C_{AL})\left(\frac{1}{\sqrt{D_A \pi . t}}\right)_{x=0} \tag{2.11}$$

substitution Eq(2.11) into Eq(2.2)

$$R = D_A(C_{Ai} - C_{AL})\left(\frac{1}{\sqrt{D_A \pi . t}}\right) = (C_{Ai} - C_{AL})\sqrt{\frac{D_A}{\pi . t}} \tag{2.12}$$

Total amount of gas absorbed for unit interfacial surface area during elapsed time t is

$$Q = \int_0^t R.dt = (C_{Ai} - C_{AL})\int_0^t \sqrt{\frac{D_A}{\pi . t}} dt = 2(C_{Ai} - C_{AL})\sqrt{\frac{D_A . t}{\pi}} \tag{2.13}$$

Therefore, the average of absorption flux over exposure time θ, can be attained as follows:

$$R' = \frac{Q(\theta)}{\theta} = \frac{2(C_{Ai} - C_{AL})\sqrt{\frac{D_A . \theta}{\pi}}}{\theta} = 2(C_{Ai} - C_{AL})\sqrt{\frac{D_A}{\pi\theta}}$$

$$R' = k_L(C_{Ai} - C_{AL}) = 2(C_{Ai} - C_{AL})\sqrt{\frac{D_A}{\pi\theta}} \tag{2.14}$$

and by definition the liquid side mass transfer coefficient is :

$$\boxed{k_L = 2\sqrt{\frac{D_A}{\pi . \theta}}} \tag{2.15}$$

The above equation shows that the mass transfer coefficient is proportional to the square root of diffusivity. Although this is again not is conformity with experimental observations in general this is definitely an improvement over the film theory for a more realistic visualization. Here the contact time is the model parameter like the film thickness δ in the film theory.

➢ Danckwerts Model (1967):

Danckwerts' proposed a model based on the concept of continues replacement of fluid elements adjacent to the interface by new elements reaching the surface as a result of turbulent mixing. He rejected the hypothesis of equal life for surface elements, as in the penetration model. He assumed that (i) the liquid elements at the interface are being randomly replaced by fresh element from the bulk, (ii) at any amount each of the liquid elements at the surface has the same probability of being replaced by a afresh element, (iii) unsteady state mass transfer occurs to an element during its stay at the interface.

The model parameter is the fractional rate of surface renewal s, Danckwerts derived the age distribution function ψ(t) as : $\psi(t) = s\, e^{-st}\, dt$

Where s is the fraction of the surface area renewed in unit time.

If the hypothesis of equal life for all surface elements of liquid is rejected, the average rate of absorption is given by:

$$R' = \int_0^{t=\infty} R\psi(t)dt = s\int_0^{\infty} R.e^{-S\theta}dt \qquad (2.16)$$

substitution the value of $R = (C_{Ai} - C_{AL})\sqrt{\frac{D_A}{\pi t}}$ from Equation (2.12) into Eq (2.16)

$$R' = s(C_{Ai} - C_{AL})\sqrt{\frac{D_A}{\pi}}\int_0^{\infty}\frac{e^{-S\theta}}{\sqrt{t}}dt \qquad (2.17)$$

we used the gamma function (Γ) integration:

and $\Gamma(0.5) = \sqrt{\pi}$

$$\int_0^{\infty} X^n e^{\lambda X} dX = \frac{1}{\lambda^{n+1}}\Gamma(n+1) \qquad (2.18)$$

from Equation(2.17) . $\lambda = s,\quad X = t \quad and \quad n = -0.5$, substitution this values into Equation (2.18)

$$R' = (C_{Ai} - C_{AL})s\sqrt{\frac{D_A}{\pi}}\int_0^{\infty} t^{-0.5}e^{-st}.dt = (C_{Ai} - C_{AL})s\sqrt{\frac{D_A}{\pi}}\left[\frac{1}{s^{(-0.5+1)}}\Gamma(-0.5+1)\right]$$

$$(C_{Ai} - C_{AL})s\sqrt{\frac{D_A}{\pi}}\left[\frac{1}{\sqrt{s}}\Gamma(0.5)\right] = (C_{Ai} - C_{AL})\sqrt{s}\sqrt{\frac{D_A}{\pi}}.\sqrt{\pi} = (C_{Ai} - C_{AL})\sqrt{D_A s}$$

$$R' = k_L(C_{Ai} - C_{AL}) = (C_{Ai} - C_{AL})\sqrt{D_A s} \qquad (2.19)$$

and, therefore, the equation for the mass transfer coefficient according to the Danckwert's theory is as follows :

$$\boxed{k_L = \sqrt{D_A s}} \tag{2.20}$$

2.2.3 Film Penetration Model (Toor and Marchello, 1958):

(Toor,1958) combined features of the film , penetration , and surface renewal theories to develop a film-penetration model , which predicts a dependency of the mass transfer coefficient k_L , on diffusivity, that varies from $\sqrt{D_A}$ *to* D_A.Their theory assumes that the entire resistance to mass transfer resides in a film of fixed thickness δ. Eddies move to and from the bulk fluid and this film. Age distribution for time spent in the film is of the Higbie or Danckwerts type.

Fick's second law still applies, but the boundary conditions are now

$$D_A\left(\frac{\partial^2 C_A}{\partial x^2}\right) = \frac{\partial C_A}{\partial t} \tag{2.7}$$

$$\left.\begin{array}{lll} t = 0 & C_A = C_{AL} \ for & 0 \le x \le \infty \\ x = 0 & C_A = C_{Ai} \ for & t > 0 \\ x = \delta & C_A = C_{AL} \ for & t > 0 \end{array}\right\} \tag{2.21}$$

Infinite-series solution are obtained by the method of laplace transform. The rate of mass transfer is then obtained in the usual manner by applying Fick's first law $R = -D\left(\frac{\partial C_A}{\partial x}\right)_{X=0}$ At the fluid-fluid interfaces. For small time, the solution, given as:

$$R = (C_{Ai} - C_{AL})\left(\frac{D_A}{\pi\theta}\right)^{1/2}\left[1 + 2\sum_{n=1}^{\infty}\exp\left(-\frac{n^2\delta^2}{D_A\theta}\right)\right] \tag{2.22}$$

and converges rapidly. For large time,

$$R = (C_{Ai} - C_{AL})\left(\frac{D_A}{\delta}\right)\left[1 + 2\sum_{n=1}^{\infty}\exp\left(--n^2\pi^2\frac{D_A\theta}{\delta^2}\right)\right] \tag{2.23}$$

The average absorption rate is given by:

$$R' = s\int_0^{\infty} R.e^{-S\theta}d\theta \tag{2.16}$$

Substitution value of R from Equation (2.22) and (2.23) for small and large time, we can write two equivalent series solution, which converge at different rates.

For small time, the solution, gives

$$R = k_L (C_{Ai} - C_{AL}) = (C_{Ai} - C_{AL})\left(sD_A\right)^{1/2}\left[1 + 2\sum_{n=1}^{\infty} \exp\left(-2n\delta\sqrt{\frac{s}{D_A}}\right)\right] \quad (2.24)$$

For large time, the solution, gives

$$R = k_L (C_{Ai} - C_{AL}) = (C_{Ai} - C_{AL})\left(\frac{D_A}{\delta}\right)\left[1 + 2\sum_{n=1}^{\infty} \exp\left(\frac{1}{1 + n^2\pi^2 \frac{D_A}{s\delta^2}}\right)\right] \quad (2.25)$$

Equations (2.24 and 2.25) contains the variable s instead of the contact time, for high rate of surface replaced,($s.\delta^2/D_A$), equation (2.24) reduces to Danckwerts's equation (Eq.(2.26)). For low rates of surface replacement, equation (2.25) reduces to the film equation (Eq. (2.27)).

$$R = (C_{Ai} - C_{AL})\sqrt{D_A s} \quad (2.26)$$

$$R = (C_{Ai} - C_{AL})\left(\frac{D_A}{\delta}\right) \quad (2.27)$$

At condition in between, k_L is proportional to D_A^n

[redacted] (2.28)

Where the value n gets the following values: n = 1 in the film model, n = 0.5 represents both penetration and surface renewal model and the film-penetration model can get values 0.5 < n < 1. The application of the film-penetration theory is difficult because of lack of data on δ and s.

2.2.4 King Diffusivity Model (Eddy):

All the theories so far reviewed agree that the absorption rate is determined by processes taking place very close to the gas-liquid interface. This underlined the importance of models based on finding a link between the mass transfer rates and the velocity fields near the various interfaces.

For (Fortescue, 1967), proposed that is effect of the turbulence on the flow field near the interface could be represented by large eddies sweeping fresh liquid to the vicinity of the interface and then remove the solute - rich liquid to be dissipated in the bulk of the absorbing fluid. The eddy diffusivity theory Equation (2.29), proposed by (King, 1966), is a steady-state theory that assumes a significant

convective contribution to the diffusion of species in the boundary layer. Near the interface, diffusion processes are dominant. Close to interface (x=0), mass transfer is dominated by the diffusion coefficient of A. As x increases (toward the bulk solution), the effect of eddies becomes more important. For describing the concentration profiles within the reactive boundary layer, (Bishnoi, 2000), used the eddy diffusivity theory (King, 1966).

$$\frac{d}{dx}\left[\left(D_A+\varepsilon(x)\right)\frac{dC_A}{dx}\right]=0 \tag{2.29}$$

$$\begin{aligned} x&=0 \qquad C_A=C_{Ai}\\ x&\to\infty. \qquad C_A=C_{AL}\end{aligned} \tag{2.30}$$

(Glasscock, 1990), showed that the eddy diffusivity theory gives a solution within 5% of the surface renewal or penetration theory without the complications of time dependence. For this reason, (Bishnoi,2000), chose this theory as the basis for his mass transfer model.

This expression excludes the effect of electrical potential onion diffusion, which (Glasscock, 1989) show to be insignificant for promoted amine systems. By making this simplifying assumption, we must assume all ion diffusion coefficients to be equal, where ε is proportionality constant ($\varepsilon = a.x^m$) We use a value of 2 for m , where [redacted] This value is suggested by (Prasher, 1974), and is consistent with the work of Glasscock. The mass transfer coefficient then becomes

[redacted] (2.31)

2.3.1 Solubility:

Solubility is a function of system temperature and, to a lesser extent, system pressure. As temperature increases, the amount of gas that can be absorbed by a liquid decreases (gases are more soluble in cold liquids than in hot liquids). Gas phase pressure can also influence solubility; by increasing the pressure of a system,

the amount of gas absorbed generally increases. However, this is not a major variable in absorbers used for air pollution control because they operate at close to atmospheric pressure (USEPA-81/12, 1981). The absorption of gas is done under low temperature, recall that the solubility of gases in liquid decreases with temperature and hence, there is always a larger driving force for the transfer of solute from the gas to the solvent. In the selection of solvent for absorption process, the solvent has to be highly soluble to absorb the solute. Several other factors determine the selection of solvent. These include volatility, viscosity, corrosiveness and toxicity. That is, an effective solvent should have low volatility which in turn, reduces the extent of solvent loss. Contrary to that will lead to high solvent loss and in turn, will create an environmental pollution as well as loss of resources. A low viscosity allows a solvent to flow easily which extensively combats the problem of flooding. (Kohl et al, 2007)

2.3.2 Equilibrium solubility and Henry's law:

Under certain conditions, Henry's law can express the relationship between the gas phase concentration and the liquid phase concentration of the contaminant at equilibrium. This law states that for dilute solutions in which the components do not interact, the resulting partial pressure (p) of a component A in equilibrium with other components in a solution can be expressed as

$$p = He\ x_A \tag{2.32}$$

Equation 2.32 is the equation of a straight line where the slope (m) is equal to He . Henry's law can be used to predict solubility only when the equilibrium line is straight — when the solute concentrations are very dilute. The units of Henry's law constants are atmosphere per mole fractions. The smaller the Henry's law constant is, the more soluble the gaseous compound is in the liquid.

2.4 Mass transfer with Chemical Reaction:

Many present-day commercial gas absorption processes involve systems in which chemical reactions take place in the liquid phase. These reactions generally enhances the rate of absorption and increase the capacity of the liquid solution to dissolve the solute, when compared with physical absorption systems, because it depletes the diffusing in the region of the interface producing a steeper concentration gradient. This introduces us to the concept of the enhancement factor, sometimes referred to as the chemical acceleration factor.

Mass transfer with chemical reaction takes place when ever two phases which are not at chemical equilibrium with one another are brought into contact. Such phenomena are made up of a number of elementary steps, which may be summarized as follows:

1- Diffusion of one reactant from the bulk of gas phase to interface between the gas-liquid.

2- Diffusion of the reactant from the interface towards the bulk of liquid phase.

3- Chemical reaction within liquid phase.

4- Diffusion of reactant initially presents within liquid phase, and/or of reaction product, within phase liquid itself, due to concentration gradients which are set up by the chemical reaction.

Mass transfer processes are coupled with a chemical reaction, in order to improve the rate and yield of the process. The mass transfer models described above can be used to help study of the effect of a chemical reaction on an absorption process. Despite the variance in the models in their representation of the processes occurring all of the models generally give useful mathematical results, and generally

it is desirable to use the easiest model to solve for the specific problem, as opposed to that which is the best resemblance of the processes occurring.

➤ In case of absorption of gas (A) into liquid, there is possibility that the dissolved gas to reacts with other solvent/ reactant dissolved in liquid with rate of reaction of r_A. Consider Fig 2.3, we make mass balance of A over volume element dv or (S.dx).

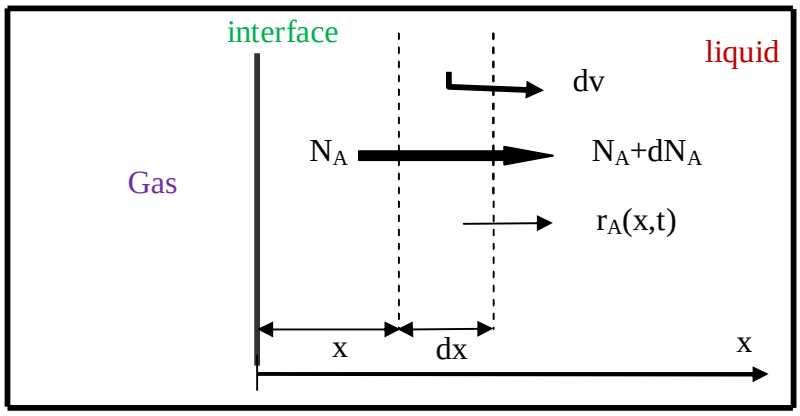

Figure 2.3 Mass transfer of gas into liquid with chemical reaction

Rate in = Rate out + Accumulation + Reaction rate

$$N_A S = (N_A + dN_A)S + \frac{\partial C_A}{\partial t}(S.dx) + r_A(S.dx) \quad (2.33)$$

$$N_A S - N_A S - dN_A S = \frac{\partial C_A}{\partial t}(S.dx) + r_A(S.dx) \quad (2.34)$$

$N_A = -D_A \frac{\partial c_A}{\partial x}$ Diffusion flux A in liquid (Fick's first law)

When the Eq(2.34) is divided by S.dx , and substitution value of N_A we get

$$-\frac{d}{dx}\left(-D_A \frac{\partial C_A}{\partial x}\right) = \frac{\partial c_A}{\partial t} + r_A \longrightarrow [redacted] \quad (2.35)$$

It becomes necessary to write such an equation (2.35) for each molecular species taking part in the reaction in order to completely describe the system.

2.5 Effects of chemical reactions on mass transfer rates:

In multiphase systems, chemical reactions affect the mass transfer rate in two distinct ways:

➤ At low reaction rate, it serves to change the bulk concentration of the transferring solute, thus increasing the driving force.

➢ On the other hand for reasonably fast reactions the concentration gradient near the interface is affected leading to an “Enhancement “of the mass transfer rate.

2.5.1 Enhancement Factor:

In gas absorption in which gas-liquid mass transfer is accompanied by a chemical reaction in the liquid phase the gas absorption rate may be enhanced significantly. Generally, the chemical reaction enhances the rate of absorption because it depletes the diffusing in the region of the interface producing a steeper concentration gradient, for describing this effect the enhancement factor concept is applied, in which the enhancement factor, E, is defined as : the ratio of the specific rate of gas absorption in a reactive liquid to the specific rate of absorption under identical conditions in a non-reactive liquid (physical mass transfer). Due to the importance of this enhancement factor for design purposes, several theoretical models have been developed to calculate this effect. Well known and frequently used one-parameter models are the film model, the Higbie penetration model and the Danckwerts surface renewal model. The Enhancement factor E can be estimated numerically by solving Equation (2.36) and using a certain interface mass transfer model. In case of irreversible second-order reaction and if the steady state conditions are further assumed, the equation (2.36) to be solved as follows for film model.

$$A + zB \longrightarrow yP$$

Figure 2.4 illustrates the gas-film and liquid-film concentration profiles one might find in an extremely fast (gas-phase mass-transfer limited) second-order irreversible reaction system. The solid curve for reagent *B* represents the case in which there is a large excess of bulk liquid reagent B^0. The dashed curve in Fig. 2.4 represents the case in which the bulk concentration B^0 is not sufficiently large to prevent the

depletion of *B* near the liquid interface and for which the equation E = 1 + B^0/zc_i is applicable.

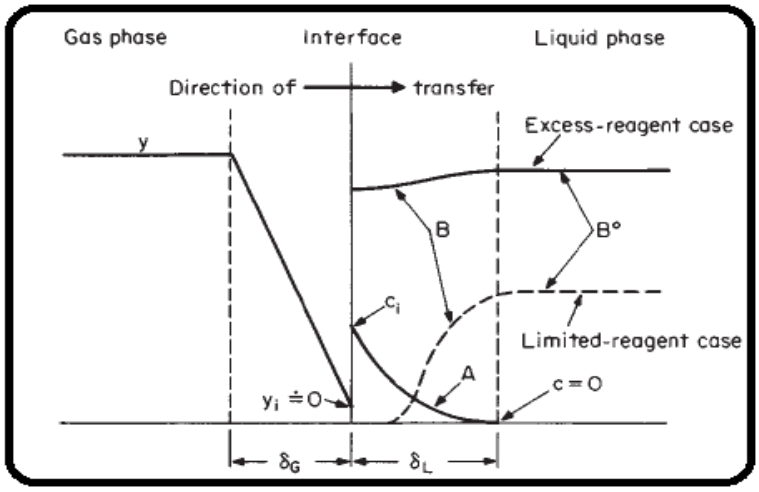

Figure 2.4: Gas phase and liquid phase solute concentration profiles for second-order reaction

$$D_A \frac{\partial^2 C_A}{\partial x^2} - k_2 C_A C_B = 0 \tag{2.36}$$

$$D_B \frac{\partial^2 C_B}{\partial x^2} - z k_2 C_A C_B = 0 \tag{2.37}$$

With Boundary condition:

$$\begin{aligned} C_A &= C_{Ai} && x = 0 \\ C_A &= C_{AL} && x = \delta \\ C_B &= C_{BL} && x = \delta \\ \frac{\partial C_B}{\partial x} &= 0 && x = 0 \end{aligned} \tag{2.38}$$

The isothermal enhancement factor can be predicted in equation (2.42), where the value of can be estimated using orthogonal collocation method. (Danckwerts', 1970). The enhancement factor for the isothermal case is defined, similarly as

$$E = \frac{\overline{R}}{k_L C_{Ai}} = \frac{-D_A [dC_A/dx]_{x=0}}{k_L C_{Ai}} \tag{2.39}$$

(Krevelen, 1948), have solved the above Equation using approximate method, and the result can be represented in Equation (2.40):

$$E = \frac{\sqrt{M \dfrac{E_i - E}{E_i - 1}}}{\tanh \sqrt{M \dfrac{E_i - E}{E_i - 1}}} \tag{2.40}$$

Where E_i = the enhancement factor corresponding to instantaneous reaction and $\sqrt{M}$

$$\sqrt{M} = \frac{\sqrt{D_A k_2 C_{BL}}}{k_L} \tag{2.41}$$

The Hatta number is actually the criterion for whether the reaction occurs completely in the liquid bulk or completely in the liquid film. The infinite enhancement factor E_i is dependent on the choice of a mass transfer model and for a film theory it is expressed by:

$$E_i = 1 + \frac{D_B C_{BL}}{z D_A C_{Ai}} \tag{2.42}$$

2.5.2 Reaction Regimes:

For example, we consider the case of gas absorption accompanied by irreversible chemical reaction of general order in liquid phase:

A +zB $\longrightarrow$ P. In this case, we assume that the reaction rate is given by the expression

$$r = k_{mn}\, C_A^m\, C_B^n \tag{2.43}$$

Reaction of this type include the first-order case (m=1, n=0) and the second-order case (m = 1, n =1). In the chemical absorption phenomena there are two competitive processes we have to consider; reaction and diffusion .This is based on the relative rate between reaction and diffusion, so it can be classified into several regimes reaction such as: very slow reaction, slow reaction, fast reaction, very fast reaction, and spontaneous reaction. For classification of these reaction regimes one usually applied Hatta Number (Ha or $\sqrt{M}$) (Hikita,1963), defined as the ratio of the maximum amount of consumed component in the liquid film and the maximum amount transferred if no chemical reaction occurs and at zero bulk concentration.

$$\sqrt{M} = \frac{1}{k_L}\sqrt{\frac{2}{m+1} k_{mn} D_A C_A^{m-1} C_B^n} \tag{2.44}$$

There are three reaction regimes based on the relative rate of reaction and diffusion

- $Ha < 0.02$ In this case very slow reaction compared to diffusion rate. If the target of process is for gas absorption, hence it can be assumed that no chemical reaction

occur in film and also in bulk of the liquid, and these is no effect of chemical reaction on the absorption rate. So the rate of absorption of gas with very slow reaction equal to the rate of physical absorption (without reaction). If the target of process is for chemical reaction hence this process is controlled with chemical reaction, and process rate equal to rate of reaction. This region is referred to as the "very slow reaction regime"

- $0.02 < Ha < 2$ The reaction is too slow to have any significant influence on the diffusion phenomena, so there is no reaction in the film and essentially no rate enhancement will take place, but the reaction is fast enough to maintain in the bulk of the liquid. This situation is referred to as the "slow reaction regime". In this regime the chemical reaction only have the effect of keeping the concentration of solute low (i.e. a larger driving force).
- $Ha > 2$ The reaction is fast enough for an appreciable fraction of the absorbed gas to react in the film, the concentration of unreacted dissolved gas in the bulk of the liquid will be negligible small (in the case of an irreversible reaction). This region is referred to as the "fast reaction regime".

2.6 Gas-Liquid Contactors:

Gas-liquid contactors are frequently encountered in chemical process industry. In these contactors a gas phase and a liquid phase are brought into contact with each other and mass transfer between the gas and the liquid phase takes place. Often, but not necessarily, the mass transfer is accompanied by the simultaneous occurrence of a chemical reaction. A good understanding of the behavior of gas-liquid contactors is essential for design purposes.

A variety of gas liquid contacting equipment is in use. In some of these, the gas is dispersed in the liquid in the form of bubbles (for example, tray towers, bubble

columns, etc) in some others the liquid is dispersed in the form of droplets or discontinuous films in a continuous gas phase (for example, spray towers, packed column, etc). Tray and packed columns are most widely used for gas liquid contacting- namely for gas absorption. Mass transfer can take place from the gas phase to the liquid phase as well as from the liquid phase to the gas phase. Chemical reactions may occur in the gas and /or in the liquid phase respectively.

2.6.1 Selection of column type (Plate or Packed):

Packed towers (columns) are also used as the contacting devices for gas absorption, liquid-liquid extraction and distillation. The gas liquid contact in a packed bed column is continuous, not stage-wise, as in a plate column. The gaseous mixture is allowed to contact continuously with the liquid counter-currently in a packed column. The liquid flows downward over the packing surface, and the gaseous mixture flows upward through the space in the packing. The performance of a packed column is very depends on the arrangement of the packings to provide good liquid and gas contact throughout the packed bed, and on the maintenance of good liquid and gas distribution throughout the packed bed, and this is an important consideration in packed-column design. The solute gas is absorbed by the fresh solvent (liquid) entering at the top of the tower where the lean gas leaves system. The liquid enriched with absorbed solute gas, leaves the column bottom through the exit port. In a plate (tray) tower, the liquid and gas are contacted in stage-wise manner on the trays; while gas-liquid contact is continuous in a packed column. There are always some uncertainly to maintain good liquid distribution in a packed tower. For this reason, it is difficult to accurately estimate the packed tower efficiency.

- Plate towers exhibit larger pressure drops and liquid holdup at higher gas flow rate. While, packed towers are not appropriate for very low liquid flow rates. Packed

column is the preferred choice than a plate column to handle toxic and flammable liquids due to lower liquid holdup to keep the unit as small as possible for the sake of safety.

- It is easier to make the provision for the installation of internal cooling coils or withdrawal of side streams from a plate column.
- Plate columns are normally suitable for fouling liquids or laden with solids. They are easier to clean and could handle substantial temperature variation during operation.
- Packed towers are more suitable for foaming and corrosive services.

2.6.1.1 Packed columns:

Packed column absorbers consist of a tower filled with packings made of metal, ceramic, glass or plastic along with a support plate for the packing material and a liquid distributing device (Perry et al, 1973). The packings can be randomly dumped in the column or they can be structurally arranged. The liquid from the liquid distributor flows down through the packings and the gas flows up through the wetted packing resulting in contact between the liquid and the gas phases. The sections of the packing are contained between a lower gas-injection support plate, which holds the packing, and upper grid or mesh hold-down plate, which prevents packing movement. A liquid distributor, placed above the hold-down plate, ensures uniform distribution of liquid as it enters the packing section. These columns are extensively used for absorption although they can also be used for rectification, humidification and dehumidification operations.

The packings in a packed column enhance the contact /interfacial area between the liquid and the vapor. This results in increased diffusion of the vapor into the liquid and subsequently higher absorption rates. But the packed column has no

arrangement to incorporate coolings coils and hence removal of heat of absorption is difficult (Perry et al, 1973). A single column can have several packed beds.

The tower shell may be made of steel or plastic, or a combination of these materials depending on the corrosiveness of the gas and liquid streams, and the process operating conditions. One alloy that is chemical and temperature resistant or multiple layers of different, less expensive materials may be used. The shell is sometimes lined with a protective membrane, often made from a corrosion resistant polymer. For absorption involving acid gases, an interior layer of acid resistant brick provides additional chemical and temperature resistance (Crowe et al, 1988).

A liquid distributor is designed to wet the packing bed evenly and initiate uniform contact between the liquid and vapor. The liquid distributor must spread the liquid uniformly, resist plugging and fouling, provide free space for gas flow, and allow operating flexibility. (Harrison, 1989) Large towers frequently have a liquid redistributor to collect liquid off the column wall and direct it toward the center of the column for redistribution and enhanced contact in the lower section of packing (Treybal, 1980). Liquid redistributors are generally required for every 8 to 20 feet of random packing depth (Letter, 2000).

Many diverse types and shapes of packing have been developed to satisfy these requirements. They can be divided into two broad classes:

2.6.1.1.1 Structured packing:

The term structured packing refers to a range of specially designed materials for use in absorption and distillation columns and chemical reactors. Structured packings typically consist of thin corrugated metal plates or gauzes arranged in a way that they force fluids to take complicated paths through the column, thereby creating a large surface area for contact between different phases.

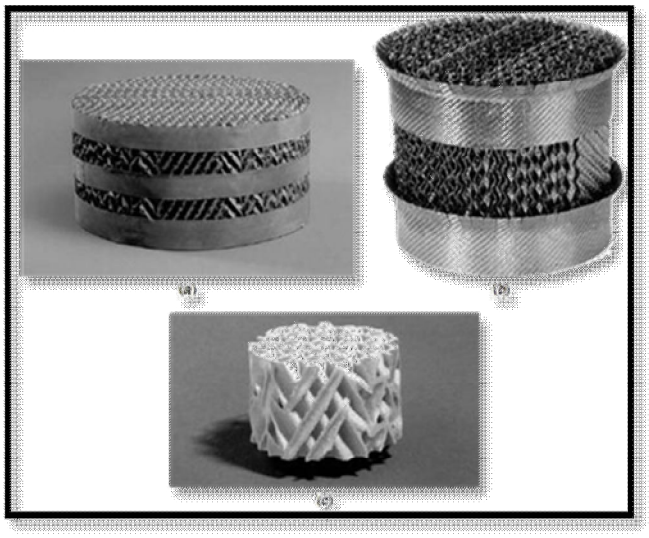

Figure 2.5 Structured packing (a) metal gauze (b) carbon (c) corrosion-resistant plastic

Structured packing is formed from corrugated sheets of perforated embossed metal or wire gauze. The result is a very open honeycomb structure with inclined flow channels giving a relatively high surface area but with very low resistance to gas flow. The surface enhancements have been chosen to maximize liquid spreading. These characteristics tend to show significant performance benefits in low pressure and low irrigation rate applications. Typical applications include vacuum and atmospheric crude oil fractionators, FCC main fractionators and TEG contactors. Structured packing is manufactured in a wide range of sizes by varying the crimp altitude. Packing surface ranges from 50 m^2/m^3 (lowest efficiency, highest capacity) to 750 m^2/m^3 (highest efficiency, lowest capacity).

2.6.1.1.2 Random packing's:

Random packing's are simply dumped-packed into the tower during installation and allowed to fall at random. The ring packing's used in the packed columns are Raschig rings, Lessing single-partition rings, and pall rings, Berl saddles and proprietary shapes, which are dumped into the column and take up a random arrangement. Grids have an open structure and are used for high gas rates, where low

pressure drop is essential; for example, in cooling towers. Random packings and structured packing elements are more commonly used in the process industries.

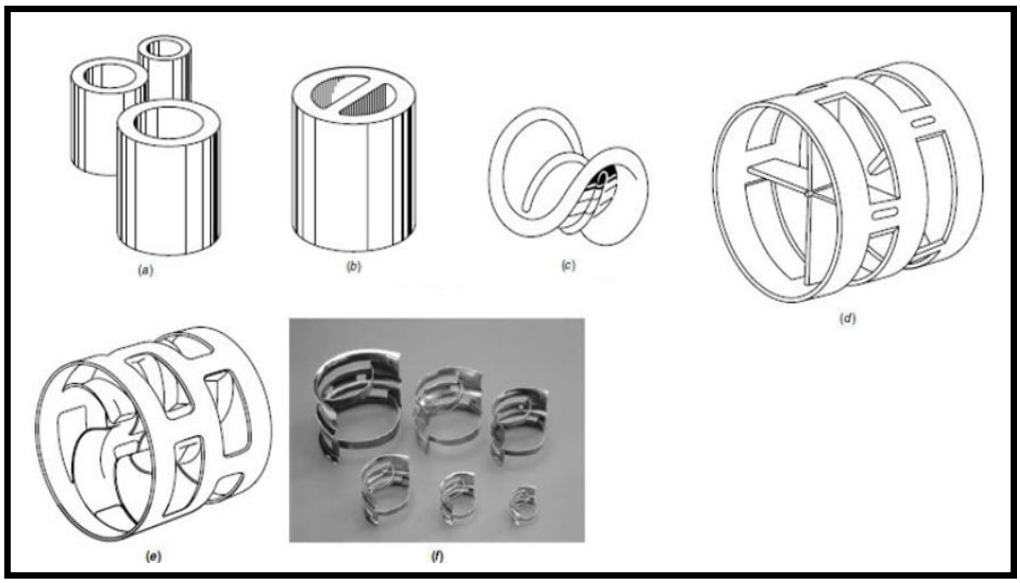

Figure 2.6 Random packing (a) Ceramic Raschig rings (b) Ceramic Lessing ring (c) Ceramic Berl saddle (d)Pall ring (plastic)(e) Pall ring (metal)(f) metal Nuter rings

2.6.1.2 The tray columns:

A tray column primarily consists of a vertical cylindrical shell and a set of 'tower internal' that include, trays or plates on which the gas-liquid contact , arrangements for flow of the liquid from one tray to lower one through downcomer, and inlet and outlet nozzles for the two phases. Tray towers do the same job as packed towers but they are very much more efficient in the separation process than packed towers and, they are also more costly. There are various types of tray in use and the type selected depends upon the degree of product purity required, the type of fluids, fluid velocity and other process parameters of the system. The types of trays used in absorption include: sieve tray, valve tray and bubble-cap trays. Mass transfer can take place from the gas phase to the liquid phase as well as from the liquid phase to the gas phase.

In a gas absorption application, the liquid enters the top tray through a nozzle. It impinges on a baffle plate, moves across the tray and flows into the lower tray through a 'downcomer'. The gas flows upwards and vigorously bubbles through the liquid on a tray, forming a turbulent 'gas-liquid dispersion' in which bubbles breakage and coalescence occur continuously. An average depth of the dispersion is maintained on a tray. A large gas-liquid contact area and a high mass transfer coefficient are achieved. Mass transfer from the gas to the liquid (or from the liquid to the gas) phase occurs depending on the direction of the driving force (the solute gets transported from the gas to the liquid phase). The gas then leaves the froth and enters the next upper tray. The liquid flows across a tray and then over a weir to enter into the downcomer. The downcomer is a region near the wall, separated by a ' downcomer plate', in which the bubbles get disengaged from the liquid. The clear liquid flows to the next lower tray. In this way, countercurrent and stage –wise gas-liquid contact takes place in the tower. Each tray acts as a stage in which the liquid flowing down from the upper tray and the gas is flowing up from the lower tray come into contact. A tray has two major functions:

- It allows the gas to flow through the holes or passages; the gas vigorously bubbles through the liquid to form a 'gas-liquid dispersion'. The tray hold the dispersion on it.
- The trays separate the column into a number of compartments each of which constitutes a stage. Mass transfer between the phases occurs on a tray. Therefore, the trays as a whole constitute the heart of a column. The performance of a column depends upon the performance of the trays.

2.6.3 The types of tray columns:

Plate contractors/ towers are vertical cylindrical columns in which a vertical stack of trays or plates are installed across the column height as shown in Figure 2.7 .

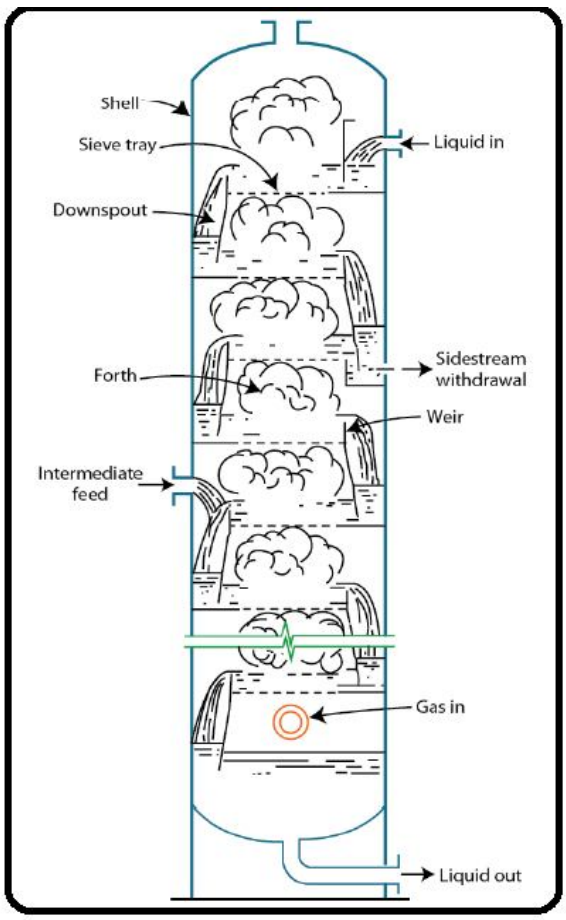

Figure 2.7 Schematic diagram of a plate contractor

The liquid enters at the top of the column and flows across the tray and then through a downcomer (cross-flow mode) to the next tray below. The gas/vapor from the lower tray flows in the upward direction through the opening/holes in the tray to form a gas-liquid dispersion. In this way, the mass transfer between the phases (gas/vapor-liquid) takes place across the tray and through the column in a stage-wise manner.

2.6.3.1 The bubble cap tray:

This is the oldest type of tray and is still in commercial use. A bubble cap consists of two major components, a bell- shaped 'cap' and a 'riser' (also called a chimney). The riser is inserted through a hole on the tray floor (or deck) and the bell-shaped cap is bolted to it. A ring gasket (not shown) is used below the nut. The riser

or chimney is a piece of tube with a flared or expanded bottom end. In fact, the riser acts as the vapour passage and also holds the cap.

A bubble cap has slots on its wall. The shape of the slots may be rectangular (most common), triangular, trapezoidal, or saw-tooth type. In the bell-shaped in Figure 2.8(a) and 2.8(b), the slots end a little above the bottom of the cap. The continuous portion of a cap below the slots is called the 'shroud ring'. The cap may be mechanically weak if there is no shroud ring and the slots extend up to the bottom. A bell-shaped cap rests on three short legs or tabs, integral to the cap, placed 120^{o} apart. The open region thus provided between the tray floor and the cap bottom is called the 'skirt clearance'. Such a design helps in reducing accumulation of sediment and provides an additional area for gas flow if there is a sudden surge of the gas. Figure 2.8(c) shows a few other designs of the bubble cap.

The cap and the risers are made of low carbon steel, stainless steel or any other suitable material that can withstand the environment within the tower. Caps are arranged on a tray on equilateral triangular pitch with rows normal to the direction of liquid flow. Bubble caps generally range from 1 inch to 6 inch in diameter.

An enhanced gas-liquid contact can be achieved having bubble caps on the tray at very low liquid flow rates. A bubble cap consists of a riser fixed to the tray through a hole and a cap is mounted over the riser .The gas flows up through the riser, directed downward by the cap through the annular space between riser and cap. Finally, the gas is dispersed into the liquid

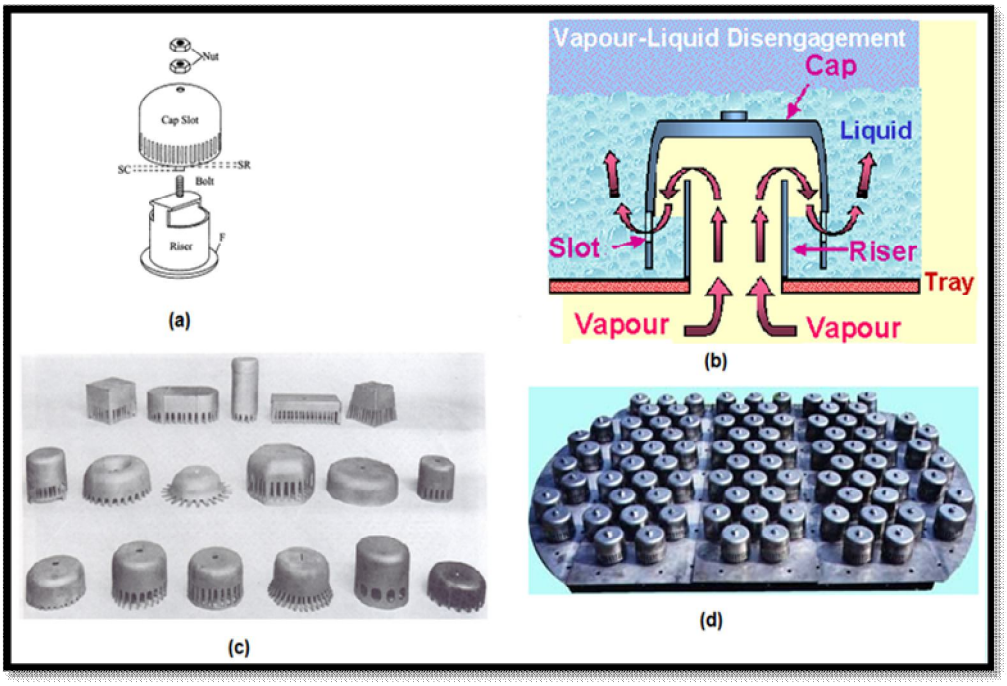

Figure 2.8 : (a) An exploded view of a bubble cap (b) sectional diagram of a bubble cap (c) different types of bubble caps and (d) a bubble cap tray

2.6.3.2 The sieve tray:

This is the simplest type of tray in which the bubble caps are replaced by holes or perforations for entrance of the gas into the liquid. The holes are of relatively small diameter – usually ranging from 0.125 to 0.5 inch. This is why the name 'sieve tray'. For clean services, use of a hole diameter of 3/16 inch is common. However, for liquid that foul or cause deposition, a hole diameter of 0.5 inch may have to be used. Small holes enhance tray capacity, reduce entrainment, reduce weeping, promote froth regime operation and exhibit better mass transfer characteristics. The sieve tray layout is a typical square or equilateral triangular pitch holes. The gas/vapor flows upward through the perforation and disperses into the flowing liquid over the plate. There is no liquid seal in case of trays without downcomer and the liquid weeps (called weeping) through the holes at low flow

rates, reducing the efficiency of plate. For this reason, sieve tray has the lowest turndown ratio. Sieve tray construction is simple and relatively cheap.

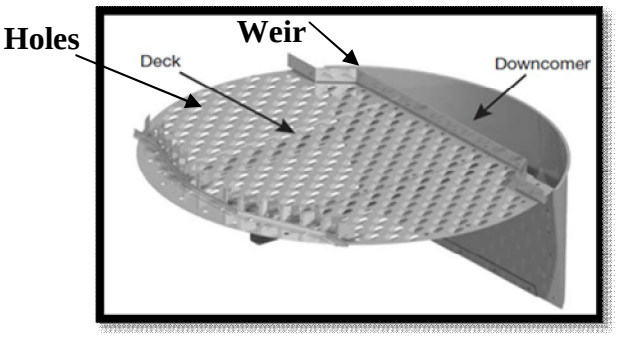

Figure 2.9: Sieve tray

2.6.3.3 The valve tray:

The valve tray is a relatively new class of tray that provides variable area for the gas flow depending upon the flow rate or 'throughput'. This is why it is called 'valve tray'. A valve tray is a proprietary (that is patented) tray. Different types of valve trays are made by different companies.

A common valve tray has sufficiently large punched holes on the tray floor, each fitted with a movable disk, generally circular. A disk has guides that can slide vertically up or down along the thickness of the tray floor [Figure 2.10(a) and 2.10(b)]. The opening for the gas flow changes in this way, but the disk is always held in the same vertical line. As the gas flow increases, the disk is automatically raised. It settles down at a low gas rate to prevent 'weeping'. The guides or retaining legs are bent at the end so that the disk does not pop up or gets detached even at a large gas rate. The valve, a part of valve tray and the gas flow rate profile through valve are all also shown in Figure 2.10(c).

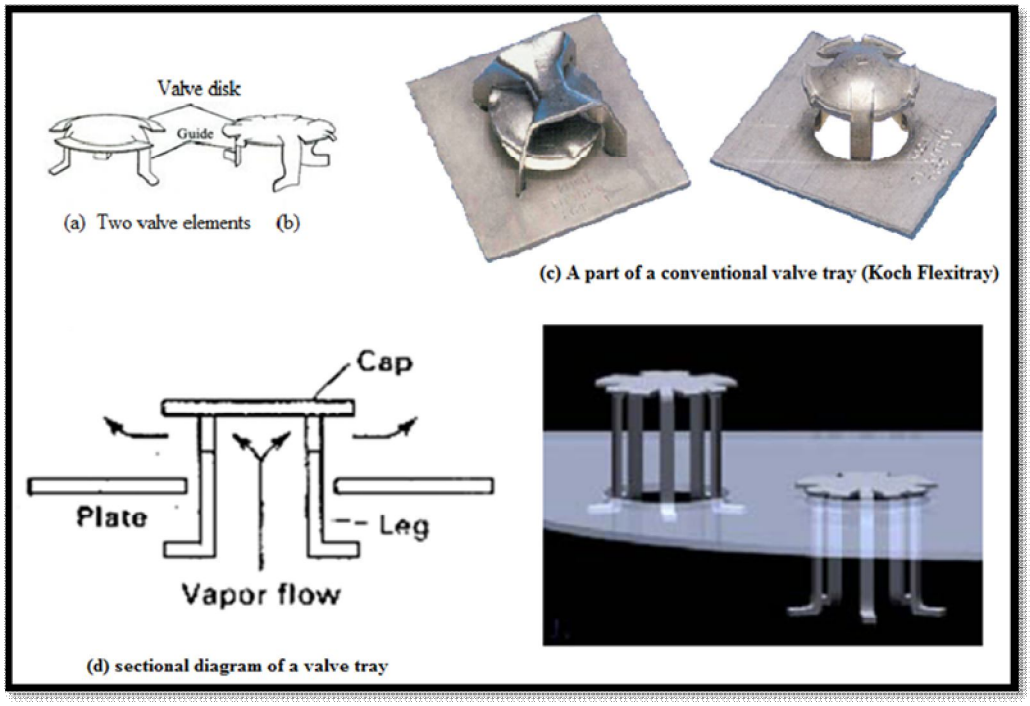

Figure 2.10 A few types of a valves, a part of a valves tray, and gas flow profile through valves

Since these are proprietary trays, the details of their design are not available in the open literature. These trays are extremely flexible because of the variable area of gas flow. The trays do not easily acquire deposits from dirty liquids, polymers or other solids because of the up and down motion of the disk and the guides. Valve units are, therefore, self-cleaning. The valve tray is a good choice for highly fouling services. In addition, they offer lower pressure drop than the bubble-cap type and generally they are cheaper than the latter type.

2.7. Selection of tray type:

The comparative performances of three common types of trays are summarized in Table 2.1. The capacity, efficiency, pressure drop and entrainment of sieve and valve trays are almost same. Bubble cap trays have lower capacity and efficiency and but higher pressure drop and entrainment compared to valve and sieve trays. The turndown ratio comes in the order of: bubble cap>valve>sieve. However,

valve trays have the best turndown ratio in case of refinery applications. Sieve trays are the least expensive and suitable for almost all applications. Valve trays can be considered where higher turndown ratio is needed. Bubble cap trays should be used at very low liquid flow rate which is not achievable using sieve trays.

Table 2.1: Comparison of three types of cross-flow trays

Tray type	Capacity	Efficiency	Pressure drop	Entrainment	Turndown ratio	Cost
Bubble cap	Medium high	Medium high	High	~3 times than sieve tray	Excellent	100-200% more than sieve tray
Valve	High to very high	High	Medium high	Medium	4 to 10.1	20-50% more than sieve tray
Sieve	High	High	Medium	Medium	2.1	Cheapest of all types

2.8. Plate Hydraulic design:

The basic requirements of a plate contacting stage are that it should:

- Provide good gas-liquid contact.
- Provide sufficient liquid hold-up for good mass transfer (high efficiency).
- Have sufficient area and spacing to keep the entrainment and pressure drop within acceptable limits.
- Have sufficient downcomer area for the liquid to flow freely from plate to plate.

A short procedure for the hydraulic design of sieve plates is given in this section. The diameter of the tower must be chosen to accommodate the flow rates, the details of the tray layout must be selected, estimates must be made of the gas-pressure drop and approach to flooding and assurance against excessive weeping and entrainment must be established.

2.9 Flow regimes on the tray:

The characteristics of gas-liquid dispersion on a tray depend upon the flow the flow rates of the two phases, besides the tray type. A few 'flow regimes' may be identified (Lockett, 1990), in this connection (Figure 2.11).

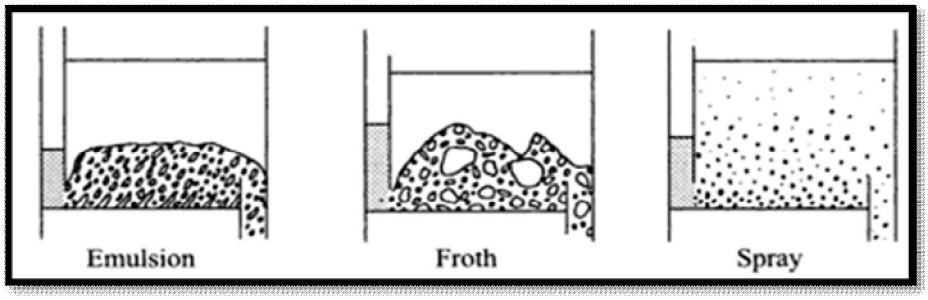

Figure 2.11 Types of gas liquid dispersion on a tray

When the gas rises through the liquid, there may be violent 'spray action' on one extreme or a 'quiescent flow' of the two phase 'emulsion' (or dispersion) on the other extreme, depending upon the flow rates of the two phase. In between, there occurs a 'froth regime' (Figure 2.11) in addition to the flow regimes, the flow rates of the two phases also govern phenomena such as weeping, dumping, entrainment, and flooding.

2.9.1 Spray regime:

It occurs at low liquid rates and high gas velocities. The gas enters at high velocity into a shallow liquid layer disintegrating the liquid into droplets which are projected up in the space between two consecutive trays. The gas becomes the continuous phase, and the liquid, the dispersed. This is called the 'spray regime'. If the gas rate is very high and the tray spacing is not sufficient, the droplets cannot settle. These are rather carried by the gas into the upper tray causing and accumulation of liquid there and eventual 'flooding'. This is more likely to occur in vacuum operation since the gas velocity remains very high. A change of flow regime

from froth to spray is called phase inversion in a tray column since the gas changes from dispersed to continuous state.

2.9.2 Emulsion regime:

This occurs if the gas flows through the liquid at a rather low rate. The gas bubbles formed at the nozzles are 'sheared off ' by the fast-moving liquid. The bubble size and its rise velocity remain low as a result. The liquid with the slowly rising entrapped bubbles appears like an 'emulsion' and hence the name of the regime.

2.9.3 Froth or mixed regime:

In between the spray and emulsion flow regimes there exists a 'froth' or 'mixed flow' regime extending over a range of gas velocities. The liquid rate is large enough to prevent spraying but not too large to cause substantial shearing of the bubbles at the stage of formation. The froth regime is the preferred flow regime in industrial tower.

2.10 Definition of tray areas:

The definition of tray areas and its nomenclature illustrated in Figures 2.12 are followed throughout the design procedure.

Total tower cross-section area (A_t): The empty tower inside cross-sectional area without trays or downspouts.

Cross-sectional area of downcomer (A_d): As 8 to12 per cent of the total tower cross-sectional area, [Ad = (8 – 12%) At]

Net area (A_n): The total tower cross-sectional area (A_t) minus the area at the downcomer (A_d). [$\boldsymbol{A}_n = \boldsymbol{A}_t - \boldsymbol{A}_d$] The net area symbolizes the smallest area available for vapor flow in the inter-tray spacing.

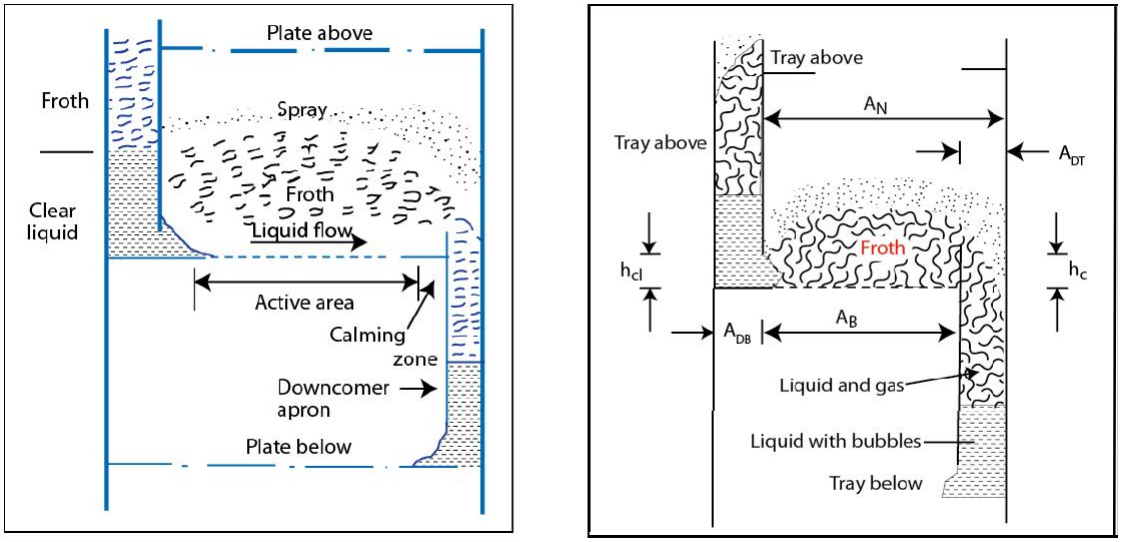

Figure 2.12 Schematic of a tray operating in the froth regime & Typical cross-flow plate

2.11 Effect of gas flow conditions on tray design:

It may be interesting to note the qualitative effect of liquid and gas loads on sieve tray performance as limited by tray dynamics. This is illustrated by Figure 2.13, where the limit of each tray dynamic factor is sketched in for typical sieve tray**.** The hydraulics of a tray column shows complex Figure 2.13 the ratio of gas to liquid flow rates should be situated in a region of satisfactory operation. This region is constrained by undesired phenomena, such as weeping, entrainment and downcomer flooding. Weeping and flooding set lower and upper bounds for gas velocity. It is desirable to work at high gas velocity to reduce both diameter and column cost. Figure 2.13 is a typical tray stability diagram. The area of satisfactory operation (shaded) is bound by the tray stability limits. These limits are discussed in the following sections. The upper capacity limit is the onset of flooding. At moderate and high liquid flow rates, the entrainment (jet) flooding limit is normally reached when gas flow is raised, while the downcomer flooding limit is normally reached when liquid flow is reused. When flows are raised while the column operates at

constant L /G either limit can be reached. At very low liquid rates, as gas rate is raised, the limit of excessive entrainment is often reached. As vapor rate is lowered, either at constant liquid rate or at a constant L /G ratio, the limit of excessive weeping is reached. This limit is not identical with the weep point, as some weeping can usually be tolerated.

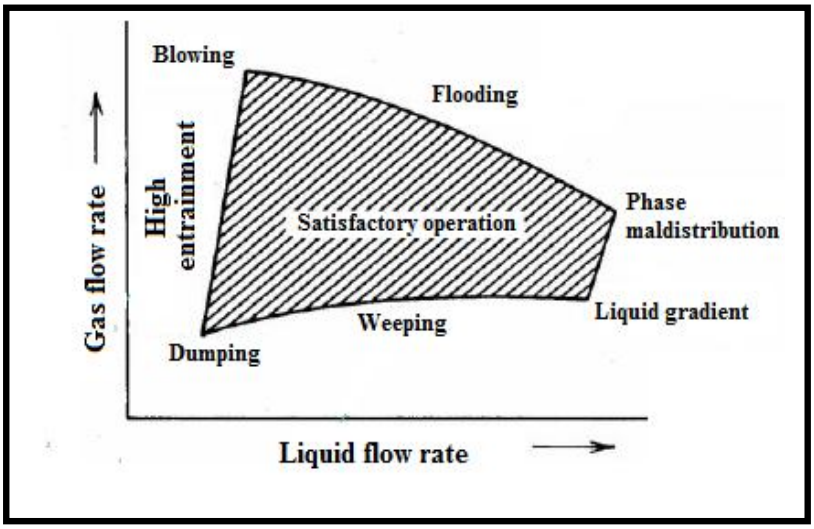

Figure 2.13 Sieve tray performance diagram.

2.11.1 Liquid entrainment:

When the velocity of the gas is sufficiently high to transport liquid droplets to the tray above, liquid entrainment occurs. This influences the mass transfer separation efficiency, as shown in Figure 2.14, since the entrained liquid contains a higher fraction of the less volatile component than the liquid on the tray above. This increases the concentration of the less volatile component on the tray above. The onset of entrainment is one of the operating parameters which constrain the mass transfer separation efficiency. The maximum allowable entrainment is achieved when the separation efficiency on each tray is reduced to the point where the overall required separation cannot be obtained with the number of trays available in the column. Therefore the onset of entrainment is a vital parameter in the design of the column and thus directly impacts the cost. The study of entrainment is categorised as

part of the hydrodynamic behavior inside the absorption column and is generally influenced by the following parameters:

1. Gas and liquid flow rates
2. Gas and liquid physical properties
3. Column and tray geometry

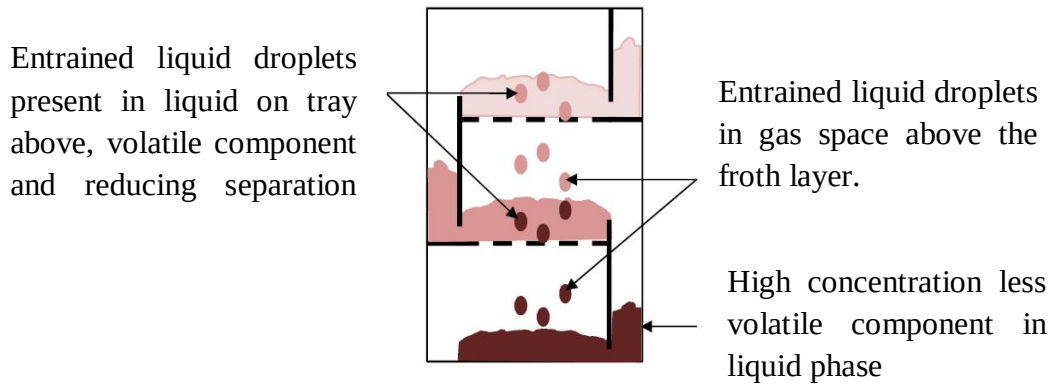

Figure 2.14 Schematic representation of the influence of entrainment on the separation efficiency.

2.11.2 Sieve tray weeping:

Another hydrodynamic phenomenon is found when the gas flow rate is low enough for liquid dumping (weeping) to occur. Under these conditions the gas flow rate is so low that the liquid weeps through the holes in the tray to the tray below. Weeping is therefore the inverse of entrainment and also negatively influences the separation efficiency.The data on incipient weeping are meager, particularly for large liquid depths, and in all likelihood there will always be some weeping. When none of the liquid reaches the downcomer at extreme weeping condition at very low gas flow rate, it is called dumping. The weeping tendency increases with increasing fractional hole area and liquid flow rates.

2.11.3 Flooding:

Excessive entrainment can cause the liquid flow rate to exceed the downcomer capacity (Seader et al, 1998). As the downcomer exceeds capacity,

liquid will build-up on the trays and go back up the column causing the column to flood. Column flooding can also occur when the liquid feed flow rate exceeds the downcomer capacity while the gas flow rate is sufficiently high enough to prevent weeping, resulting in a liquid build-up on the tray. Another mechanism for column flooding occurs during low liquid rates when the gas velocity is high enough so that the amount of liquid entrained exceeds the liquid rate flowing through the downcomer (and column).

CHAPTER THREE

3. RESEARCH METHODOLOGY

3.1 Materials and Method:

Many commercial processes are available for the removal of H_2S from gaseous streams. Most of these processes use gas-liquid contactors in which the hydrogen sulphide is contacted with a reagent to give either another dissolved sulphide-containing component for example ferric sulfate as a precipitate. Important representatives of the latter type are the so-called aqueous ferric sulfate solution $Fe_2(SO_4)_3$ based processes.

In this research, the reactive absorption of hydrogen sulfide H_2S into aqueous ferric sulfate $Fe_2(SO_4)_3$ solution has been studied and design calculations for equipment have been done and effective operation parameters on this process considered. In this process an aqueous $Fe_2(SO4)_3$ solution is used an absorbent. The basic process involves putting in contact, in an absorber, a ferric sulfate solution $Fe_2(SO_4)_3$, counter-current with refinery flue gas, contaminated with hydrogen sulfide (H_2S). H_2S absorbed and oxidized into elemental sulfur and at the same time, reducing the ferric sulfate Fe^{+3} to ferrous sulfate Fe^{+2} (FeSO4), according to this global chemical :

$$H_2S_{(g)} + Fe_2(SO_4)_{3(aq)} \rightarrow 2FeSO_{4(aq)} + H_2SO_{4(aq)} + S_{(s)}$$

Elemental sulfur is removed from the solution by solid-liquid separation, usually by gravity sedimentation, and the reactant Fe^{+3} is regenerated from Fe^{+2} by oxidation in reactor to the following reaction :

$$2FeSO_{4(aq)} + H_2SO_{4(aq)} + 0.5O_2 \rightarrow Fe_2(SO_4)_{3(aq)} + H_2O$$

3.2 Research Framework:

Firstly, this chapter we are discussing the steps of designing the sieve tray column; and determine or how to design the column diameter, number of theoretical trays, column height, was continue design of the sieve tray column like pressure drop. Was discuss the entrainment weeping and tray efficiency. The steps required for tray column design are shown in Figure 3.1 detailed discussion of each step is given below.

Secondly, this research is done in simulation to determine sieve tray column performance in absorption of H_2S gas into aqueous ferric sulfate solution $Fe_2(SO_4)_3$. Theoretical study is divided two into parts. The first part developed transfer model between phases to estimate the value of enhancement factor (E) that yielding the ordinary differential equation system in second order and it is solved by the orthogonal collocation method. Estimation of the value of (E) required several data; they are reaction kinetics data, solubility data, and mass transfer data, after that, (in the second part) the value of (E) is used for sieve tray column model of chemical absorption of H_2S yielding of ordinary differential equation system of first order solved by using Runge Kutta method. Output of sieve tray column model is % recovery of H_2S, concentration distribution of A in gas phase, concentration distribution of B in liquid phase. Research framework is shown in Figure 3.2

3.3 Design approach for absorption desorption sieve tray column:

3.3.1 General characteristics:

This phase of the design translates the process requirements (the gas and liquid loads in each section of the column) into actual hardware. The hardware design proceeds in two phases: primary (basic) and secondary (detailed layout).

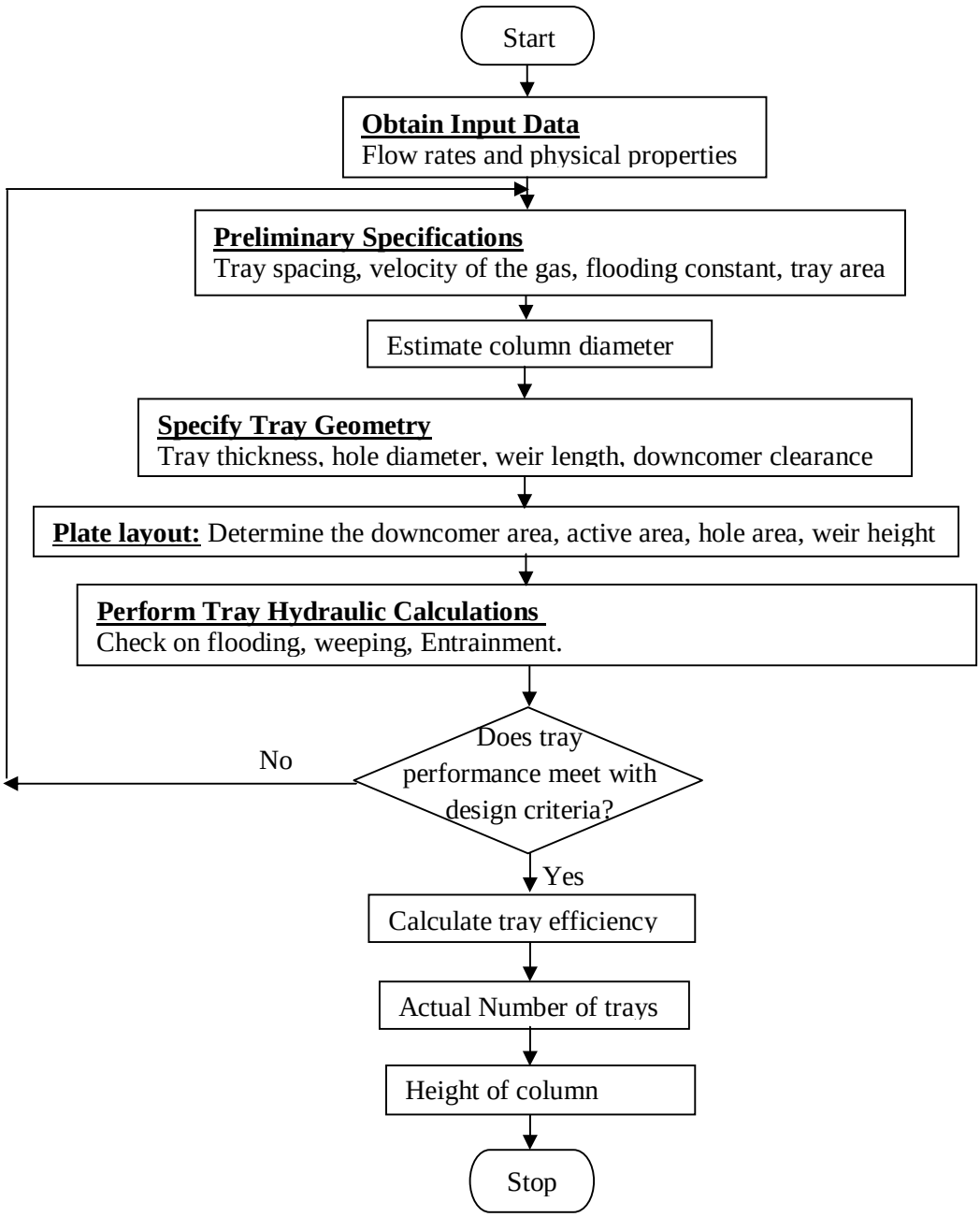

Figure 3.1 Sieve tray design procedure.

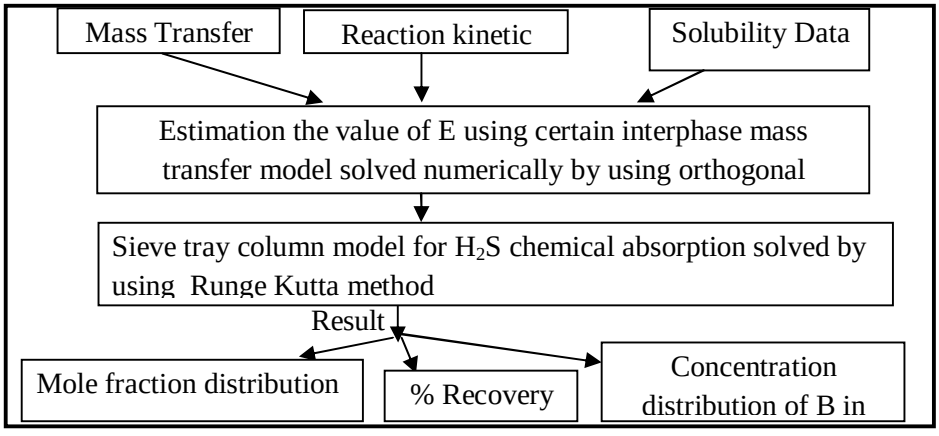

Figure 3.2 Research Simulation Frameworks

The primary phase sets column diameter, tray spacing, tray areas, and number of theoretical trays. This phase also provides a preliminary (and usually close) estimate downcomer layout such as weir height, fractional hole area, hole diameter, and clearance under the downcomer. These estimates are later firmed up in the secondary phase.

The secondary phase, describes the physical processes that constrain equipment design, including flooding, entrainment, weeping, pressure drop. This phase then describes how knowledge of these physical processes is harnessed to set hardware design.

3.4 Plate design procedure:

3.4.1 Tray spacing:

Tray spacing is usually chosen on the basis of expediency in construction, maintenance, and cost and later checked to be certain that adequate insurance against flooding and excessive entrainment is present. The tray plate spacings of 0.3 to 0.6 m will normally be used, and 0.5 m can be taken as an initial estimate (Coulson, 1999)

3.4.2 Tower diameter:

The tower diameter and consequently its cross-sectional area must be sufficiently large to handle the gas and liquid rates within the region of satisfactory operation. To calculate the column diameter an estimate of the net area A_n is required (Treybal, 1981)

$$A_n = \frac{Q}{v} \tag{3.1}$$

For a given type of tray at flooding, the superficial velocity of the gas v_F (volumetric flow rate of gas Q per net cross section for flow A_n) (Treybal, 1981). is related to fluid densities by:

$$v_F = C_F \left(\frac{\rho_L - \rho_G}{\rho_G} \right)^{0.5} \tag{3.2}$$

The flooding constant C_F of Eq (3.3) has been correlated for the data available on flooding (Treybal, 1981). The original curves can be represented by:

$$C_F = \left[\alpha \log \frac{1}{F_{LV}} + \beta\right]\left(\frac{\sigma}{0.020}\right)^{0.2} \tag{3.3}$$

The flooding constant C_F dependent on the hole area to active area ratio

$$\frac{A_o}{A_a} = \frac{hole\ \ area}{active\ \ area} = 0.907\left(\frac{d_o}{p_t}\right)^2 \tag{3.4}$$

Where, d_o = hole diameter, (3-12mm) are commonly used, 4.5 mm most frequently

p_t = equilateral triangular pitch, p_t = (2.5 - 4) d_o (Coulson, 1999)

If the $A_o/A_a > 0.1$ and F_{LV} (0.1 – 1) , $\alpha = 0.0744t + 0.01173$ and $\beta = 0.0304t + 0.015$.

If the $A_o/A_a < 0.1$. Multiply α and β by $(5A_o/A_a + 0.5)$ (Treybal, 1981)

t : tray spacing from 0.15 m to 1 m are normally used, are commonly used 50 cm most frequently (Coulson, 1999)

The flow parameter F_{LV} of Eq(3.4) (Coulson, 1999)can be represented by :

$$F_{LV} = \frac{L'}{G'}\left(\frac{\rho_G}{\rho_L}\right)^{0.5} = \frac{q}{Q}\left(\frac{\rho_L}{\rho_G}\right)^{0.5} \tag{3.5}$$

L' is liquid mass flow rate (kg/s) = q (m^3/s) ρ_L (kg/m^3)

G' is gas mass flow rate (kg/s) = Q (m^3/s) ρ_G (kg/m^3)

$$Q = \dot{n}_G.\dot{V}_s \frac{T\,(^oK)}{T_S} \tag{3.6}$$

$$q = \frac{\dot{n}_L M_{av}}{\rho_L} \tag{3.7}$$

The flooding condition fixes the upper limit of gas velocity. A high gas velocity is needed for high plate efficiencies, and the velocity will normally be between 70 to 90 per cent of that which would cause flooding. For actual design smaller value of v is used, a value of 75 to 85 per cent of the flooding velocity (v_F) should be used. (Coulson, 1999) Flooding velocity,

$$v = (75 \text{ to } 85)\ v_F \tag{3.8}$$

Net area available for gas flow (A_n)

$$A_n = \frac{Q}{v} \tag{3.9}$$

Total tower cross-section area (A_t)

$$A_t = \frac{A_n}{1 - tray\ \ area\ \ used\ \ by\ \ one\ \ downspout} \tag{3.10}$$

Tower diameter

$$D = \sqrt{\frac{4A_t}{\pi}} \tag{3.11}$$

Table 3.1 Weir length for straight, rectangular weirs, cross-flow trays (Treybal)

Weir length W	Distance from center of tower	Tower area used by one downspout %
0.55 D	0.4181 D	3.877
0.60 D	0.3993 D	5.257
0.65 D	0.2516 D	6.899
0.70 D	0.3562 D	8.808
0.75 D	0.3296 D	11.255
0.80 D	0.1991 D	14.145

3.4.3 Height of the liquid crest over the weir h_1 and weir height h_w:

The crest of liquid over a straight rectangular weir can be estimated by the well-known Francis formula (Treybal, 1981)

$$\frac{q}{W_{eff}} = 1.839\, h_1^{3/2} \tag{3.12}$$

Where q = rate of liquid flow, m^3/s. W_{eff} = effective length of the weir, m

h_1 = height of the liquid crest over the weir, m

Because the weir action is hampered by the curved sides of the circular tower, it is recommended (Treybal, 1981) that W_{eff} be represented as a chord of the circle of diameter D, a distance h_1 farther from the center than the actual weir, Equation (3.12) can then be rearranged to (Treybal, 1981)

$$h_1 = 0.666\left(\frac{q}{W}\right)^{2/3}\left(\frac{W}{W_{eff}}\right)^{2/3} \tag{3.13}$$

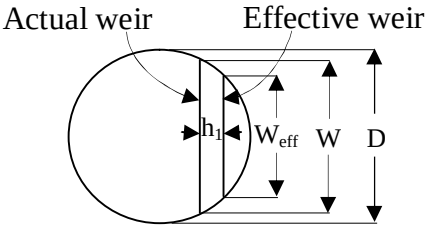

Figure 3.3 Effective weir length. (Treybal, 1981)

The geometry of Fig. 3.3 leads to

$$\left(\frac{W_{eff}}{W}\right)^2 = \left(\frac{D}{W}\right)^2 - \left[\left(\left(\frac{D}{W}\right)^2 - 1\right)^{0.5} + \frac{2h_1}{D}\frac{D}{W}\right]^2 \quad (3.14)$$

For W/D = 0.75, which typical, Eq (3.13) can be used with W_{eff} = W for h_1/W = 0.055 or less with amaximum error of only 2 % in h_1, which is negligible.

h_w = Weir height (40– 90mm), 40 – 50mm is recommended. (Coulson, 1999)

3.4.4 Pressure drop for the gas:

For convenience, all gas-pressure drops will be expressed as deads of clear liquid of density on the tray. The pressure drop for the gas h_G is the sum of the effects for flow of gas through the dry plate and those caused by the presence of liquid (Treybal, 1981):

$$h_G = h_D + h_L + h_R \quad (3.15)$$

where h_D = dry plate pressure drop, h_R = residual pressure drop.

h_L = pressure drop resulting from depth of liquid on tray

3.4.4.1 Dry pressure drop h_D

This is calculated on the basis that it is the result to a loss in pressure on entrance to the perforations, friction within the short tube formed by the perforation owing to plate thickness, and an exit loss (Treybal, 1981)

$$\frac{2h_D g \rho_l}{v_o^2 \rho_G} = C_o\left[0.4\left(1.25 - \frac{A_o}{A_n}\right) + \frac{4lf}{d_o} + \left(1 - \frac{A_o}{A_n}\right)^2\right] \quad (3.16)$$

The Fanning factor *f* is taken from a standard chart. C_o is an orifice coefficient which depends upon the ratio of plate thickness to hole diameter.Over the range l/d_o = 0.2-2

$$C_o = 1.09\left(\frac{d_o}{l}\right)^{0.25} \quad (3.17)$$

3.4.4.2 Hydraulic head h_L

Some methods of estimating h_L use a specific aeration factor to describe this. In Eq (3.18), which is the recommended relationship, the effect of the factor is included as a function of the variables which influence it (Treybal, 1981)

$$h_L = 6.1\times10^{-3} + 0.725\,h_w - 0.238\,h_w V_a \rho_G^{0.5} + 1.225\,\frac{q}{z} \qquad (3.18)$$

where z is the average flow width, which can be taken (D+W)/2.

3.4.4.3 Residual gas-pressure drop h_R:

This is believed to be largely the result of overcoming surface tension as the gas issues from a perforation. Since the bubbles do not really issue singly from the perforations into relatively quiet liquid, we substitute as an approximation the diameter of the perforations d_o (Treybal, 1981), which leads to

$$h_R = \frac{6\sigma g_c}{\rho_L d_o g} \qquad (3.19)$$

3.4.5 Pressure loss at liquid entrance h_2:

The flow of liquid under the downspout apron as it enters the tray results in a pressure loss which can be estimated as equivalent to three velocity heads (Treybal, 1981)

$$h_2 = \frac{3}{2g}\left(\frac{q}{A_{da}}\right)^2 \qquad (3.20)$$

3.4.6 Backup in downspout:

The difference in liquid level inside and immediately outside the downspout, will be the sum of the pressure losses resulting from liquid and gas flow for the tray above (Treybal, 1981)

$$h_3 = h_G + h_2 \qquad (3.21)$$

Since the mass in the downspout will be partly froth carried over the weir from the tray above, not yet disengaged, whose average density can usually be estimated roughly as half that of the clear liquid. For safe design requires that is the level of equivalent clear liquid back-up in the downspout be not more than half the tray spacing t to avoid flooding the requirement is (Treybal, 1981)

$$h_w + h_1 + h_3 < t/2 \qquad (3.22)$$

3.4.7 Check for entrainment:

Entrainment can be estimated from the correlation given by (Fair, 1961), which gives the fractional entrainment E (kg/kg gross liquid flow) as a function of the flow parameter F_{LV} and the percentage approach to flooding. (Coulson, 1999)

$$E = \frac{entrained\ liquid}{gross\ liquid\ \ flow} = \frac{e}{L+e} \quad , \quad E < 0.1 \text{ it is acceptable} \qquad (3.23)$$

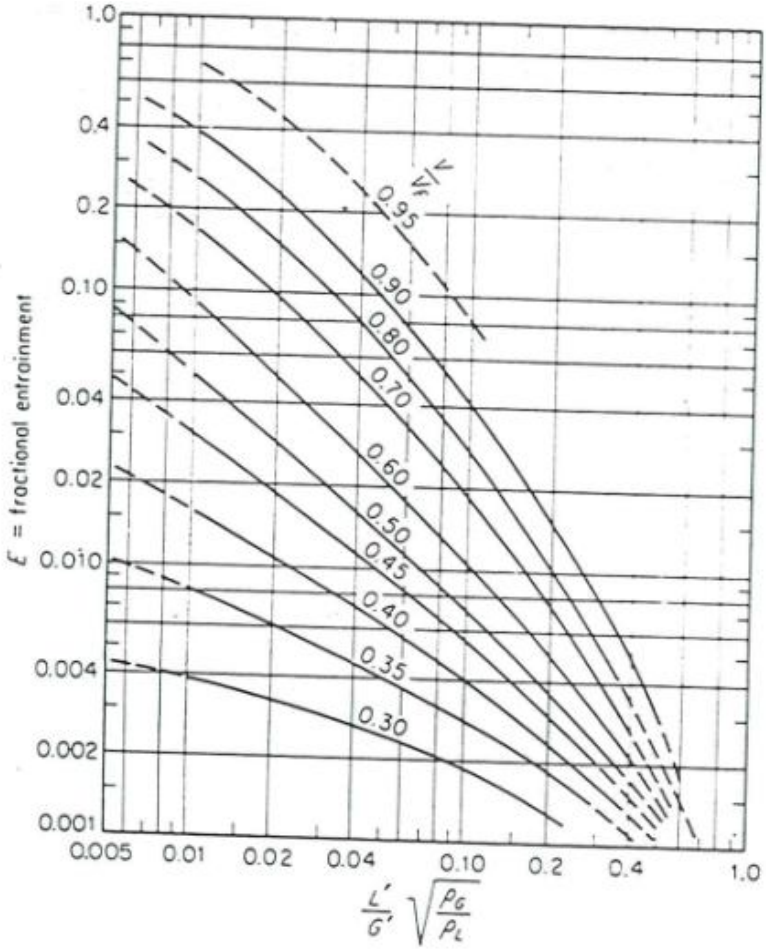

Figure 3.4: Entrainment sieve trays (from Mass Transfer Operation (Treybal))

The important influence of entrainment on tray efficiency will be considered later. Figure 3.4 represents a summary of sieve-tray entrainment data (Treybal, 1981).

3.4.8 Check for weeping:

If the gas velocity through the holes is too small, liquid will drain through them and contact on the tray for that liquid will be lost. A study of the available data

(Mdigan, 1964) led to the following as the best representation of U_{ow}, the minimum gas velocity through the holes below which excessive weeping is likely:

$$\frac{v_{ow}\mu_G}{\sigma g_c} = 0.0229\left(\frac{\mu_G^2\rho_L}{\sigma g_c \rho_G d_o \rho_G}\right)^{0.379}\left(\frac{l}{d_o}\right)^{0.293}\left(\frac{2A_a d_o}{\sqrt{3}p'^3}\right)^{2.8/(Z/d_o)^{0.724}} \quad (3.24)$$

Available data for h_L in the range 23 to 48 mm do not indicate h_L to be of important influence. It may be for larger depths. (Treybal, 1981)

3.5.1 Determine the Theoretical Number of plates:

The several methods used to determine the number of ideal plates or trays required for a given removal efficiency can become quite complicated. Equation 3.25 is a simplified method of estimating the number of theoretical plates of sieve trays needed to remove the H_2S. It can only be used if the equilibrium as well as operating lines for the system are straight, a valid assumption for most air pollution control systems. (Treybal, 1981)

$$N_P = \frac{\ln\left[\frac{y_1 - mx_2}{y_2 - mx_2}\left(1 - \frac{1}{A}\right) + \frac{1}{A}\right]}{\ln A} \quad (3.25)$$

where Np = number of theoretical plates.

y_1 = mole fraction of solute in entering gas

y_2 = mole fraction of solute in exiting gas

x_2 = mole fraction of solute entering the tower

m = equilibrium constant A = ambsorption factor = L/ mG

G = total molar flow rate of gas. kmol/hr

L = total molar flow rate of liquid . kmol/hr

4.5.2 Determine the overall plate efficiency:

Estimate of the overall stage efficiency can be obtained from the empirical correlation (Robin Smith, 2005)

$$\log_{10} E_o = -0.773 - 0.415 \log_{10} X - 0.0896 (\log_{10} X)^2 \quad (3.26)$$

Where : E_o = overall stage efficiency ($0 < Eo < 1$)

$X = mM_{wL} \mu_L/\rho_L$

3.5.3 Actual number of plates:

Actual number of plates = N_P/ overall plate efficiency

3.5.4 The height of the tower:

The height of the tower is given by (H.M.Mustafa, 2003) :

$$Z = (N_p - 1)(\text{tray spacing}) + \text{top height} + \text{bottom height} \quad (3.27)$$

The top height is the distance (freeboard) over the top plate that allows the gas–vapor mixture to separate.

3.6 Mathematical Modeling (Film Model):

The film theory is based on the assumption that when two fluid phases are brought in contact with each other, a thin layer of stagnant fluid exists on each side of the phase boundary.

3.6.1 Mass balance for component A:

The processes occurring within chemical absorption are expressed by Astarita in the form

Input – Output – Reaction = Accumulation

The film theory further simplifies the model as it is a steady state model, so there is no accumulation.

Mathematically:

$$F_{x,x=x} - F_{x,x=x+\Delta x} - k_2 C_A C_B \Delta x S = 0 \quad (3.28)$$

$$-\left[F_{x,x=x+\Delta x} - F_{x,x=x}\right] - k_2 C_A C_B \Delta x S = 0$$

$$-\left[\frac{F_{x,x=x+\Delta x} - F_{x,x=x}}{\Delta x}\right] - k_2 C_A C_B S = 0$$

$$-\lim_{\Delta x \to 0}\left[\frac{F_{x,x=x+\Delta x} - F_{x,x=x}}{\Delta x}\right] - k_2 C_A C_B S = 0$$

$$-\left[\frac{dF_x}{dx}\right] - k_2 C_A C_B S = 0 \qquad (3.29)$$

Where flux of H_2S by the following expression :

$$F_x = -D_A . S \frac{dC_A}{dx} \qquad (3.30)$$

Substitution Eq (3.30) into Eq (3.29)

$$-\frac{d}{dx}\left[-D_A S \frac{dC_A}{dx}\right] - k_2 C_A C_B S = 0$$

$$-\frac{d}{dx}\left[-D_A \frac{dC_A}{dx}\right] - k_2 C_A C_B = 0 \qquad (3.31)$$

For convenience, the following dimensionless notations are introduced:

$$\left.\begin{aligned} A = \frac{C_A}{C_{Ai}}; \quad B = \frac{C_B}{C_{Bo}}; \quad X = \frac{x}{\delta} \\ dA = \frac{dC_A}{C_{Ai}}; \quad dB = \frac{dC_B}{C_{Bo}}; \quad dX = \frac{dx}{\delta} \end{aligned}\right\} \qquad (3.32)$$

Substitution these dimensionless variables in Eq(3.32) into Eq (3.31). Then dimensionless form of Eq (3.31) can be as rewritten as follows:

$$-\frac{d}{\delta . dX}\left[-D_A \frac{C_{Ai} dA}{\delta . dX}\right] - k_2 C_{Ai} A C_{Bo} B = 0$$

$$\frac{D_A C_{Ai} d}{\delta^2 dX}\left[\frac{dA}{dX}\right] - k_2 C_{Ai} A C_{Bo} B = 0$$

$$\frac{D_A}{\delta^2}\frac{d^2 A}{dX^2} - k_2 A C_{Bo} B = 0$$

$$\frac{d^2 A}{dX^2} - \frac{k_2 A \delta^2 C_{Bo} B}{D_A} = 0 \qquad (3.33)$$

$$\frac{d^2 A}{dX^2} - MAB = 0 \qquad (3.34)$$

Where

$$M = \frac{k_2 \delta^2 C_{Bo}}{D_A} = k_2 \frac{\delta^2}{D_A^2} C_{B0} D_A = \frac{k_2 C_{B0} D_A}{k_L^2}$$

3.6.2 Mass balance for component B:

Input – Output – Reaction = Accumulation

$$F_{x,x=x} - F_{x,x=x+\Delta x} - k_2 C_A C_B \Delta x S = 0. \qquad (3.28)$$

$$-\left[F_{x,x=x+\Delta x}-F_{x,x=x}\right]-k_2C_AC_B\Delta xS=0$$

$$-\left[\frac{F_{x,x=x+\Delta x}-F_{x,x=x}}{\Delta x}\right]-k_2C_AC_BS=0$$

$$-\lim_{\Delta x\to 0}\left[\frac{F_{x,x=x+\Delta x}-F_{x,x=x}}{\Delta x}\right]-k_2C_AC_BS=0$$

$$-\left[\frac{dF_x}{dx}\right]-k_2C_AC_BS=0 \qquad (3.29)$$

Where

$$F_x=-D_B.S\ \frac{dC_B}{dx} \qquad (3.35)$$

Substitution Eq (3.33) into Eq (3.27)

$$-\frac{d}{dx}\left[-D_B\frac{dC_B}{dx}\right]-k_2C_AC_B=0 \qquad (3.36)$$

Substitution these dimensionless variables in Eq (3.32) into Eq (3.36) . Then dimensionless form of Eq (3.36) can be as rewritten as follows:

$$-\frac{d}{\delta.dX}\left[-D_B\frac{C_{Bo}dB}{\delta.dX}\right]-k_2C_{Ai}AC_{Bo}B=0$$

$$\frac{D_BC_{Bo}d}{\delta^2dX}\left[\frac{dB}{dX}\right]-k_2C_{Ai}AC_{Bo}B=0$$

$$\frac{d}{dX}\left[\frac{dB}{dX}\right]-\frac{k_2\delta^2C_{Ai}AC_{Bo}B}{D_BC_{Bo}}=0$$

$$\frac{d^2B}{dX^2}-\frac{D_A}{D_A}\left[\frac{k_2\delta^2C_{Ai}AC_{Bo}B}{D_BC_{Bo}}\right]=0$$

$$\frac{d^2B}{dX^2}-\frac{k_2\delta^2C_{Bo}}{D_A}\frac{D_AC_{Ai}}{D_BC_{Bo}}.AB=0$$

Where

$$M=\frac{k_2\delta^2C_{Bo}}{D_A}=k_2\frac{\delta^2}{D_A^2}C_{B0}D_A,=\frac{k_2C_{B0}D_A}{k_L^2},\frac{1}{S}=\frac{D_AC_{Ai}}{D_BC_{Bo}}$$

$$\frac{d^2B}{dX^2}-\frac{MAB}{S}=0 \qquad (3.37)$$

3.7 Numerical Solution Collocation Methodn(Interface Modeling) :

These method are based on the concept of interpolation of unequally spaced points; that is, choosing a function, usually a polynomial, that approximates the

solution of a differential equation in the range of integration, $x_0 \leq x \leq x_f$, and determining the coefficients of that function from set of base points. Let us again consider the set of the differential equations of orthogonal collocation method for the first derivative and the second can be written in condensed form. For the first derivative of y is then taken as:

$$\frac{dy}{dx} = f(x, y) \tag{3.38}$$

$$Ay = f(x, y) \quad \text{or} \quad \sum_{j=1}^{n+2} A_{ij} y_j = f(x, y)$$

So
$$\frac{dy}{dx} = \sum_{j=1}^{n+2} A_{ij} y_j \tag{3.39}$$

For the second derivative of y is then taken as:

$$y'' = \frac{d^2 y}{dx^2} = f(x, y, y') \tag{3.40}$$

$$By = f(x, y, y') \quad \text{or} \quad \sum_{j=1}^{n+2} B_{ij} y_j = f(x, y, y')$$

So
$$\frac{d^2 y}{dx^2} = \sum_{j=1}^{n+2} B_{ij} y_j \tag{3.41}$$

The exit improvement to be introduced into the collocation method is to choose orthogonal polynomials for trial function. For simplicity in deriving the derivative matrices we can also write the sreies as

$$y(x_j) = \sum_{j=1}^{N+2} d_i \, x_j^{i-1} \tag{3.42}$$

Taking the first and second derivatives of Eq. 3.42 we evaluate them at the collocation points. We take the collocation points as the N roots: these roots are between 0 and 1 ($x_1 = 0$ and $x_{N+2} = 1$). The location of the n internal collocation points (x_2 to x_{N+1}) are determined from the roots of the polynomial Pn (x) = 0, this points is described as following.

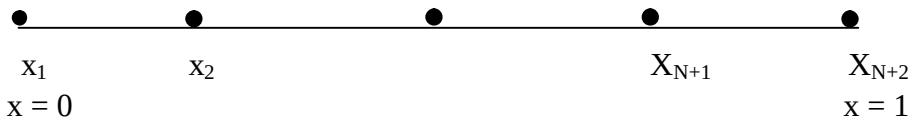

Figure 3.5 Collocation Points Position.

Table 3.2 Polynomial root and weighting (Bruce A.Finlayson)

N	x_j
1	0.5000000000
2	0.2113248654
	0.7886751346
3	0.1127016654
	0.5000000000
	0.8872983346
4	0.0694318842
	0.3300094783
	0.6699905218
	0.9305681158
5	0.0469100771
	0.2307653450
	0.5000000000
	0.7692346551
	0.9530899230
6	0.0337652429
	0.1693953068
	0.3806904070
	0.6193095931
	0.8306046933
	0.9662347571

The derivatives of Eq. 3.42 at the N+2 collocation points are

$$\frac{dy}{dx}\left(x_j\right) = \sum_{j=1}^{N+2} d_i (i-1) x_j^{i-2} \tag{3.43}$$

$$\frac{d^2y}{dx^2}\left(x_j\right) = \sum_{j=1}^{N+2} d_i (i-2)(i-2) x_j^{i-3} \tag{3.44}$$

The equations above could be written in matrix notation Q , C and D. Matrices Q , C and D are matrices of size (N+2) ×(N+2). Equations (3.42) may be presented in matrix notation as

$$y = Q.d \tag{3.45}$$

Where d is the matrices of coefficient and

$$Q_{j_i} = x_j^{i-1} \begin{cases} i=1,2,\ldots\ldots\ldots\ldots N+2 \\ j=1,2,\ldots\ldots\ldots\ldots N+2 \end{cases} \tag{3.46}$$

Solving Eq (3.42) for d we find

$$d = Q^{-1}.y \tag{3.47}$$

from the derivative of y in Eq (3.43) which in the matrix form become

$$\frac{dy}{dx} = Cd = CQ^{-1}y = Ay \tag{3.48}$$

where

$$C_{ji} = (i-1)x_j^{i-2} \tag{3.49}$$

For the derivative of y in Eq (3.44) can be written in matrix form

$$\frac{dy}{dx} = CQ^{-1}y = Ay \tag{3.50}$$

$$\frac{d^2y}{dx^2} = DQ^{-1}y = By \tag{3.51}$$

Where

$$D_{ji} = (i-1)(i-2)x_j^{i-3} \tag{3.52}$$

With *orthogonal collocation method,* the collocation equation made an A_i, B_i, explicit to solved by successive approximation method

$$\frac{d^2y}{dx^2} = \sum_{j=1}^{n+2} D_{ij}y_j ; \frac{dy}{dx} = \sum_{j=1}^{n+2} C_{ij}y_j$$

3.7.1.1. For Component A (film Model):

Equation (3.34) can be written in term of collocation method as follows:

$$\sum_{j=1}^{N+2} D_{ij}A_j - MA_iB_i = 0 \tag{3.53}$$

$$\sum_{j=1}^{N+2} D_{ij}A_j = MA_iB_i$$

$$\sum_{j=1}^{N+2} D_{ij}A_j - D_{ii}A_i + D_{ii}A_i = M.A_iB_i$$

$$\sum_{j=1}^{N+2} D_{ij}A_j - D_{ii}A_i = MA_iB_i - D_{ii}A_i$$

$$\sum_{j=1}^{N+2} D_{ij}A_j - D_{ii}A_i = A_i(MB_i - D_{ii})$$

The resulting collocation equation as follows:

$$A_i = \frac{\sum_{j=1}^{N+2} D_{ij}A_j - D_{ii}A_i}{(MB_i - D_{ii})} \tag{3.54}$$

3.7.1.2 For Component B :

Equation (3.37) can be written in term of collocation method as follows:

$$\sum_{j=1}^{N+2} D_{ij}B_j - \frac{MA_iB_i}{S} = 0 \tag{3.56}$$

$$\sum_{j=1}^{N+2} D_{ij} B_j = \frac{MA_i B_i}{S}$$

$$\sum_{j=1}^{N+2} D_{ij} B_j - D_{ii} B_i + D_{ii} B_i = \frac{MA_i B_i}{S} \longrightarrow \sum_{j=1}^{N+2} D_{ij} B_j - D_{ii} B_i = \frac{MA_i B_i}{S} - D_{ii} B_i$$

$$\sum_{j=1}^{N+2} D_{ij} B_j - D_{ii} B_i = B_i \left(\frac{MA_i}{S} - D_{ii}\right)$$

The resulting collocation equation as follows:

$$B_i = \frac{\sum_{j=1}^{N+2} D_{ij} B_j - D_{ii} B_i}{\frac{MA_i}{S} - D_{ii}} \tag{3.57}$$

3.8 The Development of plate Column Model:

The development of model is begun by forming mass balance for component A (H_2S) in gas phase and B $Fe_2(SO_4)_3$ in liquid phase. Within the element volume at thickness dz (see Figure 3.2) in tray column which will be below described:

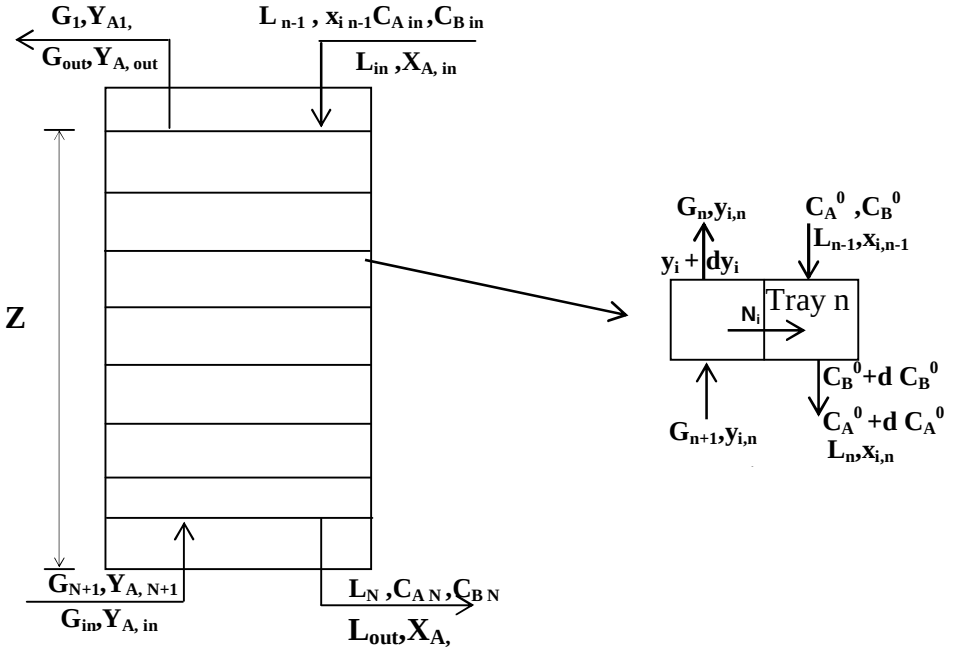

Figure 3.6 Absorption Flow Diagram in plate Column

3.8.1 Mass balance for component A (liquid phase):

If we apply the earlier assumptions, the assumption is that constant molar over flow rate that is all L will be constant and G will be constant. For steady state condition mass balance of component A can be stated as follows:

Rate of Absorption per unit cross-section = Increase in flow of unreacted A + Rate of reaction of A with B

$$L_{i,in}\, x_{i,\,in} + N_{i,z} = r_i a\, V + L_{i,out}\, x_{i,out}$$

$$0 = LC_A^{\,0}\big|_{z=z} + R' a\, S\,\Delta Z - L\,C_A^{\,0}\big|_{z=z+\Delta z} - k_2 C_A^{\,0} C_B^{\,0} S\,\Delta Z \tag{3.58}$$

$$0 = -\frac{L}{S}\frac{C_A^{\,0}\big|_{z=z+\Delta z} - C_A^{\,0}\big|_{z=z}}{\Delta Z} + \overline{R}\, a - k_2 C_A^{\,0} C_B^{\,0}$$

$$0 = -\frac{L}{S}\lim_{\Delta z \to 0}\left[\frac{C_A^{\,0}\big|_{z=z+\Delta z} - C_A^{\,0}\big|_{z=z}}{\Delta Z}\right] + \overline{R}\, a - k_2 C_A^{\,0} C_B^{\,0}$$

$$0 = -U\,\frac{d\,C_A^{\,0}}{dz} + E\,k_L\,a\left(C_{Ai} - C_A^{\,0}\right) - k_2 C_A^{\,0} C_B^{\,0}$$

$$\frac{dC_A^{\,0}}{dZ} = \frac{Ek_L a}{U}\left(C_{Ai} - C_A^{\,0}\right) - \frac{k_2}{U} C_A^{\,0} C_B^{\,0} \tag{3.59}$$

3.8.2 Mass balance for component A (Gas phase):

In the same manner mass balance of component A in gas phase (without reaction in gas phase) can be write as follows:

$$G_{i,in}\, y_{i,\,in} = G_{i,out}\, y_{i,out} + N_{i,z}$$

$$0 = G_V\, Y_A\big|_{z=z+\Delta z} - G_V\, Y_A\big|_{z=z} - E\,k_L\,a\left(C_{Ai} - C_A^{\,0}\right) S\,\Delta Z \tag{3.60}$$

$$0 = \frac{G_V}{S}\lim_{\Delta z \to 0}\left[\frac{Y_A\big|_{z=z+\Delta z} - Y_A\big|_{z=z}}{\Delta Z}\right] - Ek_L\,a\,(C_{Ai} - C_A^{\,0})$$

$$0 = \frac{G_V}{S}\frac{dY_A}{dZ} - E\,k_L\,a\left(C_{Ai} - C_A^{\,0}\right)$$

$$\frac{dY_A}{dZ} = \frac{Ek_L a}{G_m}\left(C_{Ai} - C_A^{\,0}\right) \tag{3.61}$$

3.8.3 Mass balance for component B (liquid phase):

Mass balance of component B in liquid phase can be stated as follows:

Decrease in concentration of unreacted B = Rate of reaction of B with A

$$0 = L\,C_B^{\,0}\big|_z - L\,C_B^{\,0}\big|_{z=z+\Delta z} - k_2 C_A^{\,0} C_B^{\,0} S\,\Delta Z \tag{3.62}$$

$$0 = -\frac{L}{S}\lim_{\Delta z \to 0}\left[\frac{C_B{}^0\big|_{z=z+\Delta z} - C_B{}^0\big|_{z=z}}{\Delta Z}\right] - k_2 C_A{}^0 C_B{}^0$$

$$0 = -\frac{L}{S}\frac{dC_B{}^0}{dZ} - k_2 C_A{}^0 C_B{}^0$$

$$\frac{dC_B{}^0}{dZ} = -\frac{k_2}{U} C_A{}^0 C_B{}^0 \tag{3.63}$$

When the reaction is very fast and irreversible, the absorbed gas (H_2S) to react in the film, the concentration of unreacted dissolved gas (H_2S) in the bulk of the liquid will be negligible small (we can usually put $dC_A{}^0/dZ = 0$), so the equation (3.59) lead to equation (3.64)

$$\frac{Ek_L a}{U}\left(C_{Ai} - C_A{}^0\right) = \frac{k_2 C_A{}^0 C_B{}^0}{U} \tag{3.64}$$

Substitution Eq (3.64) into Eq (3.63)

$$\frac{dC_B{}^0}{dZ} = -\frac{Ek_L a}{U}(C_{Ai} - C_A{}^0) \tag{3.65}$$

3.9 Numerical Solution Runge-Kutta Method

The most widely used method of integration for ordinary differential equations are the method of series of called Runge Kutta second, third, and fourth order, plus a number of other techniques that are variations on the Runge Kutta theme, and the Runge-Kutta integration formula is:

$$dy/dx = f(x,y) \tag{3.66}$$

$$y_{n+1} = y_n + \frac{1}{6}\left(k_1 + 2k_2 + 2k_3 + k_4\right) \tag{3.67}$$

$$k_1 = hf(x_n, y_n) \tag{3.68}$$

$$k_2 = hf\left(x_n + \frac{1}{2}h, y_n + \frac{1}{2}k_1\right) \tag{3.69}$$

$$k_3 = hf\left(x_n + \frac{1}{2}h, y_n + \frac{1}{2}k_2\right) \tag{3.70}$$

$$k_4 = hf\left(x_n + h, y_n + k_4\right) \tag{3.71}$$

3.9.1 Numerical Solution to Tray Column Modeling:

The application of Runge Kutta Metode to solve Eq (3.61) , and (3.65) yield the following equation:

$$B_1 = \Delta z \; f_1\left(C_A{}^0{}_n, C_B{}^0{}_n\right)$$

$$B_2 = \Delta z \; f_1\left(C_A{}^0{}_n + \frac{A_1}{2}, C_B{}^0{}_n + \frac{B_1}{2}\right)$$

$$B_3 = \Delta z \; f_1\left(C_A{}^0{}_n + \frac{A_2}{2}, C_B{}^0{}_n + \frac{B_2}{2}\right)$$

$$B_4 = \Delta z \; f_1\left(C_A{}^0{}_n + A_3, C_B{}^0{}_n + B_3\right)$$

$$Ay_1 = \Delta z \; f_2\left(C_A{}^0{}_n, C_B{}^0{}_n, Y_{An}\right)$$

$$Ay_2 = \Delta z \; f_2\left(C_A{}^0{}_n + \frac{A_1}{2}, C_B{}^0{}_n + \frac{B_1}{2}, Y_{An} + \frac{Ay_1}{2}\right)$$

$$Ay_2 = \Delta z \; f_2\left(C_A{}^0{}_n + \frac{A_2}{2}, C_B{}^0{}_n + \frac{B_2}{2}, Y_{An} + \frac{Ay_2}{2}\right)$$

$$Ay_2 = \Delta z \; f_2\left(C_A{}^0{}_n + A_3, C_B{}^0{}_n + B_3, Y_{An} + Ay_3\right)$$

$$C_B{}^0{}_{,n+1} = C_B{}^0{}_{,n} + \frac{1}{6}\left[B_1 + 2B_2 + 2B_3 + B_4\right]$$

$$y_{A,n+1} = y_{A,n} + \frac{1}{6}\left[Ay_1 + 2Ay_2 + 2Ay_3 + Ay_4\right]$$

Description :

$$f_1 = -\frac{Ek_La}{U}\left(C_{Ai} - C_A{}^0\right) \tag{3.72}$$

$$f_2 = \frac{E\,k_L\,a}{G_m}\left(C_{Ai} - C_A{}^0\right) \tag{3.73}$$

Where E at equations (3.61) and (3.65) above is the enhancement factor computed by using certain interface mass transfer model (film). If we used film model, the governing equation has been solved using approximate method by van Krevelen and Hoftijzer (1948) in Danckwerts (1970) approach as follows:

$$E = \sqrt{M + 1} \tag{3.74}$$

Where

$$M = \frac{D_A k_2 C_{Bo}}{k_L{}^2}; \quad and \quad E_i = \left(1 + \frac{D_B C_{B0}}{z.D_A C_{Ai}}\right)$$

The interfacial concentration of H_2S gas dissolved at interface C_{Ai}, estimated from solubility data following Henry's law and by considering gas side resistance,

the soluble gas is being transported across both films by a steady-state process, for which one can write:

$$R' = k_G(p_A - p_{Ai}) = E.k_L(C_{Ai} - C_{A0}) \quad , \quad p_{Ai} = He.C_{Ai}$$

$$C_{Ai} = \frac{k_G P_A + E.k_L C_A^{\,0}}{E.k_L + k_G He} \tag{3.75}$$

Mass transfer coefficient in liquid and gas sides appeased in the previous equation, we obtained from the empirical correlation from literature.

Sherwood and Holloway (1940) in Danckwerts (1970) give the following expression for a and k_L

$$a = 0.38\left(\frac{u}{u_t}\right)^{0.775}\left(\frac{u\rho}{nd\mu_L}\right)^{0.125}\left(\frac{g\rho}{d\sigma}\right)^{\frac{1}{3}} \tag{3.72}$$

Here u_t is the velocity of rise of the bubbles in the froth (taken to be 26.5cm/s under most conditions), n the number of holes per unit area of plate.

As regards the liquid side mass transfer coefficient k_L can be calculated from the formulae

$$k_L = 0.42\left(\frac{g\mu}{\rho}\right)^{\frac{1}{3}}\left(\frac{D_{AB}\rho}{\mu_L}\right)^{\frac{1}{2}} \tag{3.73}$$

For sieve trays, Chan and Fair (1983) give the following expression for gas-phase mass-transfer coefficient k_G a (Robert H. Perry,1999).

$$k_G a = \frac{316 D_G^{1/2}(1030 f + 867 f^2)}{h_L^{1/2}} \tag{3.74}$$

Where : f = approach to flood, fractional

The Hirschfelder, Bird, Spotz equation can be used for estimating the diffusivity of a binary gas pair of A and B molecules , as follows:

$$D_G = \frac{0.001858\ T^{1.5}\left[\frac{1}{M_A} + \frac{1}{M_B}\right]^{1/2}}{P\sigma_{AB}^2\Omega_D} \tag{3.75}$$

D_G - Binary gas phase diffusivity of A in B in cm^2/s ,

P - absolute pressure in atm , T - Absolute temperature in ^{o}K

M_A , M_B - molecular weight of constituents A and B, respectively

σ_{AB} - Lennard-Jones collision diameter in Angstroms

Ω_D - Collision integral for molecular diffusion.

If σ_{AB} is not known for a given binary system composed of a non-polar molecular pair, construct it using,

$$\sigma_{AB} = (\sigma_A + \sigma_B)/2 \qquad (3.76)$$

Table 3.3 Lennadr - Jones Potential Parameters

Molecule	Compound	σ, Å	ε/k, K
$CH_3COOC_2H_5$	Ethyl acetate	5.205	521.3
n-C_5H_{12}	n-Pentane	5.784	341.1
$C(CH_3)_4$	2,2-Dimethylpropane	6.464	193.4
C_6H_6	Benzene	5.349	412.3
C_6H_{12}	Cyclohexane	6.182	297.1
n-C_6H_{14}	n-Hexane	5.949	399.3
Cl_2	Chlorine	4.217	316.0
F_2	Fluorine	3.357	112.6
HBr	Hydrogen bromide	3.353	449.0
HCN	Hydrogen cyanide	3.630	569.1
HCl	Hydrogen chloride	3.339	344.7
HF	Hydrogen fluoride	3.148	330.0
HI	Hydrogen iodide	4.211	288.7
H_2	Hydrogen	2.827	59.7
H_2O	Water	2.641	809.1
H_2O_2	Hydrogen peroxide	4.196	289.3
H_2S	Hydrogen sulfide	3.623	301.1
Hg	Mercury	2.969	750.0
I_2	Iodine	5.160	474.2
NH_3	Ammonia	2.900	558.3
NO	Nitric oxide	3.492	116.7
NOCl	Nitrosyl chloride	4.112	395.3
N_2	Nitrogen	3.798	71.4
N_2O	Nitrous oxide	3.828	232.4
O_2	Oxygen	3.467	106.7
PH_3	Phosphine	3.981	251.5
SF_6	Sulfur hexafluoride	5.128	222.1
SO_2	Sulfur dioxide	4.112	335.4
$SnBr_4$	Stannic bromide	6.388	563.7
UF_6	Uranium hexafluoride	5.967	236.8

Values of the collision integral for molecular diffusion Ω_D as a function of a dimensionless temperature f (kT/ε_{AB}). The Ω_D in equation 3.73 is related to the absolute temperature, as follows:

$$\Omega_D = \left[44.54 \left(\frac{T}{\sqrt{\frac{\varepsilon_A}{k}\frac{\varepsilon_B}{k}}} \right)^{-4.909} + 1.911 \left(\frac{T}{\sqrt{\frac{\varepsilon_A}{k}\frac{\varepsilon_B}{k}}} \right)^{-1.575} \right]^{0.1} \qquad (3.77)$$

and

$$\frac{\varepsilon_{AB}}{k} = \sqrt{\left(\frac{\varepsilon_A}{k}\right)\left(\frac{\varepsilon_B}{k}\right)} \tag{3.78}$$

Individual values of σ_A, σ_B and ε_A/k , ε_B/k are given in Table 3.4

In liquids, it is possible to estimate the diffusivity of a non-electrolyte solute in dilute solution (in principle, at infinite dilution) using the Wilke-Chang correlation(J.D.Seader1998), given as Equation

$$D_{AB} = 7.4 \times 10^{-8} (\varphi M_B)^{0.5} \frac{T}{\mu_B V_A^{0.6}} \tag{3.79}$$

M_B - the molecular weight of the solvent B, μ_B - Viscosity of solvent B in cp

φ - Association parameter of solvent B

V_A Molal volume of solute A at normal boiling point (cm^3/gmol)

The viscosity of the ferric solution (g/cm.s) as a function of the ferric sulfate concentration could be correlated by (S. Ebrahimi, 2002)

$$\mu_B = 0.0114\, C^2_{Fe_2(SO_4)_3} + 0.0015\, C_{Fe_2(SO_4)_3} + 0.0062 \tag{3.80}$$

3.10 Kinetics of the absorption of H_2S into aqueous $Fe_2(SO_4)_3$:

The reaction rate constant (m^3/kmol.s) values were obtained as a function of temperature (S. Ebrahimi, 2002)

$$\log k = 9.3855 - \frac{2636.6}{T} \tag{3.81}$$

An important parameter that characterises how the mass transfer is affected by the chemical reaction is the reaction-diffusion modulus (Hatta number (Hatta, 1932)). In case of an irreversible reaction with second order, 1,1-reaction, species A and B are converted into one or more products

$$\sqrt{M} = \frac{\sqrt{D_A k_2 C_{BL}}}{k_L} \tag{3.82}$$

The Equations (3.61) and (3.65) is non-linear ordinary differential equation system that is solved by Runge Kutta method fourth order to produce the profile of Y_A and

C_{B0} in column. From this profile, so the percent recovery of H_2S is obtained by the equation:

$$\%\text{Recovery}H_2S = \frac{\frac{Y_{Ain}}{1-Y_{Ain}} - \frac{Y_{Aout}}{1-Y_{Aout}}}{\frac{Y_{Ain}}{1-Y_{Ain}}} \tag{3.83}$$

CHAPTER FOUR

4. RESULTS AND DISCUSSION

This research comprises two parts: design and simulation of absorption of H_2S from refinery flue gas in the sieve tray coplumn. In design and simulation steady state and isothermal condition are assumed. The refinery flue gas flow rate is fed to the bottom of the sieve tray absorption column and is sweetened by counter-currently flowing of $Fe_2(SO_4)_3$ solvent. The refinery flue gas flows upwards through the perforation and dispersed into the flowing $Fe_2(SO_4)_3$ solvent over the plate. There is no liquid seal in case of trays without downcomer and the liquid weeps through the holes at low flow rates, reducing the efficiency of plate.

4.1 Design of absorption column:

Design of plate column for absorption of H_2S from refinery flue gas is carried at 30°C, and the column is operated at atmospheric pressure, the refinery flue gas flow rate is 2401 kg/h with mole fraction of H_2S in inlet refinery flue gas of 0.29, the liquid flow rate 10000cm^3/s, the concentration of $Fe_2(SO_4)_3$ in inlet solvent 0.002mol/cm^3.

In the design of the system the sieve tray the holes layout is a ranged inequilateral triangular pitch. Design of sieve tray column for absorption H_2S involves many common steps of calculation such as determination of column diameter, split of tray area and downcomer areas, number of theoretical plates, efficiency, plate hydraulic design, etc. Tray hydraulic parameters such at weir crest, weir height, dry plate pressure drop are also needed. The effect of gas flow conditions that constrain equipment design such as flooding consideration, sieve tray weeping, liquid entrainment an also investigated.

4.1.1 Plate spacing (t)

Plate spacings of 0.3 to 0.6 m will normally be used (Chem. Eng Vol.6) , Chosen plate spacing of 0.5 m is considered for the first trial to calculate capacity parameter (C_F) for the estimation of maximum allowable gas velocity through the net plate area.

4.1.2 Plate thickness

Chosen plate thickness l = 2mm

4.1.3. Estimation of column diameter

The column diameter is determined from the flooding correlation for a chosen plate spacing. The superficial gas velocity (v_{nf}) at flooding through the net area relates to liquid and vapor densities according to Fair's correlation.C_O is an empirical constant, depends on tray spacing and can be estimated against the flow parameter (F_{LG}) based on mass flow rate of liquid (L) and vapor (G). To calculate the column diameter an estimate of the net area A_n is required.

1ST trial is started with the following considerations:

- Design is performed for 75% flooding at maximum gas flow rate.
- Total downcomer top and bottom seal area is 10% of the net area.

4.1.3.1.1 Hole diameter, hole pitch

The hole diameters (d_o) from 3 to 12 mm (Treybal, 1981) are commonly used, for this research 4.5mm is used. The centre to centre distance between two adjacent holes is hole pitch (p_t) , The normal range of p_t is from 2.5 to 5 times of do. For this research 2.5 d_o = 2.5 x 4.5 =11.25 mm is used.

The flooding constant C_F dependent on the hole area to active area ratio. For triangular pitch:

$$\frac{A_o}{A_a} = \frac{hole\ \ area}{active\ \ area} = 0.907\left(\frac{d_o}{p_t}\right)^2 = 0.907\left(\frac{4.5}{11.25}\right)^2 = 0.14512$$

$\alpha = 0.0744\mathbf{t} + 0.01173 = (0.0744 \times 0.5) + 0.01173 = 0.04893$

$\beta = 0.0304\mathbf{t} + 0.015 = (0.0304 \times 0.5) + 0.015 = 0.0302$

Flow parameter (F_{LG}) in Eq (3.5) based on mass flow rate,

$$F_{LV} = \frac{L'}{G'}\left(\frac{\rho_G}{\rho_L}\right)^{0.5} = \frac{q}{Q}\left(\frac{\rho_L}{\rho_G}\right)^{0.5} = \frac{10000}{7511447.63}\left(\frac{1899}{1.367752}\right)^{0.5} = 0.0496$$

The flooding constant C_F calculated from Eq (3.3)

$$C_F = \left[\alpha \log\frac{1}{F_{LV}} + \beta\right]\left(\frac{\sigma}{0.020}\right)^{0.2} = \left[0.04893 \times \log\frac{1}{0.0622} + 0.0302\right]\left(\frac{0.02}{0.020}\right)^{0.2}$$

$C_F = 0.0940275$

$$v_F = C_F\left(\frac{\rho_L - \rho_G}{\rho_G}\right)^{0.5} = 0.09490275 \times \left(\frac{1899 - 1.367752}{1.367752}\right)^{0.5} = 3.50233 m/s \; at \; flooding$$

The design gas velocities (v_F) is generally 75-85% of v_{nf} for non-foaming liquids and 75% or less for foaming liquids subject to acceptable entrainment and plate pressure drop.

$v = 0.75\ v_F = 0.75 \times 3.50233 = 2.63 m/s$

Net area available for gas flow (A_n)

$$A_n = \frac{Q}{v} = \frac{0.751144763}{2.63} = 0.3 m^2$$

4.1.3.2 Total tower cross-section area (A_t):

Tentatively choose a weir length W = 0.75 D. Table 3.1, the tray area used by one downspout = 11.255%

$$A_t = \frac{A_n}{1 - tray \; area \; used \; by \; one \; downspout} = \frac{0.3}{1 - 0.11255} = 0.34 m^2$$

Tower diameter

$$D = \sqrt{\frac{4A_t}{\pi}} = \sqrt{\frac{4 \times 0.34}{\pi}} = 0.7 m$$

W = 0.75 x 0.7 = 0.525 m

Downcomer area : A_d = 0.11255 x A_t = 0.11255 x 0.34 = 0.038 m^2

Active area : $A_a = A_t - 2A_d$ = 0.34 - (2 x 0.038) = 0.26 m^2

4.1.4. Tray hydraulic parameters:

4.1.4.1. Weir crest h_1 and weir height h_w :

$$\frac{q}{W} = \frac{1\times10^{-2}}{0.525} = 0.019 \ \ m^3/m.s$$

Tray h_1 = 50 mm = 0.05 m

$$\frac{h_1}{D} = \frac{0.05}{0.7} = 0.0714286 \ , \ \frac{D}{W} = \frac{1}{0.75} = 1.3333$$

From Eq. (3.14)

$$\left(\frac{W_{eff}}{W}\right)^2 = (1.3333)^2 - \left[\left((1.3333)^2 - 1\right)^{0.5} + 2\times0.0714286 \times 1.3333\right]^2 = 0.792307$$

From Eq. (3.13)

$$h_1 = 0.666\ (0.019)^{2/3}(0.792307)^{2/3} = 0.055476$$

Repeat with h_1 = 0.0055476, $\frac{h_1}{D} = 0.07925153$, $\left(\frac{W_{eff}}{W}\right)^2 = 0.763264$

h_1 = 0.05687 m

Repeat with h_1 = 0.05687 , $\frac{h_1}{D} = 0.081249$, $\left(\frac{W_{eff}}{W}\right)^2 = 0.755576$

h_1 = 0.057259 m

Repeat with h_1 = 0.057259 , $\frac{h_1}{D} = 0.0817996$, $\left(\frac{W_{eff}}{W}\right)^2 = 0.753438$

h_1 = 0.057367986 m

Repeat with h_1 = 0.0573679 , $\frac{h_1}{D} = 0.081954265$, $\left(\frac{W_{eff}}{W}\right)^2 = 0.753438$

h_1 = 0.057367986 m , OK

Set weir height h_w = 50 mm = 0.05 m.

4.1.4.2 Dry plate pressure drop h_D :

From Eq (3.17) $C_o = 1.09\left(\frac{d_o}{l}\right)^{0.25} = 1.09\left(\frac{0.0045}{0.002}\right)^{0.25} = 1.335$

$$\frac{A_o}{A_a} = 0.14512 \ \rightarrow \ A_o = 0.14512 \times A_a = 0.14512 \times 0.28 = 0.0406\ m^2$$

$$v_o = \frac{Q}{A_o} = \frac{0.751144763}{0.0406} = 18.4858\ m/s$$

μ_g = 0.0128 cp = 1.28 x 10^{-5} kg/m.s

$$Hole\ \ \text{Re}\ ynolds\ \ number = \frac{d_o v_o \rho_g}{\mu_g} = \frac{0.0045\times18.4858\times0.887904}{1.28\times10^{-5}} = 8888.9$$

Friction factor, for laminar flow conditions $f = 0.664Re^{-0.5}$ = 0.007, (Modelling in transport phenomena,Page. 67). g = 9.807m^2/s, l = 0.002 m

Dry plate pressure drop calculated from Eq. (3.16)

$$\frac{2h_D 9.807\times 1899}{18.4858^2\times 0.888} = 1.335\left[0.4\left(1.25-\frac{0.0406}{0.3}\right)+\frac{4\times 0.002\times 0.007}{0.0045}+\left(1-\frac{0.0406}{0.3}\right)^2\right]$$

h_D = 0.02 m

4.1.4.3 Hydraulic head h_L :

$$v_a = \frac{Q}{A_a} = \frac{0.751144763}{0.28} = 2.68 \ \ m/s$$

z = (D+W)/2 = (0.7 + 0.525)/2 = 0.6125 m

from Eq. (3.18)

$$h_L = 6.1\times 10^{-3} + (0.725\times 0.05) - (0.238\times 0.05\times 2.68\times (0.887904)^{0.5}) + 1.225\times \frac{0.01}{0.6125}$$

h_L = 0.025 m

4.1.4.4 Residual gas-pressure drop h_R :

From Eq. (3.19) $$h_R = \frac{6\times 0.02\times 1}{1899\times 4.5\times 9.807} = 0.00143 \ m$$

4.1.4.5 Total gas pressure drop h_G :

$h_G = h_D + h_L + h_R$ = 0.020199 + 0.02501499 + 0.00143188 = 0.046646 m

4.1.4.6 Pressure loss at liquid entrance h_2 :

A_{da} = 0.04 W = 0.04x 0.525 = 0.021 m^2

From Eq. (3.20) $$h_2 = \frac{3}{2g}\left(\frac{q}{A_{da}}\right)^2 = \frac{3}{2\times 9.807}\left(\frac{0.01}{0.021}\right)^2 = 0.034682 \ m$$

4.1.4.7 Backup in downspout h_3 :

From Eq. (3.21) $h_3 = h_G + h_2$ = 0.046646 + 0.034682 = 0.081329m

4.1.5.1 Check on Flooding:

From Eq.(3.22), $h_w+h_1+ h_3$ = 0.05 + 0.057368 + 0.081329 = 0.188697 m, which is well below t/2 = 0.5/2 = 0.25 m, No flooding and therefore the chosen t is satisfactory.

4.1.5.2 Check on Entrainment:

$$\frac{v}{v_F} = 0.75 \quad , \quad F_{LV} = \frac{q}{Q}\left(\frac{\rho_L}{\rho_G}\right)^{0.5} = 0.0496 \quad \text{(see tower diameter)}$$

From Fig. 3.4, E = 0.049. bellow 0.1 (acceptable). The recycling of liquid resulting from such enterainment is too small to influence the tray hydraulics appreciably

4.1.5.3 Check on weeping velocity :

For W/D = 0.75, the weir is set 0.3296 D = 0.3296 x 0.7 = 0.23072m, from center of the tower. Therefore Z = 2 x 0.23072 = 0.46144m.

All other quantities in Eq.(3.23) have been evaluated

$$\frac{v_{ow}\mu_G}{\sigma g_c} = 0.0229\left(\frac{\mu_G^2\rho_L}{\sigma g_c \rho_G d_o \rho_G}\right)^{0.379}\left(\frac{l}{d_o}\right)^{0.293}\left(\frac{2A_a d_o}{\sqrt{3}p'^3}\right)^{2.8/(Z/d_o)^{0.724}}$$

$$v_{ow} = \left(\frac{0.0229\times 0.02\times 1}{1.28\times 10^{-5}}\right)\times\left(\frac{\left(1.28\times 10^{-5}\right)^2\times 1899}{0.02\times 1\times\left(0.887904\right)^2\times 0.0045}\right)^{0.379}\times$$

$$\left(\frac{0.002}{0.0045}\right)^{0.293}\times\left(\frac{2\times 0.28\times 0.0045}{\sqrt{3}\times\left(0.01125\right)^3}\right)^{2.8/(0.46144/0.0045)^{0.724}} = 5.12\,m/s$$

The tray will not weep excessively until the gas velocity through the hole v_o (18.5/s) is reduced to close to this value. $v_o > v_{ow}$, So No weeping occur.

4.1.6 Determine the actul number of plates:

4.1.6.1 Determine the theoretical number of plates:

Equation 3.25 is a simplified method of estimating the number of theoretical plates. y_1= 0.288875, x_2 = 0, (no recirculated liquid), assuming 98% removal of H_2S is required, so y_2 = 0. 288875 - (0. 288875 x 0.98) = 0.00288, for solutions, H_2S-$Fe_2(SO_4)_3$ follows Henry's low constant , and at 30^{o}C m = 0.9

G = 108.78 kmol/hr , L = 170.952 kmol/hr , A = L/mG = 1.75

$$N_P = \frac{\ln\left[\frac{y_1 - mx_2}{y_2 - mx_2}\left(1-\frac{1}{A}\right)+\frac{1}{A}\right]}{\ln A} = \frac{\ln\left[\frac{0.288875-0}{0.00288-0}\left(1-\frac{1}{1.75}\right)+\frac{1}{1.75}\right]}{\ln 1.75} = 5.55$$

4.1.6.2 Determine the overall stage efficiency :

Estimation of the overall stage efficiency from Equation (3.26)

$$\log_{10} E_o = -0.773 - 0.415 \log_{10} X - 0.0896 (\log_{10} X)^2 \quad (3.26)$$

$$X = \frac{mM_{WL} \mu_L}{\rho_L} = \frac{0.9 \times 399.88 \times 0.062023}{1899} = 0.01175$$

$$\log_{10} E_o = -0.773 - 0.415 \log_{10} (0.01175) - 0.0896 (\log_{10} 0.01175)^2 = -0.306$$

$$E_o = 0.5$$

4.1.6.3 Actual number of plates:

Actual number of plates = N_P/ overall plate efficiency

$$N_a = \frac{5.55}{0.5} = 11 \; plates$$

4.1.6.4 The height of the tower:

The height of the tower is given by equation (3.27):

$$Z = (N_a\text{-}1)(\text{tray spacing}) + \text{top height} + \text{bottom height} \quad (3.27)$$

Let top height + bottom height = 2 Plate spacing = 2×0.5 = 1 m

$Z = (N_{actual} - 1)$ (tray spacing) + 2 Plate spacing = (11-1)× (0.5) + 1 = 6 m

Table 4.1 Summary of the Design Results

Parameters	Values
Total plate area, A_t (m^2)	0.340
Tower diameter D (m)	0.700
Tower Height, Z (m)	6.000
Tray spacing, t (m)	0.500
Number of theoretical stages, N_P	5.550
Overall Efficiency, E_o	0.500
Number of actual stages, N_a	11.000

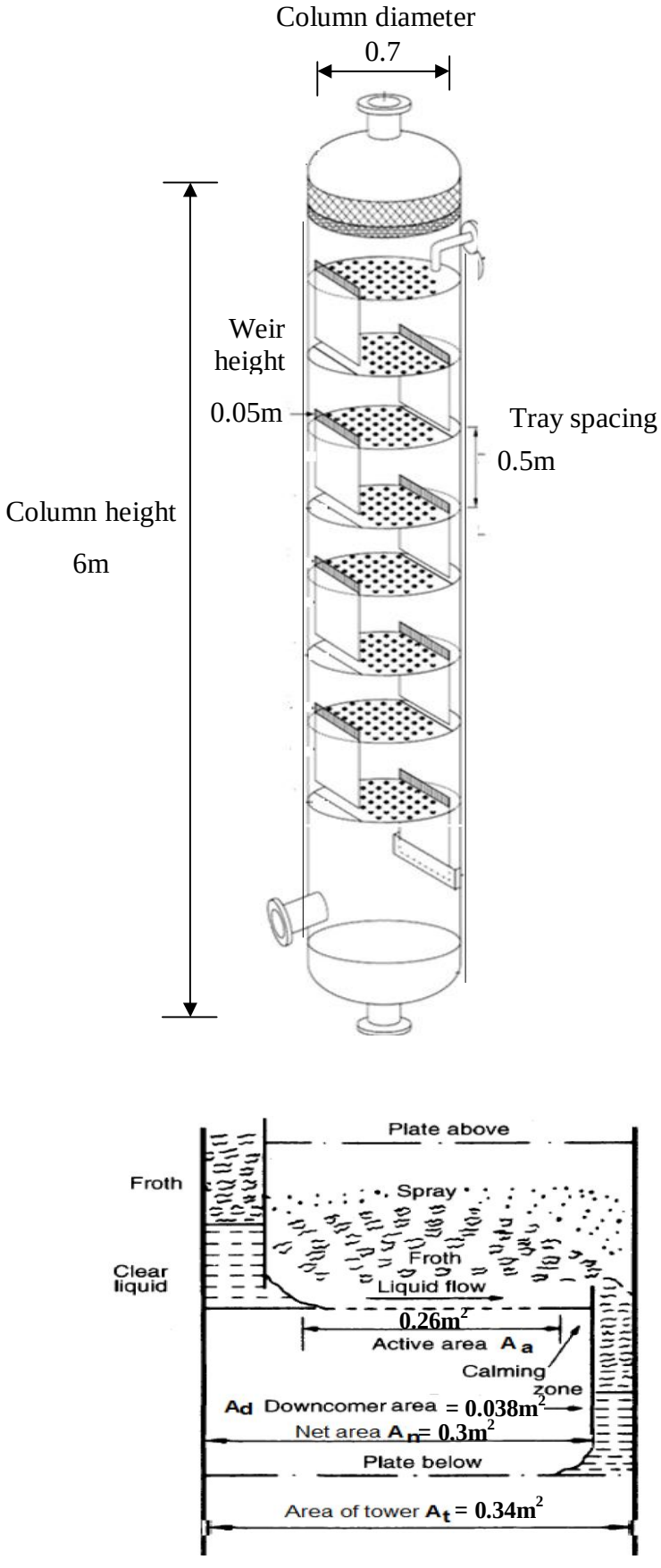

Figure 4.1 Sieve Tray Column Details.

4.2. Results and Discussion of Simulation:

In the present study, has been developed for the simulation of H_2S absorption column using $Fe_2(SO_4)_3$ solutions. The model adopts the film theory and assumes steady state and isothermal condition. In simulation research the system studied comprises a sieve tray column 70 cm in diameter filled with sieve trays 0.5 m spacing to the height of 6 m. Simulation the absorption of H_2S from refinery flue gas available at 30°C, and column is operated at atmospheric pressure, the feed refinery flue gas flow rate is 2401 kg/h with mole fraction of H_2S in inlet refinery flue gas is 0.29, the liquid flow rate 10000cm^3/s, the concentration of $Fe_2(SO_4)_3$ in inlet absorbent 0.002mol/cm^3

The distribution of mole fraction H_2S in gas phase, y_A, in tray column, and concentration distribution of $Fe_2(SO_4)_3$ in liquid phase, C_B, in tray column as a function of axial position in sieve tray column is show at Figure 4.2. Also study variation of the enhancement factor with Hatta number with E_i (enhancement factor corresponding to instantaneous reaction) as parameter are showed at Figure 4.3 to Figure 4.5. The effect of liquid flow rate, flow rate of refinery flue gas, concentration of $Fe_2(SO_4)_3$ in inlet solvent, and temperature on percentage of H_2S absorbed are shown at Figure 4.5 to Figure 4.13. Liquid flow rate was varied from 5 to 20 liter/s, refinery flue gas flow rate was varied from 700 to 950 liter/s, the concentration of $Fe_2(SO_4)_3$ in inlet absorbent was varied from 0.002 to 0.004 mol/cm^3 and temperature was varied from 30 to 50^0C.

4.2.1 Distribution of Mole Fraction and Concentration Distribution in tray Column:

Figure 4.2 depicts the prediction results of the distribution of mole fraction H_2S in gas phase, y_A, and concentration distribution of $Fe_2(SO_4)_3$ in liquid phase as a

function of axial position in sieve tray column. Simulation conditions : y_{Ain} = 0.29, G = 751144.763 cm^3/s, L= 10 liter/s $C_{(Fe\text{-}EDTA)}$ = 0.002 mol/cm^3. and temperatures 30°C. and pressure = 1 atm.

Table 4.2: Distribution of H_2S in Gas Phase and concentration of $Fe_2(SO_4)_3$ in Liquid Phase in sieve trays column.

Z(cm)	$10^2 \times C_B$	Y_A
0	0.2000	0.00335
60	0.1990	0.00536
120	0.1970	0.00858
180	0.1940	0.01370
240	0.1890	0.02182
300	0.1810	0.03461
360	0.1690	0.05455
420	0.1510	0.08511
480	0.1230	0.13082
540	0.0833	0.19664
600	0.0290	0.28649

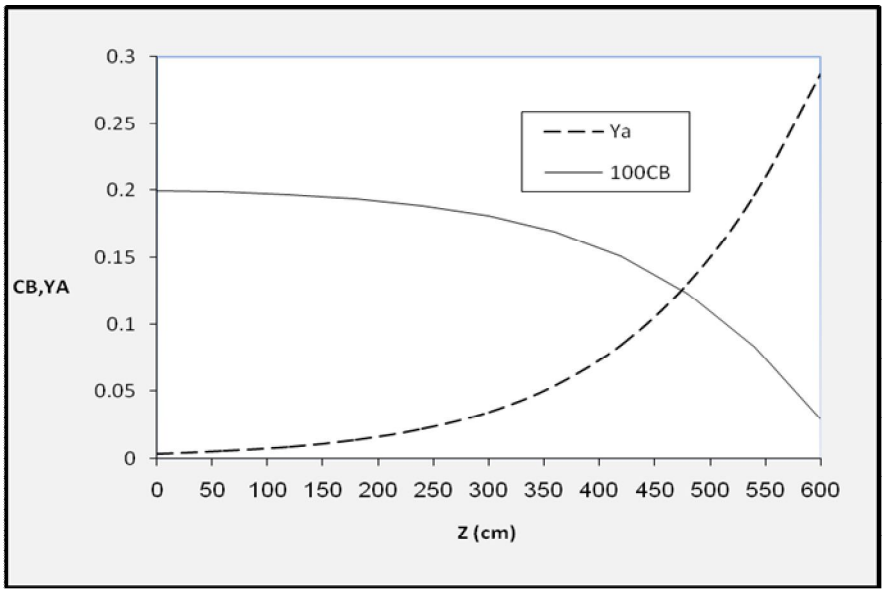

Figure 4.2 Distribution of concentration $Fe_2(SO_4)_3$ liquid phase and distribution of mole fraction H_2S in gas phase in sieve trays column.

In this figure, Z = 0 indicates the top of column and Z = 6 m indicates bottom of column. Figure 4.2 shows that the mole fraction of H_2S in gas phase increases rapidly from top to bottom while concentration of $Fe_2(SO_4)_3$ in liquid phase decreases slowly due to the amount of B as in excess to that required for theoretical reaction.

4.2.2 Variation of the Enhancement Factor with Hatta Number for Different value of E_i

This part presents a summary of the important features of the effect of chemical reaction on the absorption process expressed in the terms of enhancement factor. Figure 4.3 and Figure 4.4 shows enhancement factor (E) versus Hatta number $\sqrt{M}$ plot with E_i as parameter for absoprtion of H_2S in $Fe_2(SO_4)_3$ solution of finite depth accompanied by an irreversible second order reaction in the sieve tray column. Simulation conditions : H_2S inlet mole fraction was y_{Ain} = 0.29, G = 751144.763 cm^3/s, L= 10000 cm^3/s, $C_{(Fe2(SO4)3)}$ was 0.002 mol/cm^3, temperature 30°C.and pressure = 1 atm

Figure 4.3 shows numerical simulation results for the enhancement factor as a function of $\sqrt{M}$ according to the film theory for different values of E_i . For a given value of Ei an increase in $\sqrt{M}$ brings about an increase in E. The similarity between this figure and the familiar van Krevelen Hoftijzer plot for isothermal absorption of H_2S is apparent, one can find a remarkable similarity between Fig 4.3 and the traditional E versus $\sqrt{M}$ plots. For agiven E_i, the enhancement factor tends to reach an asymptotic value which is determined by the instantaneous reaction regime. Increasing the value of E_i will increase the amount of H_2S absorbed and value of E will increase proportionally.

Table 4.3: Variation of the Enhancement Factor with Hatta Number for different value of E_i

M^0.5	E for Ei= 4	E for Ei= 20	E for Ei= 50
00	01.000	01.000	01.000
10	3.690	07.895	08.914
30	3.979	14.182	16.942
50	3.994	16.402	19.171
70	3.996	17.502	19.991
90	3.997	18.155	20.368
100	3.997	18.390	20.482

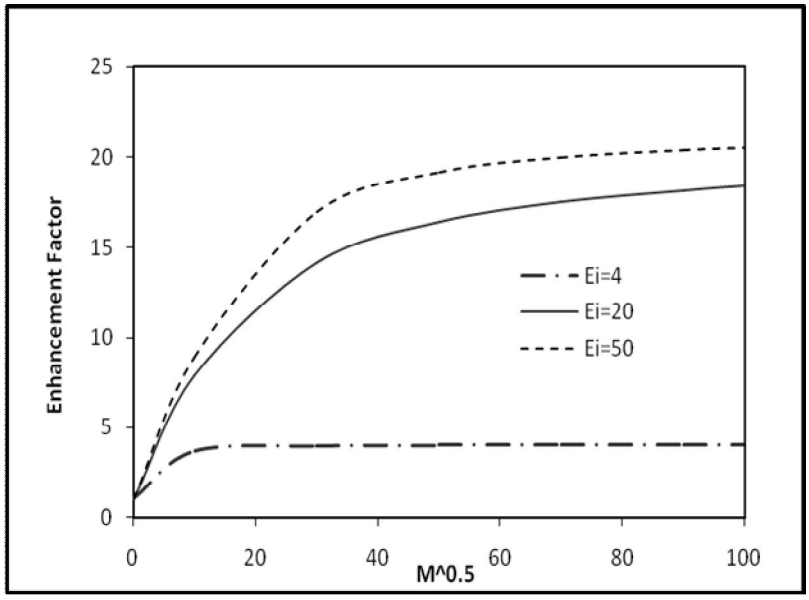

Figure 4.3 Variation of the Enhancement Factor with Hatta Number for Different values of Ei

With the same value of parameter used in Figure 4.3, E is plotted as a function of √M with the value of E_i = 6.6 in Figure 4.3. In this figure shows the compares between the numerical simulation data of the film model and Krevelen and Hoftijer equation (adapted as per Eq. (2.39)) for enhancement is given for the same asymptotic enhancement factor.

Table 4.4: Relationship between simulation data and Krevelen Equation for Enhancement factors E_i = 6.6

√M	M	(Simulation Data)	(Equation Krevelen)
0.0001	0.01	1.003	1.003
1	1	1.299	1.297
2	4	1.937	1.924
4	16	3.192	3.151
6	36	4.110	4.050
8	64	4.756	4.681
10	100	5.201	5.126

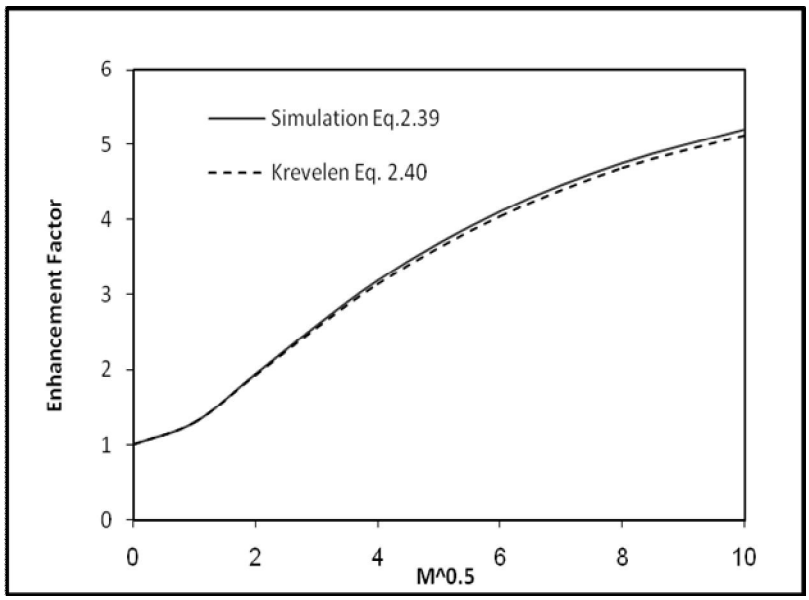

Figure 4.4 Relationship between simulation data and Krevelen and Hoftijer equation for Enhancement factors Ei = 6.6

With the same value of parameter used in Figure 4.3 with different concentrations of $Fe_2(SO_4)_3$ (0.001, 0.002, and 0.003 mol /cm^3). The variation of the

enhancement factor at different $C_{Fe2(SO4)3}$ is simulated in Figure 4.5 the result shows the effect of the concentrations of $Fe_2(SO_4)_3$ on the enhancement factor.

Table 4.5 Effect of $C_{Fe2(SO4)3}$ on Enhancement factors as function of √M

√M	E for C_B=0.001	E for C_B=0.002	E for C_B= 0.003
0	1.000	1.000	1.000
1	1.286	1.299	1.306
2	1.828	1.937	2.002
4	2.682	3.192	3.550
6	3.148	4.110	4.888
8	3.148	4.751	5.993
10	3.542	5.201	6.901

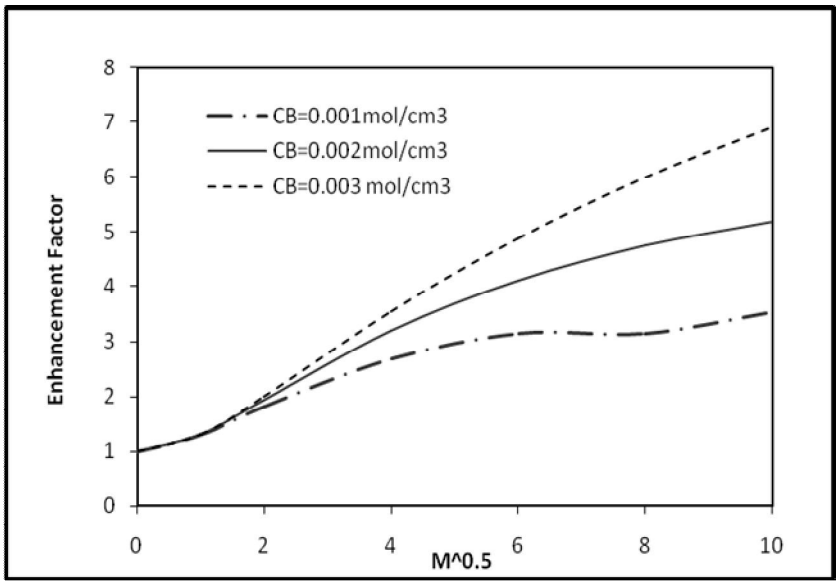

Figure 4.5 Effect of $C_{Fe2(SO4)3}$ on Enhancement factors as function of √M

The enhancement factor increases with increased concentration of $Fe_2(SO_4)_3$ because with increasing $C_{Fe2(SO4)3}$ increasing chemical reaction rate, i.e. increasing Hatta number, enhancement of mass transfer occurs resulting in an increased

concentration. They are better known when the solution behaves more like pure H_2O. A decrease in the $Fe_2(SO_4)_3$ concentration will decrease the amount of H_2S removed from the refinery flue gas and this could affect the statistical results; the difference of removal from one run to another could be so small that there would not be much difference between results.

4.2.3 Effect of Temperature on H_2S Removal Efficiency

In general, temperature is an important parameter influencing reaction kinetics. This indicates that the reaction rate constant is temperature dependent and that elevated temperatures lead to a greater reaction rate constant, k. If the rise in temperature is large enough it will affect the rate of mass transfer (absorption) because of its affect on solubility, diffusivity and reaction rate constant.

Figure 4.6 and Figure 4.7 shows the measurements of H_2S absorption removal into $Fe_2(SO_4)_3$ solution under different temperatures in the sieve tray column. In these cases, simulation conditions: H_2S inlet mole fraction is $y_{Ain} = 0.29$, G = 751144.763 cm^3/s, L= 10000 cm^3/s, $C_{(Fe\text{-}EDTA)} = 0.002$ mol/cm^3, pressure = 1 atm and the operating temperatures are range between 30-50 ℃.

Figure 4.6 shows; An increase in the value of the temperature also produces an increase on the %removal of H_2S. According to the principle of molecular dynamics, the rate constant of reaction and the diffusion coefficient increase with the increase in the temperature, and this is beneficial to improve the absorption rate .In an absorber, the transfer of H_2S from refinery flue gas into $Fe_2(SO_4)_3$ liquid brings about a heating effect.

Also Figure 4.7 shows indicates that the effect of temperature but with difference concentration of $Fe_2(SO_4)_3$ (0.002, 0.0025, and 0.003 mol/cm^3). For %removal of H_2S is given the same result in Figure 4.5 .

Nevertheless, The increasing of temperature of course will reduce the solubility of H_2S in $Fe_2(SO_4)_3$ liquid absorbent and raise the liquid side resistance, but the increasing of temperature would also increase gas phase mass transfer coefficient that caused gas side resistance become decreases . An increase in temperature causes a rise in the energy levels of the molecules involved in the reaction, so the rate of the reaction increases. Similar to previous results, the observed absorption rate increases with increasing temperature and decrease with a decrease in temperature

Table 4.6 Effect of Temperature on H_2S Removal Efficiency

T(C)	% Removal Efficiency
30	97.327
35	97.697
40	98.137
45	98.594
50	99.013

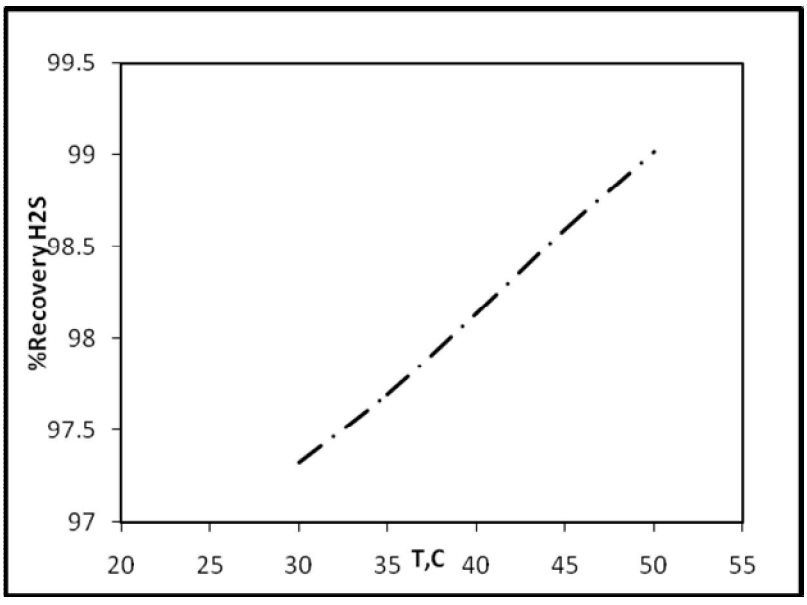

Figure 4.6: Temperature influence on the % Removal

Table 4.7: Temperature Influence on the % Removal with different solvent concentration of $Fe_2(SO_4)_3$

T(C)	C_{Bin}= 0.002	C_{Bin}= 0.0025	C_{Bin}= 0.003
30	97.327	97.884	98.308
35	97.697	98.298	98.721
40	98.137	98.730	99.108
45	98.594	99.123	99.428
50	99.013	99.440	99.662

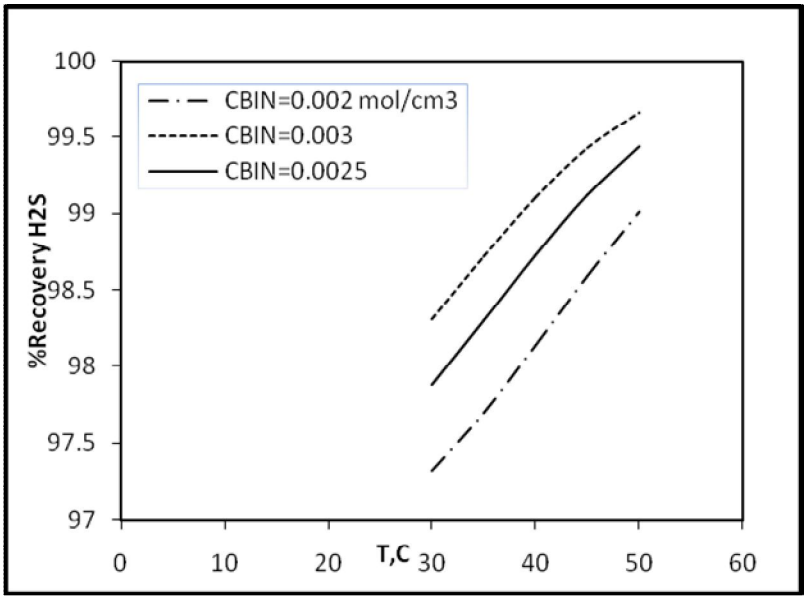

Figure 4.7 Temperature Influence on the % Removal with different solvent concentration of $Fe_2(SO_4)_3$

4.2.4 The Effect of Concentration of $Fe_2(SO_4)_3$ Solution on H_2S Removal Efficiency:

Figure 4.8 and Figure 4.9; shows the measurements of H_2S absorption removal into $Fe_2(SO_4)_3$ solution under different concentration of $Fe_2(SO_4)_3$ in the sieve tray column. In these cases, simulation conditions: H_2S inlet mole fraction is

y_{Ain} = 0.29, G = 751144.763 cm^3/s, L= 10000 cm^3/s, pressure = 1 atm and, temperatures 30 °C and $C_{(Fe\text{-}EDTA)}$ are range between 0.002-0.004 mol/cm^3.

Table 4.8 The Effect of Concentration of $Fe_2(SO_4)_3$ on H_2S Removal Efficiency

C_{Bin}	% Removal Efficiency
0.002	97.325
0.0025	97.884
0.003	98.308
0.0035	98.635
0.004	98.889

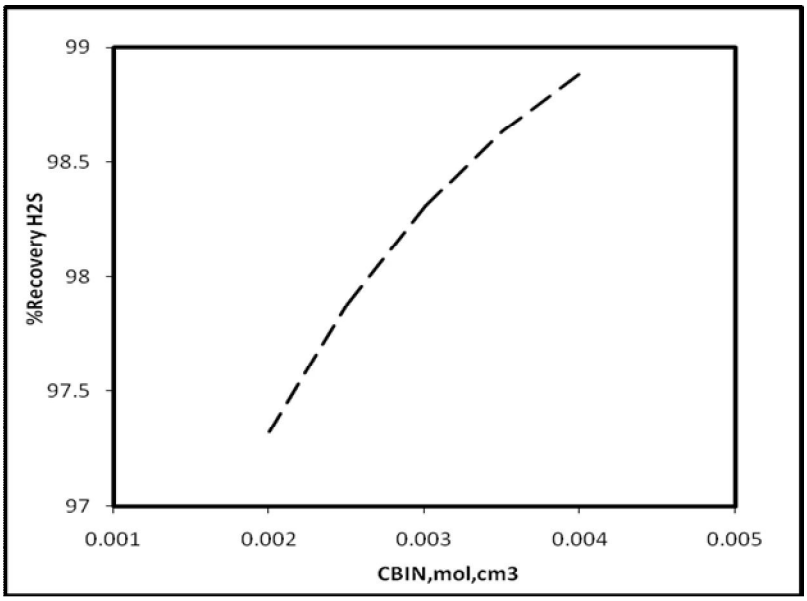

Figure 4.8 Solvent concentration of $Fe_2(SO_4)_3$ Influence on the % Removal

Figure 4.8; shows indicates that the increase in the value of $Fe_2(SO_4)_3$ concentration is still give influence to increase of H_2S removal efficiency. This is because when the concentration of $Fe_2(SO_4)_3$ is high, more H_2S must be introduced into the system to react with $Fe_2(SO_4)_3$, and this thing of course is caused because at

higher concentration of $Fe_2(SO_4)_3$ in solution, the ferric ion would be more reactive with sulphur ion, so that will increase absorption rate of H_2S from refinery flue gas.

Also Figure 4.9 shows indicates that the effect the $Fe_2(SO_4)_3$ concentration but with difference temperature (30 – 50^oC). For %removal of H_2S is given the same result in Figure 4.8 .

Table 4.9: The Effect of Concentration of $Fe_2(SO_4)_3$ on H_2S Removal Efficiency but with different Temperature

C_{Bin}	T=30^oC	T=40 ^oC
0.0020	97.325	98.138
0.0025	97.884	98.730
0.0030	98.308	99.108
0.0035	98.635	99.359
0.0040	98.889	99.529

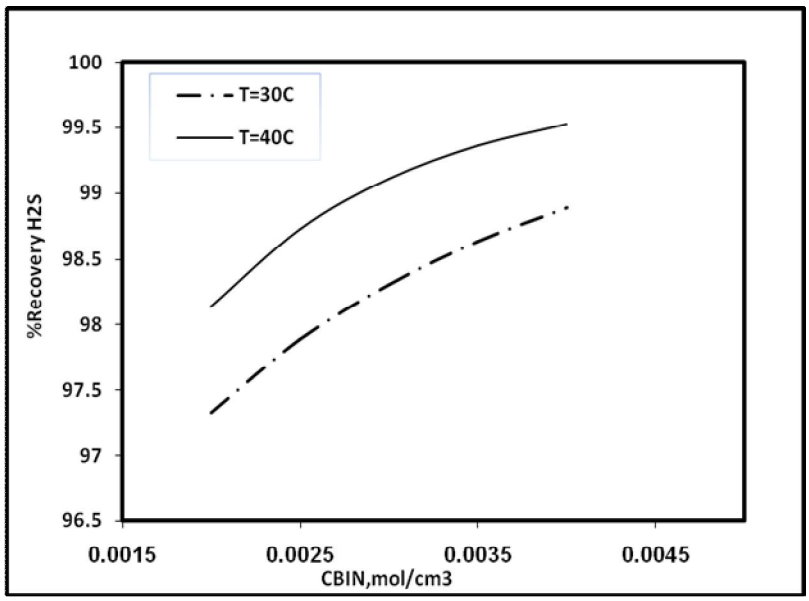

Figure 4.9 Solvent Concentration of $Fe_2(SO_4)_3$ Influence on the % Removal with different Temperature

4.2.5 The Effect of Flow Rate of $Fe_2(SO_4)_3$ Solution on H_2S Removal Efficiency:

The liquid flow rate has an important influence on H_2S removal efficiency. Figure 4.10 and Figure 4.11; shows the measurements of H_2S absorption removal into $Fe_2(SO_4)_3$ solution under different flow rate of $Fe_2(SO_4)_3$ in the sieve tray column. In these cases, simulation conditions: H_2S inlet mole fraction is $y_{Ain} = 0.29$, G = 751144.763 cm^3/s, pressure = 1 atm, temperatures 30 °C $C_{(Fe\text{-}EDTA)}$ = 0.002mol/cm^3, and L are range between 5000 -20000 cm^3/s

Figure 4.10; shows indicates that the increase in the value of $Fe_2(SO_4)_3$ flow rate is still give influence to increase of H_2S removal efficiency. Liquid flow rate determines how readily Component H_2S will absorb into the liquid phase. When the liquid flow rate is large, component H_2S will be absorbed more readily into the liquid phase.

Table 4.10 The Effect of Flow Rate of $Fe_2(SO_4)_3$ Solution on H_2S Removal Efficiency

L (cm^3/s)	% Removal Efficiency
5000	96.349
7500	97.070
10000	97.325
12500	97.455
15000	97.535
17500	97.587
20000	97.629

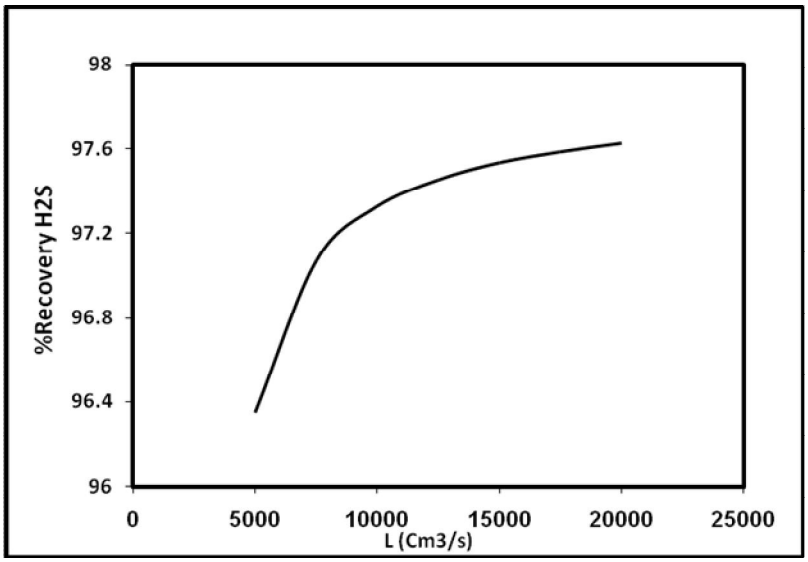

Figure 4.10 Flow Rate of $Fe_2(SO_4)_3$ Influence on the % Removal

This increase of H_2S removal efficiency occurred because the increasing of absorbent flow rate the liquid disturbance is enhanced, increase of driving force concentration that caused as result of decrease of concentration of H_2S in liquid bulk, which results in a higher speed of H_2S diffusing into the liquid. The consumed absorbents at the boundary layer could diffuse into the liquid phase at a higher speed due to the increase of liquid flow rate.

Table 4.11 The Effect of Flow Rate of $Fe_2(SO_4)_3$ Solution on H_2S Removal Efficiency but with different Temper

L(cm^3/s)	T=30°C	T=40 °C
5000	96.349	96.511
7500	97.070	97.816
10000	97.325	98.138
12500	97.455	98.284
15000	97.535	98.368
17500	97.587	98.422
20000	97.626	98.460

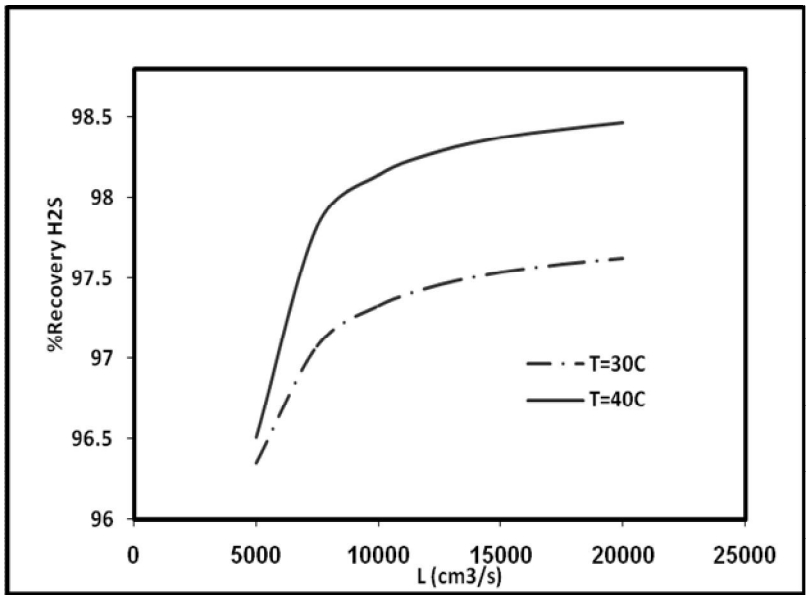

Figure 4.11 Flow Rate of $Fe_2(SO_4)_3$ Influence on the % Removal with different Temperature

Also Figure 4.11 shows indicates that the effect of $Fe_2(SO_4)_3$ flow rate but with difference temperature (30-50^oC) . For %removal of H_2S is given the same result in Figure 4.10

In addition, as the increase of liquid flow rate, the thicknesses of gaseous and liquid-phase boundary layers decrease, leading to enhancement of the mass transfer rate, also it can be explained when the flow rate increased, the interfacial area between gas-liquid places increased. Therefore, the result is to enhance gas-liquid mass transfer rate and improving the H_2S absorption efficiency.

4.2.5 The Effect of gas Flow Rate of Refinery flue gas on H_2S Removal Efficiency:

Figure 4.12, Figure 4.13 and Figure 4.14; shows the measurements of H_2S absorption removal into $Fe_2(SO_4)_3$ solution under different flow rate of refinery flue gas in the sieve tray column. In these cases, simulation conditions: H_2S inlet mole fraction is y_{Ain} = 0.29, pressure = 1 atm, temperatures 30 °C, $C_{(Fe2(SO4)3)}$ = 0.002mol/cm^3, L = 10000 cm^3/s, and G are range between (700-950 liter/s).

Table 4.12 The Effect of gas Flow Rate of Refinery flue gas on H_2S Removal Efficiency

$G_A(cm^3/s)$	% Removal Efficiency
700000	97.435
750000	97.327
800000	97.220
850000	97.112
900000	97.002
950000	96.891

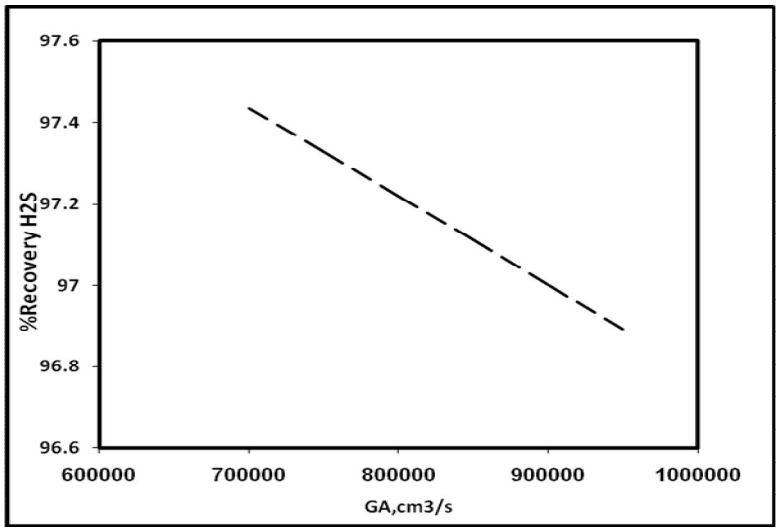

Figure 4.12 Flow Rate of Refinery flue gas Influence on the % Removal

Figures 4.12; shows indicates that the increase in the value of inlet refinery flue gas flow rate is give to declines and main negative effects on removal efficiency H_2S removal efficiency. This is because when the flow rate of refinery flue gas is high would a decrease the gas - liquid two phase contact time in the absorption column so the reaction rate of H_2S absorption slowed down. It was also that the increasing refinery flue gas flow rate carried spray absorbent out from the tower, and

led to the loss of the absorbent. Therefore, be concluded that the gas flow rate condition tends to become unfavorable to H_2S absorption when the gas flow rate increases within the operation range investigated.

Table 4.13 The Effect of gas Flow Rate of Refinery flue gas on H_2S Removal Efficiency but with different concentration of $Fe_2(SO_4)_3$

$G_A(cm^3/s)$	C_{BIN} =0.002	C_{BIN}=0.003
700000	97.435	98.378
750000	97.327	98.310
800000	97.220	98.242
850000	97.112	98.174
900000	97.002	98.105
950000	96.891	98.036

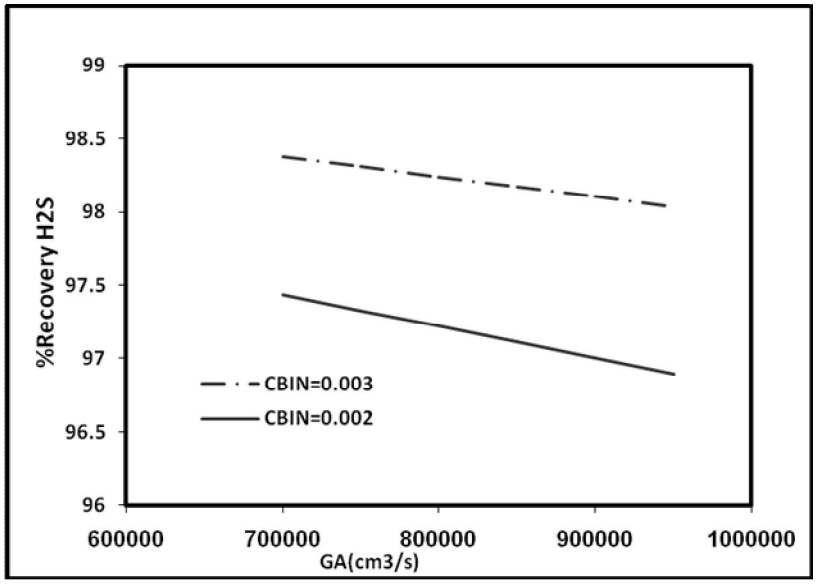

Figure 4.13 Flow Rate of Refinery flue gas Influence on the % Removal with different concentration of $Fe_2(SO_4)_3$

Also Figures 4.13 and Figures 4.134 shows indicates that the effect of refinery flue gas flow rate but with difference concentration 0.002-0.003 mol/cm^3 in Figure 4.13 and difference temperature (30-40^oC) in Figures 4.14. For %removal of H_2S is given the same result in Figure 4.12.

Table 4.14 The Effect of gas Flow Rate of Refinery flue gas on H_2S Removal Efficiency but with different Temperature:

$G_A(cm^3/s)$	T=30^oC	40 ^oC
700000	97.435	98.240
750000	97.327	98.140
800000	97.220	98.036
850000	97.112	97.929
900000	97.002	97.816
950000	96.891	97.816

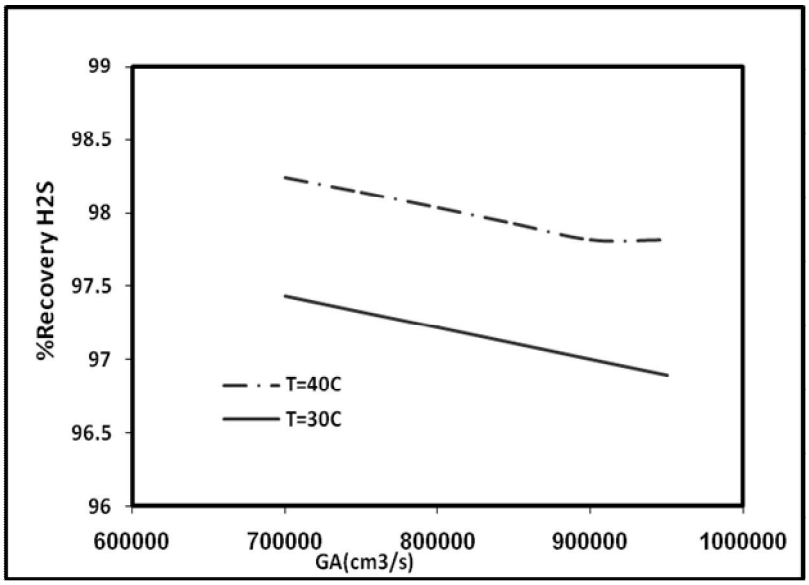

Figure 4.14 Flow Rate of Refinery flue gas Influence on the % Removal with different Temperature

CHAPTER FIVE

5. Conclusions and Recommendations

5.1 Conclusions

H_2S removal from refinery flue gas using aqueous ferric solution $Fe_2(SO_4)_3$ is an advanced air pollution control device to reduce greenhouse gas emissions and as absorbent has been studied theoretically, calculations for absorber have been done, and their dimensions are obtained for a known refinery flue gas flow rate.

This thesis describes the hardware design of sieve tray column and describes the physical processes that constrain equipment design, including flooding, entrainment, weeping, pressure drop, clear liquid height, and flow regimes. This thesis then describes how knowledge of these physical processes is harnessed to set hardware design.

Absorption of H_2S by $Fe_2(SO_4)_3$ solutions was performed in this study to clarify the H_2S absorption efficiency. The absorption of H_2S into aqueous solutions of $Fe_2(SO_4)_3$ as encountered in refinery flue gas was carried out using sieve plate column.

Various important operating factors affecting the H_2S absorption efficiency were discussed in this research. Various operating parameters, including liquid flow rate, $Fe_2(SO_4)_3$ concentration, temperature, and gas flow rate, were tested to determine the effect of these variables on the H_2S absorption efficiency. The simulation results showed that the percentage of absorbed H_2S can be enhanced and should have higher efficiency by increasing temperature, liquid flow rate, and $Fe_2(SO_4)_3$ concentration and decreasing flow rate of refinery flue gas.

The model can be implemented in any program for the design of absorption processes. A program for the calculation and display of phase diagrams and for the optimal design of gas liquid absorption processes was developed.

5.2 Recommendations

1- Study the effect of varying different design parameters on the required number of theoretical stages and stage efficiencies and design of differential contactors.

2- The obtained results may be helpful in estimating the scavenger injection dose for similar fields and condition.

3- It is hoped that with the continuous for this study to absorption NH_3 remaining in refinery flue gas which also pollutes environment.

4- Other absorption equipment needs to the considered (spray column).

5- Contains for effecting factors should be observed.

REFERENCES

A. C. a. N. Mostoufi. (1999). "Numerical Methods For Chemical Engineers With Matlab Applications". The State University , New Jersey.

Asai, S., Konishi, Y., & Yabu, T. (1990). "Kinetics of absorption of hydrogen sulfide into aqueous ferric sulfate solutions". AI.Ch.E. Journal, 35: 1271–1281

Astarita, Giovanni, (1967). "Mass Transfer With Chemical Reaction". Elsevien publishing Company, Amsterdam.

Bruce A.Finlayson, (2003). "Nonlinear Analysis In Chemical Engineering". Professor of Chemical Engineering And Applied Mathematics University of Washington,.

C. a. Y. P. . Wang. (2012). "The removal of hydrogen sulfide in solution by ferric and alum water treatment residuals". Chemosphere,Volume 88 (10) P 1178–1183

Coulson & Richardson's, (1999). "Chemical Engineering Design Volume.6" Department of Chemical and Biological Process Engineering University of Wales Swansea.

DeCoursey, W.J. (1982). "Enhancement factors for gas absorption with reversible reaction. Chemical Engineering Sciences", 37: 1483-1489.

Danckwerts, P. V.(1970)." Gas liquid reactions". New York: McGraw-Hill Book Co

G. Astarita, (1967). "Mass Transfer With Chemical Reaction". Amsterdam: Elsevien publishing Company.

Horikawa, M.S., Rossi, F., Gimenes, M.L., Costa, C.M.M., and da Silva. M.G.C. (2004). "Chemical Absorption of H_2S For Biogas Purification". Brazilian Journal of Chemical Engineering Vol. 21, No. 03, pp. 415 – 422,.

M. S. Horikawa, Rossi, F., Gimenes, M.L., Costa, C.M.M., and da Silva. M.G.C. (2004). "Chemical Absorption of H2S For Biogas Purification". Brazilian Journal of Chemical Engineering, vol. 21 : 415 – 422 .

Mohammadtaghi , Zahra and Fatemeh. (2012). "Removal of Hydrogen Sulfide from Gaseous Streams by a Chemical Method using Ferric Sulfate Solution". World Applied Sciences Journal, 19 (2) : 241-245

Perry, R.H. and D.W. Green. (1997). "Perry's Chemical Engineers' Handbook (7Edition)". McGraw-Hill.

P.S. Kumar, J.A. Hogendoorn, P.H.M. Feron and G.F. Versteeg. (2003) "Approximate solution to predict the enhancement factor for the reactive absorption of a gas in a liquid flowing through a microporous membrane hollow fiber". Journal of Membrane Science, 231–245.

R.W.Holhlfeld. (1980). "Selective Absorption of H_2S from Sour gas". journal of petroleum Technology, 32: 1083-1089.

Robert E. Treybal. (1981). "Mass Transfer Operation Third edition". McGraw Hill Book.

Roger A. Svehla, (1995). "Transport Coefficients for the NASA Lewih Chemical Equilibrium Program". Lewih Research Center Cleveland, Ohio 44135.

Reinalldo Caban and Thomas W, (1979). "Solution of Boundary layer Transport Problems by Orthogonal Collocation". Chemical Engineering Department University of Wisconsin Madison.

S. Ebrahimi,R.Kleerebezem,M.C.M.van Loosdrecht, J.J.Heijnen. (2003). "Kinettics of the reactive Absorption of Hydrogen Sulfide into Aqueous Ferric Sulfate Solutions". Chem Eng Sci, 58(2): pp 417-427.

Sungbum Han.(2004). "Absorption of Hydrogen Sulfide into Aqueous Ferric Sulfate Solutions through a Flat Gas-Liquid Interface in an Agitated Vessel". Chem. Eng. Res, Vol. 42(2) : 163-167.

Yung Ji Tarng and Rayford G. Anthony, (1987). "Nonlinear Boundary Value Problems. A Decoupling Technique with Quasi-Linearization and Orthogonal Collocation". Department of Chemical Engineerin Texas A&M University, College Station, Texas 77843.

Z. Gholami, M. Torabi Angaji, F. Gholami, and S. A. Razavi Alavi. (2009). "Reactive Absorption of Hydrogen Sulfide in Aqueous Ferric Sulfate Solution". International Journal of Chemical, Molecular, Nuclear, Materials and Metallurgical Engineering, Vol:3, No:1.

APPENDIX A

LISTING PROGRAM

% Listing Matlab Program for Film Model

```
clear all;
clc;
% initial input
   %N=input('value input N=');
   N=4;% Number of boundary collocation points
   NK=11;% Actual Number of plates
   ZT=600; %Height of the tower cm
   dz=ZT/(NK-1);
   % Costant of matrix for orthogonal collcation, from Nonlinear Analysis in
Chemical Engineering page77
   if N==1
      Xj=[0; 0.50000; 1];
   end
   if N==2
      Xj=[0; 0.2113248654; 0.7886751346; 1];
   end
   if N==3
      Xj=[0; 0.1127016654; 0.5000000000; 0.8872983346; 1];
   end
   if N==4
      Xj=[0; 0.0694318442; 0.3300094783; 0.6699905218; 0.9305681558; 1];
   end
```

```
    if N==5
      Xj=[0; 0.0469100771; 0.2307653450; 0.5000000000; 0.7692346551;
0.9530899230; 1];
    end
    if N==6
      Xj=[0; 0.0337652429; 0.1693953068; 0.3826904070; 0.6193095931;
0.8306046933; 0.9662347571; 1];
    end
    if N==7
      Xj=[0; 0.0254; 0.1292; 0.2971; 0.5; 0.7029; 0.8708; 0.9746; 1];
    end
    if N==8
      Xj=[0; 0.0199; 0.1017; 0.2372; 0.4083; 0.5917; 0.7628; 0.8983; 0.9801; 1];
    end
       for j= 1:N+2
       for i= 1:N+2
    % The derivatives at the N+2 Collocation points, Nonlinear Analysis in Chemical
Engineering page76
          Q(j,i)=Xj(j,1)^(i-1);
          R(j,i)=(i-1)*(Xj(j,1))^(i-2);
          H(j,i)=(i-1)*(i-2)*(Xj(j,1)^(i-3));
          R(1,1)=0;
          H(1,1)=0;
          H(1,2)=0;
       end
```

```
end
C=R*inv(Q);
D=H*inv(Q);
A(1,1)=1;
A(1,N+2)=0;
B(1,N+2)=1;
%CBIN=input('value input CBIN='); % mol/cm3 -------> Concentration of solvent
CBIN=0.002;
CB(1)=CBIN;
CA=0;
%LA=input('value input LA=');% cm3/s -------> Volumetric flow rate of solvent
LA=10000;%cm3/s
YaIN=0.288875;% mole fraction of solute in inlet Sour gas
GV=751144.763;% cm3/s -------> Volumetric flow rate of sour gas
Dcolumn=70;%cm -------> column diameter
AC=(0.785*Dcolumn^2);%cm2
%calculates a -------> interfacial area
RoL=1.899;%g/cm3 ----> density of solvent, From Wikipedia, the free encyclopedia
L=(LA*RoL/AC);% g/cm2.s
MwG=34;% Molecular weight of solute
Rg=82.057;%cm3.atm/mol.K -------> Universal Gas Constant
P=1;%atm -------> preassure
%P=input('P (atm)=');
T=30;%C
T=input('T (C)=');%;;C -------> Temperature
```

```
CC=P/(Rg*(T+273.15));% mol/cm3
RoG=CC*MwG;%g/cm3
e=2.718281828;
SIGMAL=20;%dyne/cm
ut=26.5 ;%cm/s-------> velocity of rise of the bubbles in the forth (gas liquid reaction , Danckwerts)
d=0.45;%cm -------> hole diameter
n=2597;%number of holes per unit area of plate
MuL=(0.0114*CBIN^2)+(0.0015*CBIN)+0.0062;%g/cm.s------>viscosity of solvent, Kinetics of the reactive absorption of hydrogen sulfide into aqueous ferric sulfate solutions
g=987;%cm/s2 -------> gravitational acceleration
u=GV/AC;%cm/s  -------> the superficial gas velocity
a=0.38*((u/ut)^0.775)*(((u*RoG)/(n*d*MuL))^0.125)*(((g*RoG)/(d*SIGMAL))^(1/3));%cm-1------> interfacial area per unit volume of froth(gas liquid reaction , Danckwerts)Eq3.71
% calculate diffusion coefficient
VH2S= 32.9;% cm3/mol  -------> molecular volume
phi= 1; % association factor
MwL= 399.88; %Molecular weight of solvent
DB = ((7.4*10^-8)*((phi*MwL)^0.5)*(T+273.15))/(MuL*(VH2S)^0.6);%cm2/s----> diffusion coefficient of H2S in fe2(so4)3 solution Equation 3.75
%calculate kL
RHO=RoL;
```

```
    kL=0.42*(((g*MuL)/RHO)^(1/3))*(((DB*RHO)/MuL)^(1/2));%cm/s ------>
%Mass transfer coefficient in liquid phase Equation 3.72
%calculate DG
    sigmaA=3.623;%Lennard-Jones force constants for A=H2S ,
sigmaB=2.9;%Lennard-Jones force constants for B=NH3,
 epskA=301.1; % K
    epskB=558.3;%  K
    sigmaAB=(sigmaA+sigmaB)/2;% Eq. 3.75
    epskAB=(epskA*epskB)^0.5;% Eq.3.77
    MA=34;
    MB=17;
    TB=(T+273)/epskAB;
    omegaD=((44.54*(TB^-4.909))+(1.911*(TB^-1.575)))^0.1;%Eq.3.76
DG=0.001858*(T+273)^1.5*((MA+MB)/(MA*MB))^0.5/(P*sigmaAB^2*omegaD);
%cm2/s ------> Binary gas phase diffusivity of A in B Eq3.74
    Dg=DG*10^-4;%m2/s
    %calculate DG
     G=GV* RoG;%g/s
     Gm=G/(AC*MwG);% mol/cm2.s
     GG=G/AC;%g/cm2.s
     MuG=0.0128 ;%g/cm.s
     hw=5;%cm-------> weir height
    f=0.75;%approach to flood, fractional
    hL=0.025;%liquid holdup on plate, mm
```

```
    kga=(316*Dg^0.5*((1030*f)+(867*f^2)))/hL^0.5;%Perry's Chemical Engineers' Handbook (7th Edition)
    kg=kga/a;% m/s------->gas-phase mass-transfer coefficient,
    kG=kg*100;%cm/s
    U=LA/AC;
    Z=1;
    k1 = 9.3855-(2636.6/(T+273));
    k11=10^k1;%m3/kmol.s  --------> reaction rate constant, Kinetics of the reactive absorption of hydrogen sulfide into aqueous ferric sulfate solutions
    k=k11*1000;%cm3/gmol.s --------> reaction rate constant
    Hs=358.8842;
    O=-975.267;
    konvH=1000;
    He=Hs*(2.718282^(O/(T+273.15)))*konvH;
     %k1 = 9.3855-(2636.6/(T+273));
     %k11=10^k1;%m3/kmol.s  --------> reaction rate constant, Kinetics of the reactive absorption of hydrogen sulfide into aqueous ferric sulfate solutions
     %k=k11*1000;%cm3/mol.s --------> reaction rate constant
     %He=(((273.1+T)-266.6)/3.168)*1000;% cm3.atm/mol--------> Compilation of Henry’s Law Constants for Inorganic and Organic Species of Potential Importance in Environmental Chemistry
    DA=DG;
% Dimension Column and Operating condition
% ------------------------------------------------------------
% Calculates CA,CB,YA every stage by using Runge Kutta
```

```
%GUESS YAout
%first trial
er_kolom=1;
iter_k=0;
inkYa=YaIN/2000;
Ya(1)=0;
while er_kolom > 0.01
   iter_k=iter_k+1;
   incrementsYa=inkYa;
   if iter_k>1
      dev=YaIN-Ya(NK);
      inka=20*inkYa;
      inkb=100*inkYa;
      inkc=-100*inkYa;
      inkd=-2*inkYa;
      if dev < inkc
         incrementsYa=-inkYa/2;
      else
         if dev < 0
            incrementsYa=-inkYa/100;
         else
            if dev < inka
               incrementsYa= inkYa/100;
            else
               if dev > inkb
```

```
                incrementsYa=inkYa/2;
            else
                incrementsYa=inkYa/5;
            end
        end
    end
  end
end
Ya(1)=Ya(1)+incrementsYa
Ya1=Ya(1)
for ik=1:NK-1
   Pa=P*Ya(ik);
   CBb=CB(ik);
   % Calculation E
   E=1.1;
   tol=0.001 ;
   Error=1 ;
   while Error>tol
     ES=E;
     CAi=((kG*Pa)+(E*kL*CA))/((E*kL)+(kG*He));
     M=(k*CBb*DB)/(kL^2);
     S=DB*CBb/(Z*CAi*DA);
     for i=2:N+1
        A(1,i)=1-Xj(i,1);
     end
```

```
for i=1:N+1
   B(1,i)=0.09+0.91*Xj(i,1);
end
%starts iteration
tol=0.0001;
Err_max=1;
it=0;
while (Err_max >tol);
   it=it+1;
   j=1:N+2;
   Bi(1,1)=B(1,1);
   B(1,1)=-(sum(C(1,j).*B(1,j))-(C(1,1)*B(1,1)))/C(1,1);
   for i=2:N+1;
      Ai(1,i)=A(1,i);
      Bi(1,i)=B(1,i);
      A(1,i)=((sum(D(i,j).*A(1,j)))-(D(i,i)*A(1,i)))/(M*B(1,i)-D(i,i));
      B(1,i)=((sum(D(i,j).*B(1,j)))-(D(i,i)*B(1,i)))/((M/S)*A(1,i)-D(i,i));
   end
   %pemilihan error terbesar ... The election error
   if it>1
      Err_max=0;
      for i=2:N+1;
         if (abs((B(1,1)-Bi(1,1))/Bi(1,1))>Err_max);
            Err_max= (abs((B(1,1)-Bi(1,1))/Bi(1,1)));
         end
```

```
            if (abs((A(1,i)-Ai(1,i))/Ai(1,i))>Err_max);
               Err_max= (abs((A(1,i)-Ai(1,i))/Ai(1,i)));
            end
            if (abs((B(1,i)-Bi(1,i))/Bi(1,i))>Err_max);
               Err_max= (abs((B(1,i)-Bi(1,i))/Bi(1,i)));
            end
         end
      end
   end
   E=-(sum(C(1,j).*A(1,j)));
   Error=abs((E-ES)/ES);
end
A1=dz*(E*kL*a/Gm)*(CAi-CA);
B1=dz*(-2*E*kL*a/U)*(CAi-CA);
Pa=P*(Ya(ik)+A1/2);
CBb=CB(ik)+B1/2;
%Calculation E
E=1.1;
tol=0.001 ;
Error=1 ;
while Error>tol
   ES=E;
   CAi=((kG*Pa)+(E*kL*CA))/((E*kL)+(kG*He));
   M=(k*CBb*DA)/(kL^2);
   S=DB*CBb/(Z*CAi*DA);
```

```
for i=2:N+1
   A(1,i)=1-Xj(i,1);
end
for i=1:N+1
   B(1,i)=0.09+0.91*Xj(i,1);
end
%starts iteration
tol=0.0001;
Err_max=1;
it=0;
while (Err_max >tol);
   it=it+1;
   j=1:N+2;
   Bi(1,1)=B(1,1);
   B(1,1)=-(sum(C(1,j).*B(1,j))-(C(1,1)*B(1,1)))/C(1,1);
   for i=2:N+1;
      Ai(1,i)=A(1,i);
      Bi(1,i)=B(1,i);
      A(1,i)=((sum(D(i,j).*A(1,j)))-(D(i,i)*A(1,i)))/(M*B(1,i)-D(i,i));
      B(1,i)=((sum(D(i,j).*B(1,j)))-(D(i,i)*B(1,i)))/((M/S)*A(1,i)-D(i,i));
   end
   %pemilihan error terbesar
   if it>1
      Err_max=0;
      for i=2:N+1;
```

```
            if (abs((B(1,1)-Bi(1,1))/Bi(1,1))>Err_max);
               Err_max= (abs((B(1,1)-Bi(1,1))/Bi(1,1)));
            end
            if (abs((A(1,i)-Ai(1,i))/Ai(1,i))>Err_max);
               Err_max= (abs((A(1,i)-Ai(1,i))/Ai(1,i)));
            end
            if (abs((B(1,i)-Bi(1,i))/Bi(1,i))>Err_max);
               Err_max= (abs((B(1,i)-Bi(1,i))/Bi(1,i)));
            end
         end
      end
   end
   E=-(sum(C(1,j).*A(1,j)));
   Error=abs((E-ES)/ES);
end
A2=dz*(((E*kL*a/Gm)*(CAi-CA)));
B2=dz*(((-2)*(E*kL*(a/U))*(CAi-CA)));
Pa=P*(Ya(ik)+A2/2);
CBb=CB(ik)+B2/2;
%perhitungan E
E=1.1;
tol=0.001 ;
Error=1 ;
while Error>tol
   ES=E;
```

```
CAi=((kG*Pa)+(E*kL*CA))/((E*kL)+(kG*He));
M=(k*CBb*DA)/(kL^2);
S=DB*CBb/(Z*CAi*DA);
for i=2:N+1
   A(1,i)=1-Xj(i,1);
end
for i=1:N+1
   B(1,i)=0.09+0.91*Xj(i,1);
end
%starts iteration
tol=0.0001;
Err_max=1;
it=0;
while (Err_max >tol);
   it=it+1;
   j=1:N+2;
   Bi(1,1)=B(1,1);
   B(1,1)=-(sum(C(1,j).*B(1,j))-(C(1,1)*B(1,1)))/C(1,1);
   for i=2:N+1;
      Ai(1,i)=A(1,i);
      Bi(1,i)=B(1,i);
      A(1,i)=((sum(D(i,j).*A(1,j)))-(D(i,i)*A(1,i)))/(M*B(1,i)-D(i,i));
      B(1,i)=((sum(D(i,j).*B(1,j)))-(D(i,i)*B(1,i)))/((M/S)*A(1,i)-D(i,i));
   end
   %pemilihan error terbesar .... The election error
```

```
        if it>1
            Err_max=0;
            for i=2:N+1;
                if (abs((B(1,1)-Bi(1,1))/Bi(1,1))>Err_max);
                    Err_max= (abs((B(1,1)-Bi(1,1))/Bi(1,1)));
                end
                if (abs((A(1,i)-Ai(1,i))/Ai(1,i))>Err_max);
                    Err_max= (abs((A(1,i)-Ai(1,i))/Ai(1,i)));
                end
                if (abs((B(1,i)-Bi(1,i))/Bi(1,i))>Err_max);
                    Err_max= (abs((B(1,i)-Bi(1,i))/Bi(1,i)));
                end
            end
        end
    end
    E=-(sum(C(1,j).*A(1,j)));
    Error=abs((E-ES)/ES);
end
A3=dz*(((E*kL*a/Gm)*(CAi-CA)));
B3=dz*(((-2)*(E*kL*(a/U))*(CAi-CA)));
Pa=P*(Ya(ik)+A3);
CBb=CB(ik)+B3;
%Calculation E
E=1.1;
tol=0.001 ;
```

```
Error=1 ;
while Error>tol
   ES=E;
   CAi=((kG*Pa)+(E*kL*CA))/((E*kL)+(kG*He));
   M=(k*CBb*DA)/(kL^2);
   S=DB*CBb/(Z*CAi*DA);
   for i=2:N+1
      A(1,i)=1-Xj(i,1);
   end
   for i=1:N+1
      B(1,i)=0.09+0.91*Xj(i,1);
   end
   %starts iteration
   tol=0.0001;
   Err_max=1;
   it=0;
   while (Err_max >tol);
      it=it+1;
      j=1:N+2;
      Bi(1,1)=B(1,1);
      B(1,1)=-(sum(C(1,j).*B(1,j))-(C(1,1)*B(1,1)))/C(1,1);
      for i=2:N+1
         Ai(1,i)=A(1,i);
         Bi(1,i)=B(1,i);
         A(1,i)=((sum(D(i,j).*A(1,j)))-(D(i,i)*A(1,i)))/(M*B(1,i)-D(i,i));
```

```
            B(1,i)=((sum(D(i,j).*B(1,j)))-(D(i,i)*B(1,i)))/((M/S)*A(1,i)-D(i,i));
        end
        %pemilihan error terbesar .... The election error
        if it>1
            Err_max=0;
            for i=2:N+1
                if (abs((B(1,1)-Bi(1,1))/Bi(1,1))>Err_max);
                    Err_max= (abs((B(1,1)-Bi(1,1))/Bi(1,1)));
                end
                if (abs((A(1,i)-Ai(1,i))/Ai(1,i))>Err_max);
                    Err_max= (abs((A(1,i)-Ai(1,i))/Ai(1,i)));
                end
                if (abs((B(1,i)-Bi(1,i))/Bi(1,i))>Err_max);
                    Err_max= (abs((B(1,i)-Bi(1,i))/Bi(1,i)));
                end
            end
        end
    end
    E=-(sum(C(1,j).*A(1,j)));
    Error=abs((E-ES)/ES);
end
A4=dz*(((E*kL*a/Gm)*(CAi-CA)));
B4=dz*(((-2)*(E*kL*(a/U))*(CAi-CA)));
Ya(ik+1)=Ya(ik)+(A1+2*A2+2*A3+A4)/6;
CB(ik+1)=CB(ik)+(B1+2*B2+2*B3+B4)/6;
```

```
  end
  er_kolom=abs((Ya(NK)-YaIN)/YaIN)
end
YYaIN=Ya(NK)/(1-Ya(NK));
YYaOUT=Ya(1)/(1-Ya(1));
Persen_Recovery=((YYaIN-YYaOUT)/YYaIN)*100;
disp(['Persen_Recovery = ',num2str(Persen_Recovery)]);
disp(['Ya = ',num2str(Ya)]);
disp(['CB = ',num2str(CB)]);
```

APPENDIX B